

## INFORMATION TO USERS

This material was produced from a microfilm copy of the original document. While the most advanced technological means to photograph and reproduce this document have been used, the quality is heavily dependent upon the quality of the original submitted.

The following explanation of techniques is provided to help you understand markings or patterns which may appear on this reproduction.

1. The sign or "target" for pages apparently lacking from the document photographed is "Missing Page(s)". If it was possible to obtain the missing page(s) or section, they are spliced into the film along with adjacent pages. This may have necessitated cutting thru an image and duplicating adjacent pages to insure you complete continuity.
2. When an image on the film is obliterated with a large round black mark, it is an indication that the photographer suspected that the copy may have moved during exposure and thus cause a blurred image. You will find a good image of the page in the adjacent frame.
3. When a map, drawing or chart, etc., was part of the material being photographed the photographer followed a definite method in "sectioning" the material. It is customary to begin photoing at the upper left hand corner of a large sheet and to continue photoing from left to right in equal sections with a small overlap. If necessary, sectioning is continued again — beginning below the first row and continuing on until complete.
4. The majority of users indicate that the textual content is of greatest value, however, a somewhat higher quality reproduction could be made from "photographs" if essential to the understanding of the dissertation. Silver prints of "photographs" may be ordered at additional charge by writing the Order Department, giving the catalog number, title, author and specific pages you wish reproduced.
5. PLEASE NOTE: Some pages may have indistinct print. Filmed as received.

**Xerox University Microfilms**

300 North Zeeb Road  
Ann Arbor, Michigan 48106

75-1177

**PLOTCH, Stephen J., 1943-  
RABBIT MUSCLE ALANINE AMINOTRANSFERASE: PURIFICATION  
AND PROPERTIES.**

**The City University of New York, Ph.D., 1974  
Chemistry, biological**

**Xerox University Microfilms, Ann Arbor, Michigan 48106**

RABBIT MUSCLE ALANINE AMINOTRANSFERASE:  
PURIFICATION AND PROPERTIES

---

A Dissertation Presented to the  
Faculty of the Department of Biochemistry  
of the City University of New York

---

In Partial Fulfillment of the  
Requirements for the Degree of Doctor  
of Philosophy

---

by

Stephen Plotch

1974

This manuscript has been read and accepted for the Graduate Faculty in Biochemistry in satisfaction of the dissertation requirement for the degree of Doctor of Philosophy.

August 23, 1974  
date

Aaron Laktion  
Chairman of Examining Committee

August 23, 1974  
date

Aaron Laktion  
Executive Officer

Morton Glantz  
Norman Indictor  
Stanley Salthe  
James Hogg  
Supervisory Committee

ABSTRACT

ABSTRACT

1. Rabbit muscle alanine aminotransferase has been purified to a state of homogeneity based upon analytical ultracentrifugal analysis, disc gel electrophoresis, and SDS gel electrophoresis. The enzyme has a molecular weight of  $110,000 \pm 4000$ , a  $S_{20}^{\circ, w}$  of 6.45, and is a dimer consisting of two polypeptide chains of molecular weight  $55,000 \pm 2000$ .

2. Analytical and preparative isoelectric focusing indicate that the enzyme is actually a heterogeneous mixture of 12-14 isozymes with isoelectric points between pH 7 and 9. The isozymes are enzymatically active.

3. The enzyme contains approximately 2 moles of PLP per mole of enzyme. The PLP is tightly bound and is not readily resolved. Borohydride reduction results in complete loss of enzymatic activity.

4. PCMB titration results in about 95% loss of activity after 6-7 cysteinyl residues have reacted.

5. The pH activity optimum range is between pH 7.5 - 8.1. Increasing ionic strength decreases enzymatic activity in a manner which points to a primary kinetic salt effect. Phosphate retards this inhibition.

6. The enzyme is virtually specific for the substrate pairs alanine plus  $\alpha$ -ketoglutarate and pyruvate plus glutamate. Mesoxalate, 2-ketobutyrate and  $\alpha$ -amino valerate can act as very weak substrates.

7. The Michaelis constants, measured in 0.1M phosphate, pH 7.5 at 30°C are: pyruvate and ketoglutarate - 0.64mM;

glutamate - 17.5mM; alanine - 43mM.

8. The enzyme is inhibited by a wide variety of amino, keto, mono and dicarboxylic acids, with proline, cysteine, phenylpyruvate and the longer monocarboxylic acids being especially effective.

9. Aminooxyacetate is a potent inhibitor, with a  $K_i$  of  $3 \times 10^{-8}$ M.

10. An Arrhenius plot demonstrates 3 activation energies between 12°C and 42°C.

## ACKNOWLEDGEMENT

I would like to thank Professor Aaron Lukton for his many years of advice and guidance in the preparation of this work.

DEDICATION

To My Mother

TABLE OF CONTENTS

	<u>Page</u>
APPROVAL.....	i
ABSTRACT.....	ii
ACKNOWLEDGEMENT.....	v
DEDICATION.....	vi
TABLE OF CONTENTS.....	vii
LIST OF TABLES.....	ix
LIST OF ILLUSTRATIONS.....	x
LIST OF ABBREVIATIONS.....	xii
I. INTRODUCTION.....	1
A. Transamination.....	2
B. Gluconeogenesis.....	22
II. MATERIALS AND METHODS.....	31
A. Enzymes and other proteins.....	32
B. Reagents.....	32
C. Column chromatography.....	33
D. Instrumentation.....	33
E. PCMB titration.....	34
F. PLP content.....	35
G. Reduction with NaBH <sub>4</sub> .....	35
H. Attempted resolution of PLP.....	36
I. Disc gel electrophoresis.....	37
J. SDS gel electrophoresis.....	38
K. Analytical gel isoelectric focusing.....	39
L. Preparative isoelectric focusing.....	40
M. Sedimentation coefficient.....	40
N. Molecular weight.....	41
O. Enzyme assay.....	42
P. Enzyme purification.....	46
III. RESULTS.....	51
A. Disc gel electrophoresis.....	54
B. Analytical isoelectric focusing.....	55
C. Preparative isoelectric focusing.....	56
D. SDS gel electrophoresis.....	57
E. Sedimentation coefficient.....	58
F. Molecular weight.....	59
G. Tryptophan and tyrosine content.....	59
H. PLP content.....	60

	<u>Page</u>
III. RESULTS (Cont.)	
I. Sodium borohydride reduction.....	61
J. Removal of PLP from holoenzyme.....	61
K. PCMB titration.....	62
L. Spectra.....	63
M. Effect of pH on enzyme activity.....	64
N. Ionic strength effects.....	65
O. Effect of temperature on enzyme activity.....	67
P. Enzyme specificity.....	68
Q. Kinetic theory and parameters.....	69
R. Inhibitors.....	71
S. Phosphorylase-Transaminase complex.....	76
IV. DISCUSSION.....	78
V. TABLES.....	84
VI. ILLUSTRATIONS.....	91
VII. REFERENCES.....	163

LIST OF TABLES

<u>Table No.</u>		<u>Page</u>
I	Summary of enzyme purification procedure.....	85
II	Michaelis constants and maximal velocities.....	86
III	Inhibition by keto, mono and dicarboxylic acids of the forward reaction.....	87
IV	Inhibition by keto, mono and dicarboxylic acids of the reverse reaction.....	88
V	Inhibition by amino acids of the forward reaction.....	89
VI	Inhibition constants for various inhibitors....	90

LIST OF ILLUSTRATIONS

<u>Fig. No.</u>		<u>Page</u>
1	DEAE-Sephadex A-50 Chromatography	92
2	Hydroxylapatite Chromatography	94
3	Disc gel electrophoresis of purified enzyme-pH 4.3	95
4	Disc gel electrophoresis of purified enzyme-pH 9.5	96
5	Isoelectric focusing of purified enzyme-pH 3-10	97
6	Isoelectric focusing of purified enzyme-pH 7-9	98
7	Activity vs slice number for pH 7-9 isoelectric focusing	100
8	Preparative isoelectric focusing	102
9	SDS gel electrophoresis of purified enzyme	103
10	Mobility of alanine transaminase and 5 marker proteins on 10% Acrylamide SDS gels	105
11	Sedimentation velocity of purified enzyme-photos	106
12	Sedimentation velocity of purified enzyme-in distance vs time	108
13	Plot of $S_{20,w}$ at several protein concentrations	110
14	Equilibrium sedimentation of purified enzyme	112
15	Fluorescence intensity vs PLP-standard curve	114
16	Loss of enzyme activity with PCMB	116
17	Spectra of alanine aminotransferase at pH 7.0 PLP and PMP forms	118
18	Effect of pH on the spectrum of alanine aminotransferase	120
19	pKa determination	122
20a	Spectrum of alanine <sub>5</sub> aminotransferase in the presence of $1 \times 10^{-5}$ M aminooxyacetate	124
20b	Spectrum of alanine aminotransferase in the presence of 0.1M L-proline	124
21	Enzyme activity vs pH	126
22	Per cent inhibition by aminooxyacetate vs pH	128
23	Per cent inhibition by proline vs pH	130
24	Per cent inhibition by phenylpyruvate vs pH	132

<u>Fig. No.</u>		<u>Page</u>
25a	Activity vs ionic strength-.01M phosphate buffer	134
25b	Log activity vs the square root of the ionic strength-.01M phosphate buffer	136
25c	Log rate constant vs the square root of the ionic strength-.01M phosphate buffer	138
26	Log activity vs the square root of the ionic strength-0.1M phosphate buffer	140
27	Log activity vs the square root of the ionic strength - ionic strength is a function of phosphate concentration	142
28	Arrhenius plot	144
29	Double reciprocal plot of initial velocity vs alanine concentration at a series of fixed ketoglutarate concentrations	146
30	Double reciprocal plot of initial velocity vs pyruvate concentration at a series of fixed glutamate concentrations	148
31	Secondary plots of data from Fig. 29	150
32	Secondary plots of data from Fig. 30	152
33	Dixon plot of enzyme inhibition by lauric acid	154
34	Dixon plot of enzyme inhibition by phenylpyruvate	156
35	Dixon plot of enzyme inhibition by L-cysteine	158
36	Dixon plot of enzyme inhibition by L-proline	160
37	Lineweaver-Burke plot of enzyme inhibition by aminoxyacetate	162

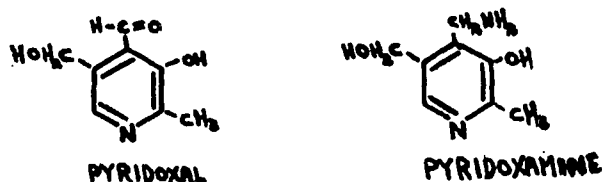
LIST OF ABBREVIATIONS

PLP	Pyridoxal-5'-Phosphate
PMP	Pyridoxamine-5'-Phosphate
DTNB	5,5'-Dithiobis(2-Nitrobenzoic Acid)
PCMB	p-Chloromercuribenzoate
AMP	Adenosine Monophosphate
Gl-1-Ph	Glucose-1-Phosphate
UDPG	Uridinediphosphoglucose
TCA	1. Tricarboxylic Acid 2. Trichloroacetic Acid
DPN(H)	Diphosphopyridine Nucleotide (Reduced)
DTT	Dithiothreitol
LDH	Lactate Dehydrogenase
GLDH	Glutamate Dehydrogenase
EDTA	Ethylenediamine Tetraacetate
SDS	Sodium Dodecyl Sulfate
TRIS	TRIS(hydroxymethyl) aminomethane

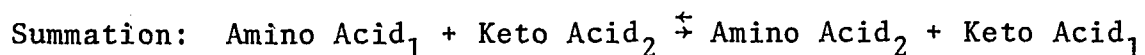
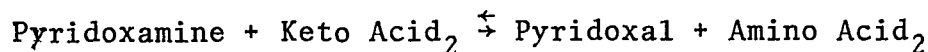
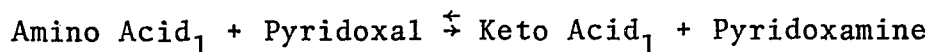
**INTRODUCTION**

TRANSAMINATION

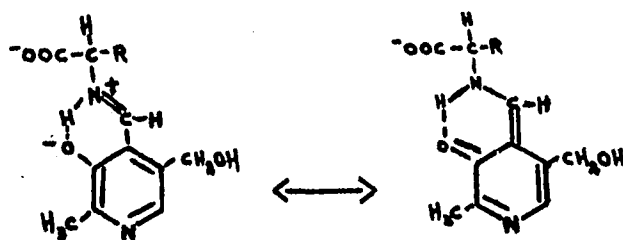
In 1945, Snell demonstrated that pyridoxal was converted to pyridoxamine by autoclaving it with a variety of amino acids. The reaction was completely reversible.<sup>1</sup>



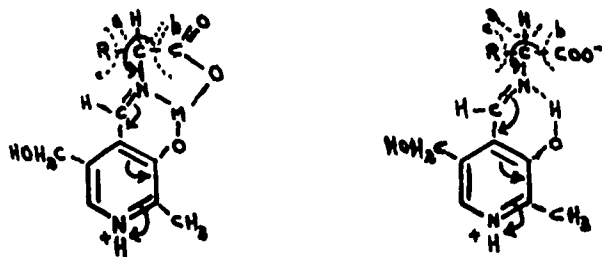
This chemical transamination reaction led to the suggestion that pyridoxal and pyridoxamine might serve as amino group carriers in vivo by catalyzing the following coupled reaction pair:



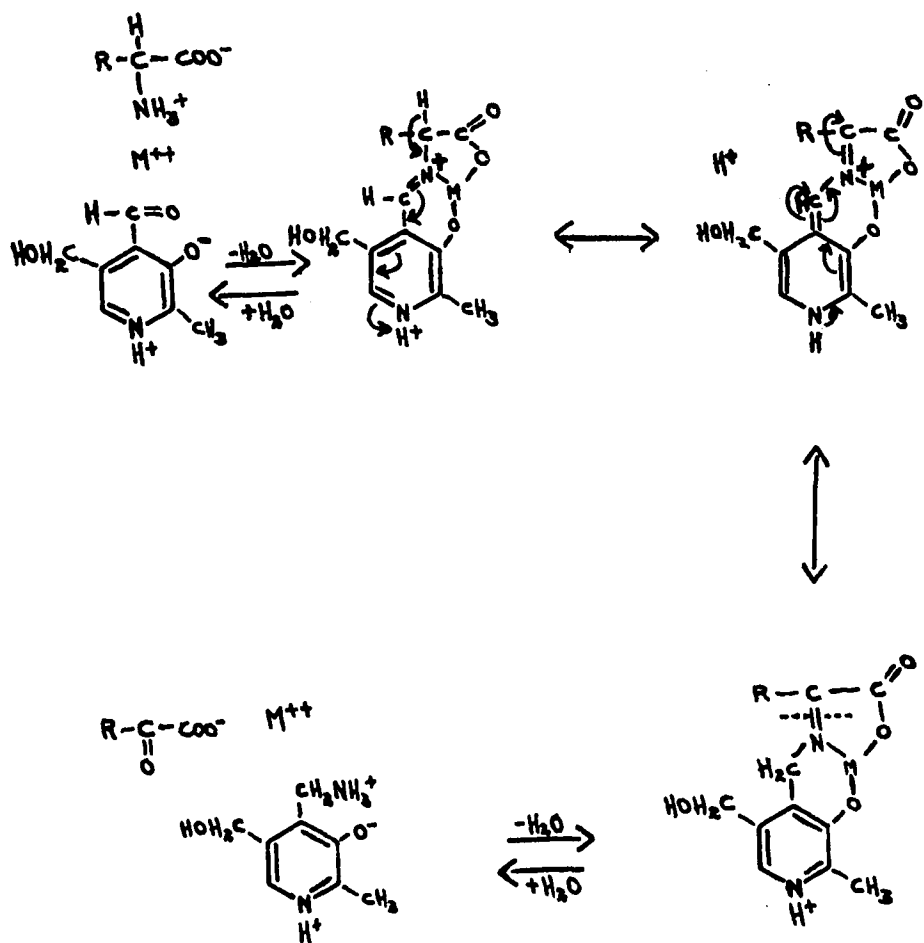
Further studies showed that it was the 5'phosphorylated derivatives of pyridoxal and pyridoxamine that were the active metabolites in enzymatic transamination.<sup>2,3</sup> In the non-enzymatic reaction, metal ions were found to accelerate the transamination reaction between pyridoxal and amino acids.<sup>4</sup> During the course of the transamination reaction, a distinct yellowing of the solution occurs which was demonstrated by spectrophotometric studies to be due to imine or Schiff base formation between pyridoxal or its phosphate and amino acids. Later studies showed the equilibrium to greatly favor imine formation.<sup>5</sup> In neutral aqueous solution the imines exist in the following resonance and tautomeric structures:



These findings confirmed the previously postulated suggestions that imine formation was a necessary intermediate in the course of both non-enzymatic and enzymatic transamination.<sup>6,7</sup> Studies with pyridoxal analogues demonstrated that the minimum structural requirement for effective catalysis of non-enzymatic transamination is a heterocyclic nitrogen or electronically similar nitro group, the formyl group, and a phenolic group ortho to it.<sup>8,9</sup> Formation of an imine between pyridoxal and an amino acid results in a conjugated system of double bonds that acts as an "electron sink", which in turn, weakens the bonds a,b, and c of the alpha carbon atom, with a resultant shift of electrons towards the electrophilic heterocyclic nitrogen. Labilization of the C-H bond activated the amino acid for transamination. The system of conjugated double bonds is maintained in the planar configuration necessary for electron withdrawal by hydrogen bonding between the imine nitrogen and phenolic oxygen, or in the case of the metal catalyzed reaction, by chelate formation of 5 and 6 membered rings. The metal ion also serves as an electron sink. These interactions are illustrated in the structures below.<sup>10</sup>

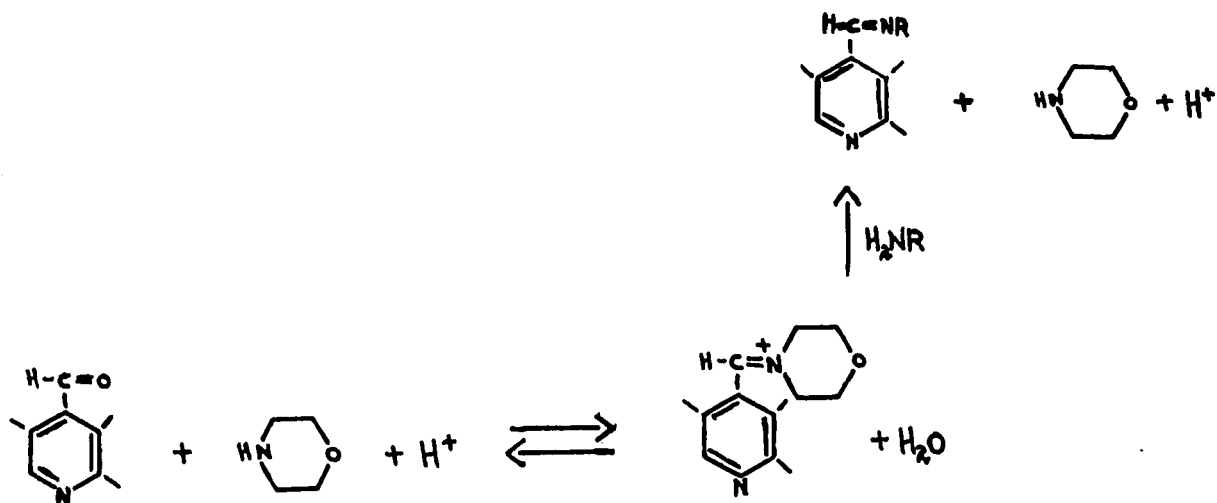


The demonstration of the central role of pyridoxal in the catalysis of transamination led finally to proposals of transamination mechanisms both in the presence<sup>8</sup> and absence<sup>11</sup> of metal ions. Except for the presence of the chelate structure, both are essentially the same. The metal catalyzed non-enzymatic reaction is illustrated below:



The mechanism features labilization of the alpha hydrogen of the aldimine, formation of a semiquinoid intermediate, and subsequent protonation on the formyl carbon to form a ketimine intermediate, followed by hydrolysis to the keto acid and pyridoxamine. The reaction is fully reversible and depends only on the concentration of amino and keto acid. Coupling of two such half reactions results in the overall transamination described earlier between different amino acid and keto acid pairs.

Enzymatic transamination proceeds at a rate  $10^7 - 10^8$  times faster than the non-enzymatic reaction.<sup>12,13</sup> Studies of pyridoxal phosphate (PLP) semicarbazone formation have shown the reaction to be catalyzed by amines. Since secondary amines such as morpholine are even more effective catalysts, the reaction must, therefore, proceed through a reactive, cationic Schiff base intermediate which is structurally similar to a protonated Schiff base.<sup>12</sup>



In all PLP enzymes so far investigated, the carbonyl group does not exist free, but is bound in an aldimine Schiff bond linkage with an  $\epsilon$ -NH<sub>2</sub> group of a lysine at the active center of the apoenzyme.<sup>14</sup> Reduction with borohydride followed by acid hydrolysis yields  $\epsilon$ -N-pyridoxyl lysine. The first step in enzymatic transamination, therefore, must be a transaldimination whereby the internal aldimine linkage is displaced by the amino group of the substrate.<sup>15</sup> Transaldimination proceeds in two steps; the formation and breakdown of a tetrahedral addition product. In order to account at least in part for the tremendous rate accelerations of the enzymatic transaldimination over the non-enzymatic reaction, an enzyme promoted addition of a proton to the internal Schiff base must be postulated.<sup>12</sup> Other factors, such as steric and electronic distortions undoubtedly also play a role.

The slow rate determining step of both non-enzymatic<sup>16</sup> and enzymatic<sup>17</sup> transamination is the prototropic shift between PLP-aldimine and pyridoxamine phosphate (PMP) ketimine. The rate of transamination between  $\alpha$ -amino phenylacetic acid and pyridoxal is greatly accelerated by an imidazole - imidazolium buffer which catalyzes this prototropic rearrangement by a concerted general acid - base mechanism.<sup>18</sup>



spectrum, a different amino acid content and is immunologically quite distinct from the anionic cytoplasmic isozyme. The Michaelis constant of the cytoplasmic enzyme for aspartate is about one order of magnitude larger than for ketoglutarate, whereas the opposite is true for the mitochondrial enzyme. The apoenzyme of each isozyme is capable of catalyzing reversible transamination between pyridoxal or pyridoxamine (not PLP and PMP) and the normal amino and keto acid substrates. The mitochondrial apoenzyme, however, is specific only for oxaloacetate - ketoglutarate is ineffective. In addition, phosphate ions are obligatory for activity. The cytoplasmic apoenzyme utilizes either keto acid and is inhibited by phosphate. Differential sensitivities to heat, pH, urea and PCMB titration also distinguish between the two isozymes.<sup>22</sup>

The isozymes exhibit still greater complexity. Each isozyme contains several subforms; the cytoplasmic ones have been most intensely studied.<sup>13</sup> There are four separable cytoplasmic subforms designated alpha, beta, gamma and delta. The  $\alpha$  and  $\beta$  forms can be converted into the  $\gamma$  and  $\delta$  forms by treatment with ammonium sulfate at high pH.<sup>23</sup> No differences can be detected in the immunochemical properties, amino acid composition, peptide maps, molecular weight or PLP content. Each subform has a MW of 93,000 and consists of two identical subunits.<sup>24</sup> The subforms do differ in the rate of recombination between apoenzyme and PLP, in specific activity, and in the mode of binding of the coenzyme.

The alpha subform binds the coenzyme in the active mode characterized by spectral absorption peaks at 362 m $\mu$  in basic medium and 430 m $\mu$  in acid. The alpha subform reacts with carbonyl reagents, engages in reversible transamination with amino acid substrates, reacts with borohydride to produce an inactive, covalently linked enzyme - coenzyme reduced secondary amine. The active alpha enzyme, therefore, contains PLP bound as an internal aldimine to a protein amino group. The less active subforms contain increasing amounts of material with an absorption peak at 340 m $\mu$ . Their spectral properties are not affected by pH, and they do not react with carbonyl reagents, substrates or borohydride. Resolution, however, removes stoichiometric amounts of PLP, as in the active subform. The PLP, therefore, is probably bound as a substituted aldamine in the inactive subforms, as has been postulated for the mode of binding of PLP in phosphorylase.<sup>25</sup> That this difference in the mode of binding of the coenzyme in the various subforms is a consequence and not a cause of the electrophoretic differences is demonstrated by the fact that they all retain their characteristic electrophoretic mobilities even after the coenzyme has been removed.<sup>13</sup> The subforms may, therefore, be considered as "conformation isomers" whose tertiary structure determine the nature of the apoenzyme - coenzyme covalent linkage. The fact that the four subforms can be isolated from a single pig heart excludes the possibility that the heterogeneity arises from different animals.

The detailed mechanism of the aspartate aminotransferase reaction has been investigated by steady state kinetics, spectrophotometric and equilibrium studies with substrates and substrate analogues, and fast reaction kinetics. All of these approaches have substantiated the classical Snell-Braunstein shuttle mechanism and have elucidated the nature of the reaction intermediates. The studies of Velick and Vavra<sup>17</sup> and Jenkins<sup>26-30</sup>, have shown that only binary complexes of aldehydic enzyme with amino substrates and aminic enzyme with keto substrates are active. Only the non-protonated aldimine enzyme (with the phenolic proton removed) reacts with amino acid substrates, the pKa for this protonation being 6.2. Keto acid substrates and dicarboxylic acids of similar size and configuration act as competitive inhibitors of the amino acids by forming inactive abortive complexes with the protonated aldimine enzyme. These dicarboxylic acids also bind to the unprotonated aldimine enzyme less well and in addition, bind quite well to the aminic enzyme. The amino acid substrates, however, do not form abortive complexes with the aminic enzyme. Binding of keto acid substrates and dicarboxylic acid inhibitors to the protonated enzyme results in a shift upward of the aforementioned pKa, which explains why velocity vs pH curves exhibit a pKa dependence on substrate concentration, the pKa's always substantially higher than 6.2. The dissociation constants of the aldimine enzyme with amino acid sub-

strates and substrate analogues does not display a pH dependence between pH 6-10. In addition, the  $V_{max}$  is constant in the region pH 6-10. This pH independence of enzyme-substrate intermediates indicates that the catalytic site is strongly shielded from the surrounding aqueous media.

Spectral studies of enzyme-substrate and substrate analog intermediates at high enzyme concentration have demonstrated absorption maxima at 330, 362, 430 and 492  $m\mu$ <sup>26-30</sup>. Comparison with spectra of model compounds suggests that absorbancy at 430 and 362  $m\mu$  is due to aldimine derivatives, absorbancy at 330  $m\mu$  is due to ketimine and tetrahedral addition complexes and absorbancy at 492  $m\mu$  is due to semiquinoid formation. Alpha-methyl aspartate, which participates in transaldimination with enzyme bound PLP, but which cannot form the ketimine intermediate, produces an enzyme-amino acid complex with peaks at 362 and 430  $m\mu$ .<sup>31</sup> Erythro- $\beta$ -hydroxy aspartate reacts rapidly forming the presumed semiquinoid intermediate absorbing at 492  $m\mu$ , followed by slow transformation to ketimine, and finally to pyridoxamine enzyme and keto acid.<sup>28</sup> Threo- $\beta$ -hydroxy glutamate behaves similarly.<sup>13</sup> Unfortunately, identification of these spectral peaks with specific reaction intermediates is not straightforward since as has already been indicated, the PLP enzyme and enzyme-dicarboxylic acid abortive complexes also absorb at 362 and 430  $m\mu$  and the PMP enzyme absorbs at 330  $m\mu$ .

ORD studies<sup>32</sup>, however, have been able to distinguish between enzyme spectral peaks and those due to enzyme-substrate complexes resulting from transaldimination, since the former are associated with strong positive Cotton effects whereas the latter are not and may even produce negative Cotton effects. This technique has allowed the assignment of the various absorption peaks to various intermediates along the reaction pathway to be made with greater confidence.

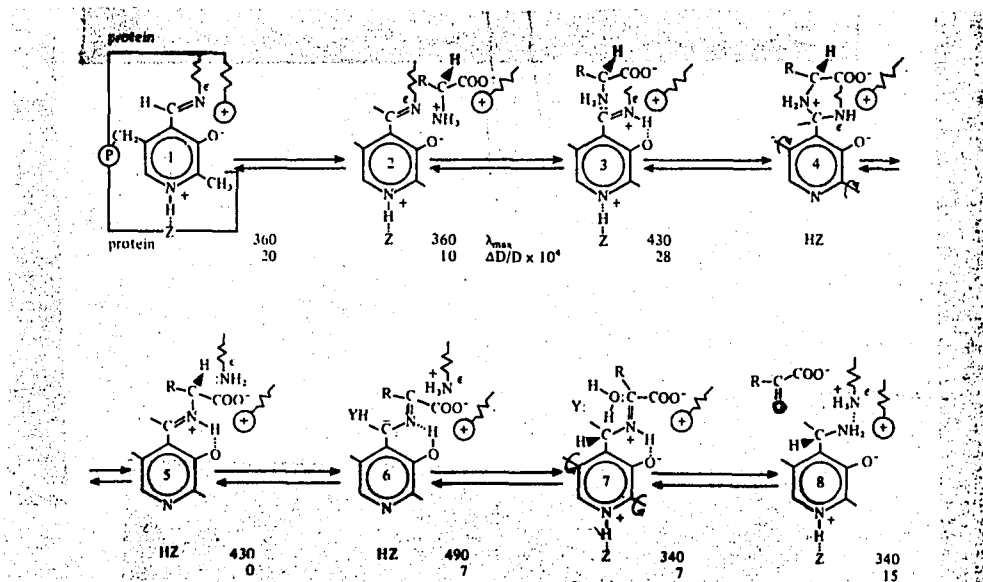
Fast reaction kinetics experiments, in addition to determining the rate constants of the several steps in the reaction mechanism, have also demonstrated that the intermediates with spectral peaks of 430, 362 and 492 m $\mu$  are on one side of the rate controlling step, and the intermediates with absorption at 330 m $\mu$  are on the other side.<sup>13</sup>

Chemical modification of the enzyme has been quite fruitful in implicating (or not implicating) various amino acid residues as components of the catalytic site. Photo-oxidation of the apoenzyme<sup>33</sup> or treatment with the difunctional reagent, 3-bromopropionyl chloride,<sup>34</sup> results in disappearance of one histidine residue and consequent 100% loss of activity. Dinitrodifluorobenzene crosslinking of the lysine residue that normally reacts with PLP to a nearby tyrosine,<sup>34</sup> places this tyrosine near the active site and supports earlier studies that implicated a tyrosine residue as necessary for activity.

In addition to the lysine residue engaged in aldimine linkage, a nearby second lysine has also been implicated by acetylation studies as part of the active site.<sup>35</sup> Five cysteine residues per monomer are present in the enzyme. Two residues react rapidly with -SH group reagents causing no loss in enzymatic activity. The third thiol group reacts two orders of magnitude more slowly and its blocking by a large number of reagents including DTNB, PCMB, N-ethylmaleimide, sulfite and tetranitromethane results in essentially complete loss of activity.<sup>36</sup> Bromopyruvate can both alkylate this thiol group with concomitant inactivation of the enzyme and also act as a substrate.<sup>37</sup> The last two thiol groups react only under denaturing conditions. That thiol group III, however, is not part of the catalytic site, is shown by the fact that incorporation of one mole of cyanide into it to form the uncharged S-CN product results in retention of over 60% activity. Inactivation by the other reagents occurs apparently by producing bulky or charged substituents on thiol group III which interfere with the activity of the nearby catalytic site.

These intensive investigations into the structure and function of aspartate aminotransferase have resulted in the presentation of a detailed reformulation of the mechanism of transamination in which a stepwise, dynamic scheme of the interconversion of intermediates along the reaction pathway

is postulated.<sup>38</sup> This mechanism updates earlier detailed schemes by accounting for most of the known facts presented in this discussion and is shown below:



The essential feature of the mechanism is that the active site comprises two spatially distinct regions, one of which binds the coenzyme in the absence of substrate, while the other includes the substrate binding site and the catalytic groups that participate in the prototropic aldimine-ketimine rearrangement. Sequential steps in the mechanism are linked with sequential changes in the orientation of the coenzyme as it rotates between these two regions.

Stage I - Ordinary aldimines of PLP have pKa's between 10-11. The lowering of the pka to 6.2 in aspartate aminotransferase is explained by the combined effect of protonation of the heterocyclic nitrogen by a group Z on the protein and a positively charged group proximal to the phenolic oxygen.

Group Z is thought to be the tyrosine residue that reacts with difluorodinitrobenzene. The cationic group may be the lysine residue next to the one involved in the internal aldimine linkage.

Stage 2 - Binding of the substrate carboxylate group to the cationic group results in a rise in the pKa of the phenolic group to about 8. At the same time, neutralization of the substrate carboxylate group lowers its amino group pKa from 9.5 to 7.4.

Stage 3 - Proton transfer from substrate to coenzyme occurs. Protonation enhances the electrophilicity of the C=N bond. Neutralization of the phenolic anion lowers the pKa of the ring nitrogen.

Stage 4 - Nucleophilic attack by the substrate amino group to form a tetrahedral addition product follows. This can only occur if the nucleophile is in a plane perpendicular to the C=N bond. This is made possible by loss of the proton by the ring nitrogen to group Z, followed by rotation of the coenzyme about an axis through positions 2 and 5 of the ring.

Stage 5 - The protonated substrate-coenzyme aldimine intermediate forms.

Stage 6 - The  $\epsilon$ -amino group of lysine, acting as a general base, abstracts a proton from the  $\alpha$ -carbon of the substrate, producing a carbanion which is in resonance with the previously postulated semiquinoid intermediate.

Stage 7 - Proton donation by a general acid YH (possibly the essential histidine) to atom C'<sub>4</sub> produces a tetrahedral configuration which allows the ring to rotate back to its original position where the ring nitrogen is reprotonated. This lowers the pKa of the phenolic group and the phenolic hydrogen shifts to the ketimine nitrogen, thereby increasing the electrophilicity of the ketimine carbon. Group Y abstracts a proton from a molecule of water, and the Schiff base is hydrolyzed.

Stage 8 - A product keto acid is released. The amino group of PMP is unionized since it is positioned near two cationic groups. It is therefore capable of reacting with the ketosubstrate in the reverse half reaction.

The mechanism explains several previously puzzling facts. In model systems, positively charged Schiff bases are most reactive, whereas in the enzyme, activity is present at pH's where only an ionized phenolic group is possible (pKa 6.2). In the mechanism, protonation does occur, but only subsequent to binding of the substrate. In addition, the mechanism demonstrates why no transamination occurs between the coenzyme and the lysine residue forming the internal aldimine. Finally, the pH independence of V<sub>max</sub> and enzyme-substrate dissociation constants can be explained, since none of the steps in the sequence involves

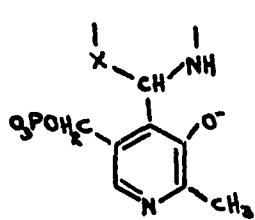
acceptance or release of protons from or to the medium - all exchanges occur between intermediates in the reaction. Although some aspects of this mechanism may be peculiar only to aspartate aminotransferase, its essential features are probably common to all transaminases and it may have wider significance by serving as a model for other enzyme mechanisms where alternation in the mutual orientation of interacting components in enzyme substrate complexes may explain otherwise incompatible facts.

Alanine aminotransferase (EC. 2.6.1.2) has been investigated with far less vigor, probably because there is considerably less of it in most tissues under normal conditions.<sup>39</sup> The enzyme has been isolated from pig heart,<sup>40</sup> rat liver<sup>41</sup> and beef heart.<sup>42</sup> Alanine aminotransferases are found in both cytoplasmic and mitochondrial varieties in both heart and liver with more than 90% of the total of cytoplasmic origin.<sup>40,43</sup> The mitochondrial enzyme is both labile and difficult to solubilize; the purified enzyme from both tissues is the cytoplasmic one. With the rat liver enzyme no amino or keto acids tested other than the normal substrates gave any activity, although a number were inhibitory.<sup>44</sup> PCMB is a potent inhibitor. The kinetics of the forward and reverse reaction fit the previously proposed shuttle mechanism of other transaminases.<sup>45</sup> Aminoxyacetate inhibits the reaction on an almost stoichiometric basis by combining with the PLP form of the enzyme. It is competitive

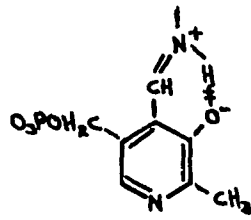
with amino acid substrates and uncompetitive with keto acid substrates. Maleate and acrylate inhibit weakly by binding to both forms of the enzyme. The enzyme exhibits an absorption maximum at 430 m $\mu$  at pH 5 and at 335 m $\mu$  at pH 8.3, with the former peak decreasing and the latter increasing, as the pH is raised from acidic to basic values. A pKa of 7.3 for this shift can be determined.<sup>41</sup> Reaction with aminooxyacetate shifts the 430 m $\mu$  peak to 370 m $\mu$  as a result of oxime formation.<sup>46</sup> The molecular weight of the enzyme is 114,000 and appears to exist in at least two closely related subforms as judged by mobility on acrylamide gel.<sup>46</sup> Two moles of PLP and 23-30 titratable -SH groups per 114,000 daltons can be detected.<sup>41</sup> Amino acid analysis indicates 34 half-cystine residues. Reaction of the first seven or eight -SH groups with PCMB or DTNB results in no loss of activity, after which there is a proportional loss of activity over the next 6-9 -SH groups reacting with PCMB. Complete resolution of the PLP from the enzyme with PCMB and  $(\text{NH}_4)_2\text{SO}_4$  is possible, although only 40% reconstitution can be achieved.\* L-Proline is a competitive inhibitor of the PLP enzyme and reacts to form a quaternary, cationic Schiff base with an absorption maximum at 380 m $\mu$ .<sup>47</sup> The various spectral forms of the coenzyme and their absorption maxima as postulated by Segal are illustrated on the following page:<sup>41,46,47</sup>

---

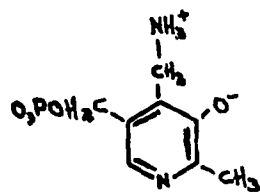
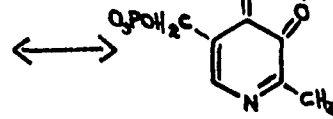
\*Treatment with borohydride results in complete loss of activity.



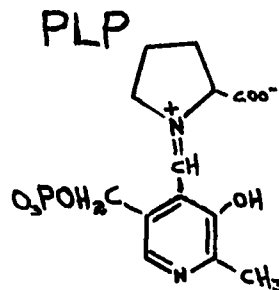
ALDIMINE 335 m $\mu$   
BASE



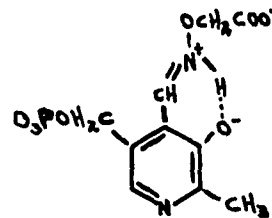
PROTONATED ALDIMINE 430 m $\mu$   
ACID



325 m $\mu$   
PMP



380 m $\mu$   
PLP-PROLINE



370 m $\mu$   
PLP-AMINOXYACETATE

Unlike aspartate aminotransferase, the unprotonated aldimine (362 m $\mu$ ) does not occur in this enzyme.

The beef heart enzyme was isolated in a very low yield and no attempt at physical or chemical characterization was made.<sup>42</sup> Kinetic studies indicated that the reaction mechanism is the familiar binary shuttle type. At high concentrations, both alanine and glutarate are inhibitory. The keto acids, even at concentrations 100 fold greater than their  $K_m$ 's, were not. Product inhibition studies showed the product amino acid to be a competitive inhibitor with respect to substrate amino acid and noncompetitive with respect to substrate

keto acid. Glutarate is a noncompetitive inhibitor of all four substrates, indicating it combines with both PLP and PMP forms of the enzyme, although it binds 10 times more tightly with the PLP form. Maleate is an uncompetitive inhibitor with respect to alanine and competitive with  $\alpha$ -ketoglutarate, indicating it combines only with the PMP enzyme.  $\alpha$ -Aminobutyrate is non-competitive with both alanine and  $\alpha$ -ketoglutarate, indicating it combines with both forms of the enzyme. Unlike the rat liver enzyme,  $\alpha$ -amino butyrate could act as a substrate for the beef heart enzyme, but only at 2% of the rate with alanine.

Pig heart alanine aminotransferase has a subcellular distribution similar to that in the liver. The cytoplasmic enzyme has been obtained in high yield.<sup>40</sup> It has a molecular weight of  $115,000 \pm 15,000$  and a  $S_{20}$  of about 6. It has a similar activity and absorption spectrum vs pH dependence as the liver enzyme, with a pH optimum of about 8 and a pKa for the spectral shift of 7.3. The reversible shuttle mechanism explains the kinetics adequately. Unlike the beef heart enzyme, pyruvate was found to competitively inhibit the amino acid substrates by binding to the PLP form of the enzyme, but only at very high concentrations ( $K_i = 30\text{mm}$ , which is about 100x's  $K_m$ ). Only  $\alpha$ -aminobutyrate besides alanine had any substrate activity (about 2% that of alanine), although a large number of amino acids acted as weak competitive inhibitors. Formate was found to stimulate activity

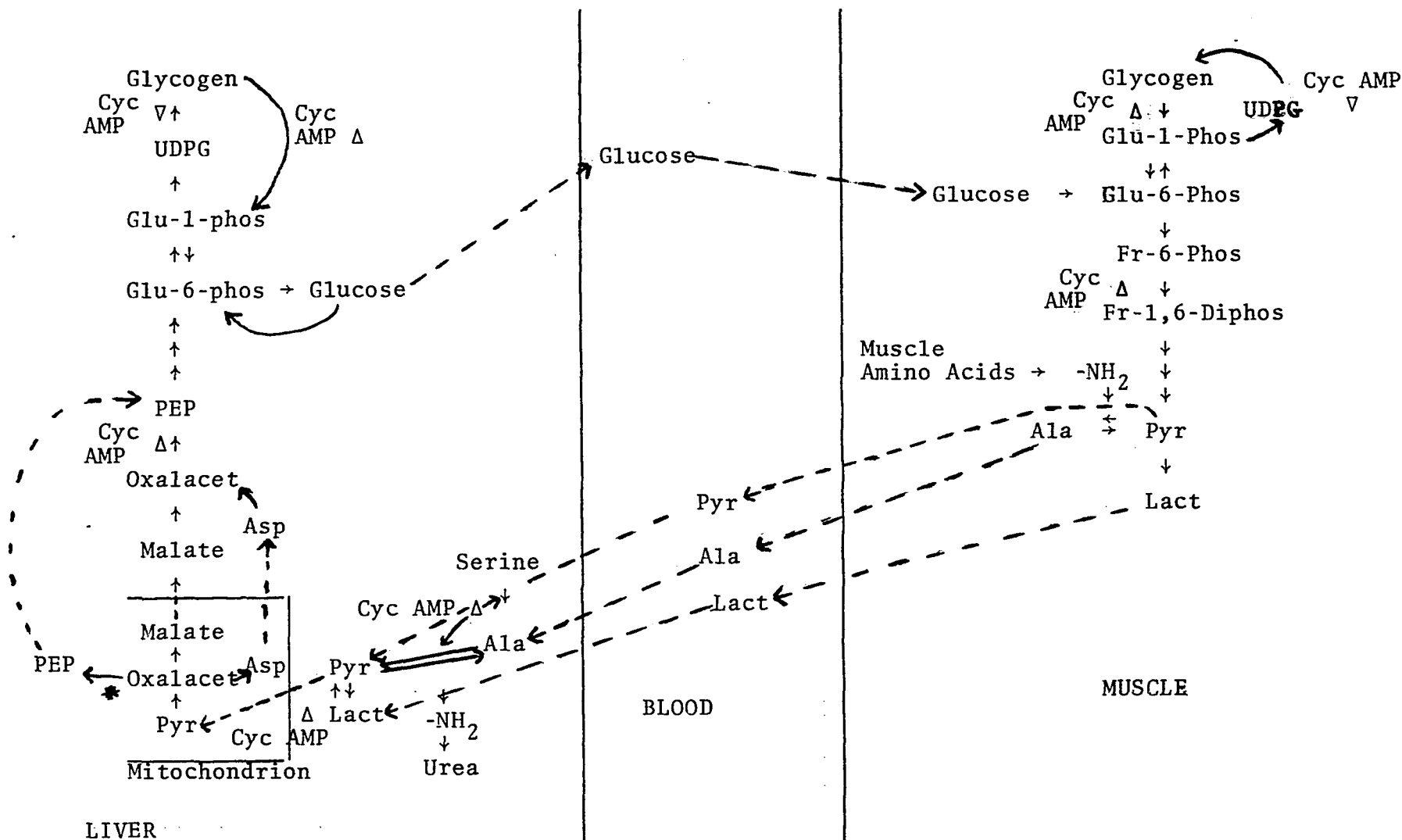
in the direction of glutamate and pyruvate formation but to inhibit it in the opposite direction. Other monocarboxylic acids were inhibitory in both directions. This was interpreted to mean that formate activates by binding to the site that normally binds the  $\gamma$  carboxyl group of glutamate. The spectra of the enzyme in the presence of mixtures of amino and corresponding keto acid substrates exhibits peaks at 330, 360 and 490  $m\mu$  which presumably correspond to several enzyme substrate complexes in equilibrium.<sup>48</sup> These peaks are remarkably similar to those observed with aspartate aminotransferase under comparable conditions. Finally, when examined by starch gel electrophoresis, the enzyme appeared heterogeneous, although only one distinct band of activity could be observed, leading to the conclusion that the smearing was due to impurities rather than the presence of subforms.

Although the physical and chemical properties of alanine aminotransferase are not especially unique, its role in the regulation of alanine and pyruvate levels under different physiological conditions is probably of critical importance to gluconeogenesis, as will be shown in the following section.

GLUCONEOGENESIS

Amino acids account for greater than 50% of total gluconeogenic carbon and alanine is the principle amino acid precursor of glucose.<sup>49,50</sup> In livers from fasted rats, perfused with a mixture of amino acids, glucose production is half-maximal at normal amino acid concentrations and approaches saturation at three times normal concentrations. In livers from fed rats, maximum gluconeogenesis from alanine is reached when the perfusate concentration is twenty times the physiological level and the increase in the gluconeogenic rate is essentially linear with increasing alanine concentration. With high concentrations of alanine, hepatic transamination becomes rate limiting for gluconeogenesis. Since alanine is the principal amino acid released by muscle,<sup>51</sup> the rate of release of alanine from peripheral tissues can, therefore, be most important in controlling hepatic gluconeogenesis. These facts support the existence of an alanine cycle,<sup>50,51,99</sup> which together with the well known Cori cycle,<sup>52</sup> account for the flow of metabolites from peripheral tissues to the liver and unifies glycolysis, glycogenolysis, glycogenesis and protein catabolism in a harmonious cyclical pattern (See Diagram).

In addition, glycerol (not shown) derived from lipolysis also contributes to gluconeogenesis.



### The Cori and Alanine Cycles

Cyc Amp  $\Delta$  - Enzyme level or activity involved in the reaction is increased by cyclic AMP.

Cyc AMP  $\nabla$  - Reduced by cyclic AMP.

The mechanisms, where known, are considered in the text below.

\*Oxalacetate  $\rightarrow$  PEP occurs in guinea pig and rabbit liver to a significant extent.<sup>100,101</sup>

The conversion of alanine to glucose is enhanced by glucagon and epinephrine by mediating an increase in the level of cyclic 3',5'-AMP.<sup>49</sup> Exogenous cyclic 3',5'-AMP produces a similar effect. These agents also act to increase gluconeogenesis from pyruvate and lactate. In the case of pyruvate, this stimulation is thought to occur at the level of increased transport into the mitochondria<sup>53</sup> and increased synthesis of the gluconeogenic enzyme, phosphoenolpyruvate carboxykinase (EC 4.1.1.32).<sup>54</sup> The mechanism by which enzyme synthesis is induced by cyclic 3',5'-AMP is not known, but Langan's demonstration that the nucleotide activates a specific histone kinase points to a mechanism whereby histone phosphorylation could act to cause conformational changes in histone structure with consequent derepression of portions of chromosomal structure and resultant increased transcription rates.<sup>55,56</sup> More recently, a posttranscriptional site of action of cyclic AMP has been postulated for the induction of PEP carboxykinase.<sup>102</sup>

Increased glycogenolysis<sup>57</sup> and decreased glycogen synthesis<sup>58</sup> are also mediated by cyclic AMP (and the hormones that stimulate its production in the various organs) by conformationally activating a kinase that activates phosphorylase kinase which, in turn, converts the physiologically inactive phosphorylase b to phosphorylase a.<sup>59</sup> This same cyclic 3',5'-AMP dependent kinase converts the physiologically active I form of glycogen synthetase to the inactive D form.<sup>60</sup>

Other enzymes involved in or related to carbohydrate metabolism whose activity or levels are raised by cyclic 3',5'-AMP are muscle phosphofructokinase<sup>61</sup> and liver serine dehydratase.<sup>62</sup>

The stimulation of enzymes in muscle which favor glycolysis and the stimulation of enzymes and processes in liver which favor gluconeogenesis by a substance whose level is increased by hormones known to raise gluconeogenic rates, together with the fact that gluconeogenesis in muscle is insignificant, supports the thesis that the direction of metabolite flow is as outlined in the diagram above. It may safely be assumed that whatever physiological conditions raise the level of cyclic 3',5'-AMP in these tissues activates the rates of the Cori and alanine cycles over basal values.

As for the stimulation of gluconeogenesis from alanine by cyclic AMP, the site of action is unknown but the following observations are at least indicative of certain conclusions. At high alanine concentrations in the rat liver perfusate, where hepatic transamination to pyruvate becomes rate limiting for gluconeogenesis, a higher concentration of alanine is found intracellularly than extracellularly in the presence of glucagon than in controls.<sup>49,50</sup> This "crossover" is indicative of active transport of alanine being under cyclic AMP mediated control, since a similar crossover occurs between the levels of pyruvate and PEP in glucagon treated versus control livers, the latter effect being stimulated by cyclic AMP induction of PEP carboxykinase and increased transport of pyruvate across the mitochondrial membrane. At physiological levels of alanine in the perfusate, this

crossover between intra and extracellular levels is not seen, probably because of the rapid utilization of the intracellular alanine, which keeps its concentration low despite its faster entry. With regard to the transamination step itself, glucagon and cyclic 3',5'-AMP are stimulatory at high alanine concentrations. Mallette et. al<sup>50</sup> feel that this occurs because of the lowering of pyruvate which reduces the back reaction and not through the stimulation or induction of alanine aminotransferase. However, other studies have shown<sup>39,44,63</sup> that hepatic cytoplasmic alanine and aspartate aminotransferase can be raised as much as eight fold over basal levels under gluconeogenic conditions, whereas the mitochondrial enzymes are either not affected or are only transiently affected under some, but not all, gluconeogenic conditions.<sup>43</sup> The cytoplasmic isozymes are the ones chiefly involved in the gluconeogenic pathway in rat liver since penicillamine, which inhibits cytoplasmic aminotransferases and does not inhibit mitochondrial ones, also inhibits gluconeogenesis from amino acids.<sup>63</sup> The conditions which brought about these increased enzyme levels included a low carbohydrate-high protein diet, alloxan induced diabetes and daily hydrocortisone injections. Low carbohydrate intake stimulates glucagon secretion, which in turn, raises cyclic 3',5'-AMP levels. The high protein level undoubtedly stimulates gluconeogenesis by mass action. The effect of

glucocorticoids is complex. Adrenalectomy has no effect on the ability of glucagon to stimulate cyclic 3',5'-AMP production, whereas it increases the response to epinephrine.<sup>49,64</sup> However, in both cases, gluconeogenesis from lactate is severely reduced in adrenalectomized animals and can be restored to near normal by injection of dexamethasone. Exogenously added cyclic AMP stimulated gluconeogenesis in these adrenalectomized animals only at very high concentrations.<sup>65</sup> These results would indicate that glucocorticoids exert a permissive effect on the action of cyclic AMP. However, in the case of the inducible rat liver enzymes PEP carboxykinase and tyrosine transaminase, the effect of dexamethasone has been shown to be additive and even synergistic to that of cyclic AMP in organ and tissue cultures, thereby complicating any simple interpretation.<sup>102</sup>

The glucocorticoids also stimulate gluconeogenesis from amino acids,<sup>66</sup> although in this case a permissive effect on the action of cyclic AMP was not demonstrated under the non-physiological conditions employed. Finally, glucocorticoids act to stimulate protein catabolism in peripheral tissues, leading to an increase in the rate at which alanine is made available for conversion to glucose in the liver.<sup>67</sup>

Insulin lowers cyclic AMP levels in the liver,<sup>49</sup> although it has no such effect in muscle.<sup>68</sup> Conversely, alloxan diabetes raises cyclic AMP levels and this can be reduced to normal by injection of insulin.<sup>69</sup> The mechanism by which

this occurs was unknown until recently as it affects neither adenylyl cyclase<sup>70</sup> nor phosphodiesterase<sup>71</sup> in broken cell preparations. However, insulin does act in vivo on liver in normal, diabetic and hypophysectomized rats and in vitro on fat cells in culture to increase the activity of a membrane-bound, high affinity cyclic AMP phosphodiesterase.<sup>103,104</sup>

In their excellent review, Robison et al.<sup>72</sup> suggest that insulin may stimulate the conversion of cyclic AMP to another metabolite which would oppose its action. It is now thought that insulin may also stimulate cyclic GMP synthesis, which acts as a cyclic AMP antagonist in many systems.<sup>105</sup>

In summary then, de novo synthesis of hepatic alanine aminotransferase is stimulated many fold under conditions where the level of or the sensitivity of target systems to cyclic 3',5'-AMP is enhanced, strongly suggesting that this gluconeogenic enzyme is under hormonal regulation in the liver.

The central role of alanine in gluconeogenesis, together with the dramatic rise in hepatic aminotransferase levels under just those conditions where alanine utilization by the liver is maximized, points to the possibility that alanine aminotransferase levels in peripheral tissues, especially muscle, may be regulated by hormonal controls as well. Although amino acid levels in the blood are most certainly determined in part by diet and protein catabolic activity, the conversion of pyruvate to alanine in muscle and its release is a process that suggests itself to be

one that is under strict hormonal control. The work of Bailin and Lukton<sup>73</sup> bears strongly on this suggestion. These workers isolated a phosphorylase a - alanine aminotransferase complex from rabbit muscle. The enzymes coeluted from DEAE and G-200 columns and were subject to reciprocal controls. Glutamate and pyruvate, the transaminase substrates, inhibited transglucosylase activity. Conversely, glycogen and gl-1-Ph, substrates, glucose and UDPG, inhibitors, and 5' AMP, the positive effector of phosphorylase, inhibited the transaminase activity. Inhibition by gl-1-Ph was competitive with both transaminase substrates. 5' AMP inhibited only at temperature below 37°C, and it acted non-competitively. At 37°C, 5' AMP reversed the inhibitory effects of gl-1-phos, glycogen, UDPG and glucose on the transaminase activity. These observations indicate the existence of a protein-protein complex whereby the binding of ligands by one enzyme conformationally affects the activity of the second. The physiological purpose for such a complex is not known, but the suggestion of Krebs<sup>74</sup> that phosphorylase serves as a repository for PLP raises the possibility that transfer of the coenzyme between PLP enzymes occurs via protein-protein interaction. Another possibility is that each enzyme acts to dampen the activity of the other in vivo. During the initial periods of active glycogenolysis, when the phosphorylase substrate levels are high, the energy needs of the cell would require that the end product of glycolysis, pyruvate, be

shunted into the TCA cycle rather than be transaminated. At the same time, the high pyruvate levels would tend to moderate glycogenolytic activity. During periods of starvation, when glycogen levels are low, transamination would be favored, followed by release of alanine to the liver through the blood where it is eventually converted to glucose. During refeeding, and periods of glycogen synthesis, the raised glucose and UDPG levels, by inhibiting transamination from pyruvate, would decrease gluconeogenesis via alanine, which need would now be markedly reduced.

This postulated scheme of feedback inhibition modulated via protein-protein interaction is quite unique and deserves further investigation. It must be added that highly purified phosphorylase normally isolated by multiple recrystallization contains only minute traces of alanine aminotransferase activity.<sup>75</sup>

All of the observations noted above point to the fact that the purification and characterization of muscle alanine aminotransferase may be quite important for the development of a firmer understanding of the relationship between glycolytic and gluconeogenic pathways in mammalian systems.

**MATERIALS AND METHODS**

## Materials

### Enzymes and other proteins:

Lactate Dehydrogenase (beef heart) and Glutamate Dehydrogenase (beef liver) were obtained from Sigma Chemical Co. Prior to use in assays, the enzymes were dialyzed against .05M potassium phosphate, pH 7.5, to remove excess  $(\text{NH}_4)_2\text{SO}_4$ . Phosphorylase "b" was prepared by the method of Fischer and Krebs<sup>76</sup> and recrystallized three times. Phosphorylase "a" was prepared by the method of Cori et.al.<sup>77</sup> and was recrystallized three times. Bovine serum albumin (crystalline) and ovalbumin were from Pentex. Pepsin and chymo-trypsinogen were obtained from Worthington. For preparation of alanine aminotransferase, frozen rabbit muscle, Type I, deboned, from Pel-Freeze Corp. was used.

### Reagents:

L- $\alpha$ -alanine was obtained from Nutritional Biochemicals Co. Sodium pyruvate, glutamic acid and  $\alpha$ -ketoglutaric acid and DPNH, were obtained from Sigma. PLP, 5'AMP, DTT, PCMB, DTNB, 2-mercaptoethanol and all other keto acids were obtained from Calbiochem. Enzyme grade  $(\text{NH}_4)_2\text{SO}_4$ , guanidine-HCl and sucrose, as well as all other amino acids were obtained from Schwarz-Mann. Aminoxyacetic acid and sodium borohydride came from K & K Laboratories. All other reagents used were the purest grades commercially obtainable.

Acrylamide, N, N'-methylene bisacrylamide, N,N,N,N'-tetramethylethylenediamine (TEMED), ammonium persulfate, riboflavin and other chemicals used for disc gel electrophoresis came from Canalco. Ampholine pH 3-10 and pH 7-9 used in

isoelectric focusing were from LKB.

#### Column Chromatography:

Sephadex G-200 and DEAE-Sephadex A-50 was obtained from Pharmacia, Inc. Hydroxylapatite, dry powder, came from Bio-Rad Corp.

#### Instrumentation:

For all pH determinations, a Radiometer Model TTT1C pH meter was used. Kinetic assays were performed in a water jacketed, Beckmann DU spectrophotometer with Gilford attachment. Absorption spectra were obtained with a Cary Model 14 spectrophotometer. PLP determinations were done with an Aminco-Bowman recording spectrofluorometer. Equipment for disc gel electrophoresis and isoelectric focusing was from Canalco. Preparative isoelectric focusing was performed in the 110 ml column designed by LKB. Fractions from column chromatography were collected in an Isco fraction collector model 820 with double channel UV lightsource set at 280 m $\mu$  and elution profile determined with an Isco chart recorder. Preparative centrifugation was done with the Sorvall model RC2-B. Analytical ultracentrifugation was performed on a Spinco model E analytical ultracentrifuge with Schlieren and Rayleigh interference optics.

#### Methods:

##### Chemical and Physical Characterization:

Tryptophan and tyrosine were determined by dissolving the

enzyme in 6M guanidine HCl, .02M potassium phosphate, pH 6.5, and measuring absorbance at 280 m $\mu$  and 288 m $\mu$  according to the method of Edelhoch.<sup>78</sup> By solving the two simultaneous equations

$$\text{Ext. Coeff.}_{288} = N_{\text{TRP}} 4815 + M_{\text{TYR}} 385$$

$$\text{Ext. Coeff.}_{280} = N_{\text{TRP}} 5690 + M_{\text{TYR}} 1280$$

N and M, the numbers of moles of tryptophan and tyrosine, respectively, per mole of protein, can be determined.

PCMB titration was performed essentially according to the method of Boyer.<sup>79</sup> The enzyme was dialyzed against several changes of .02M potassium phosphate, pH 6.5, to remove EDTA and DTT. 1.5 ml was pipetted into a cuvette containing a micro spinning bar at a concentration of .193 mg/ml ( $1.75 \times 10^{-6}$  M for a molecular weight of 110,000). Two  $\mu$ l PCMB at  $1.32 \times 10^{-3}$  M in H<sub>2</sub>O was added; the solution mixed, and allowed to stand 20-30 minutes at room temperature. The change in optical density against a similarly treated blank at 255 m $\mu$  was noted and a 5  $\mu$ l aliquot was removed for assay under standard conditions (see Enzyme Assay Section). The process was repeated until enzyme activity was negligible. Then 5  $\mu$ l aliquots of PCMB were added at a time and the absorbance, corrected for dilution, was measured 20-30 minutes after each addition. Each 2  $\mu$ l addition of PCMB titrates approximately 1.0 SH group/mole enzyme. The same procedure was followed with the enzyme dissolved in 6M

guanidine-HCl except that aliquots were not removed for activity determinations.

PLP content was determined by a slight modification of the fluorometric method of Yamada et al.<sup>80</sup> 33.2  $\mu$ l and 66.4  $\mu$ l of a 0.90 mg/ml enzyme solution were diluted to 2.0 ml with H<sub>2</sub>O in two 15 ml pyrex centrifuge tubes. Two ml of 10% TCA was then added and the precipitate centrifuged at 27,000g. The supernatants were pipetted into 6 inch test tubes and extracted three times with equal volumes of ether. The ether was carefully removed and 2.0 ml of the aqueous phase were pipetted into 4 inch tubes. To these were added 20  $\mu$ l of 1M acetic acid, followed by 0.2 ml of 0.2M phosphate, pH 7.5, followed by 0.1 ml of .05M KCN. The mixture was heated to 50°C in a water bath for 30 minutes and then adjusted to pH 3.8 by adding 1.0 ml of 0.5M tartaric acid. After cooling to room temperature, the fluorescence intensity was determined on an Aminco-Bowman spectrofluorometer at an excitation wavelength of 325 m $\mu$  and an emission wavelength of 420 m $\mu$ . A standard curve was constructed by following the same procedure with 0.25, 0.5, 1.0 and 1.5 ml of a  $6 \times 10^{-7}$ M solution of PLP. Two ml H<sub>2</sub>O treated similarly served as the blank.

Reduction with NaBH<sub>4</sub>:

To an enzyme solution at 0.25 mg/ml in .05M phosphate, pH 7.5, was added 10  $\mu$ l of freshly prepared .05% NaBH<sub>4</sub>.

Aliquots were removed every minute, diluted 1:3000 in assay medium to stop the reaction, and assayed. Assuming 2 moles of PLP per mole enzyme, the molar ratio of  $\text{BH}_4^-$  to PLP was 125:1.

Attempted Resolution of PLP from Holoenzyme:

Method 1:

Method similar to that of Matsuzawa and Segal.<sup>41</sup> To 0.5 ml of a 0.47 mg/ml solution of enzyme dialyzed against .05M phosphate, pH 7.5, was added 0.1 ml of  $5 \times 10^{-3}$ M PCMB. After standing 30 minutes at 0°C, 200 mg of  $(\text{NH}_4)_2\text{SO}_4$  was added and the suspension centrifuged. The precipitate was washed with 1.0 ml of a saturated  $(\text{NH}_4)_2\text{SO}_4$  solution containing .01M DTT. It was then dissolved in 0.5 ml of .05M phosphate, .001M EDTA, .01M DTT, pH 7.5, dialyzed, and an aliquot removed for assay. For reconstitution, PLP was added to a final concentration of  $1 \times 10^{-4}$ M and incubated for 30 minutes at 30°C.

Method 2:

Method of Shaltiel, Hedrick and Fischer<sup>81</sup> for resolution and reconstitution of phosphorylase b.

To 0.1 ml of enzyme at 2.35 mg/ml in .05M phosphate, .001M DTT, .001M EDTA, pH 7.5, was added 0.4 ml of a solution containing 0.5M imidazole, 0.125M cysteine-HCl previously adjusted to pH 6.2 at 0°C with citric acid. After 1 hour at 0°C, the solution was warmed to room temperature and 0.5 ml

of a saturated  $(\text{NH}_4)_2\text{SO}_4$  solution was added. The suspension was centrifuged and the precipitate taken up in 0.4 ml phosphate-DTT-EDTA buffer, dialyzed and assayed.

Protein concentration was determined by the microbiuret method of Zamenhof.<sup>82</sup> Absorption was measured at 310 m $\mu$  and 390 m $\mu$  without correcting for the presence of DNA. Bovine serum albumin was used for the standard curve.

#### Disc Gel Electrophoresis:

##### Method 1:

Low pH method of Williams and Riesfeld.<sup>83</sup>

The gels were prepared according to the instructions of the Canalco manual. The separating gel contained 7.5% acrylamide in a 0.375M acetate buffer, pH 4.3. The stacking gel contained 2.5% acrylamide in a .0625M acetate buffer, pH 6.7. No sample gel was used. The separatory gel catalyst was 0.14% ammonium persulfate, the stacking gel catalyst .0005% riboflavin. The upper and lower electrode buffer was .035M  $\beta$ -alanine-acetate, pH 4.7. Protein in 10-30% sucrose was applied to the top of the stacking gel, allowed to enter at a current of 2 mamps/gel, and then the current was raised to 4-5 mamps/gel for 1 hour. The gels were removed from their tubes, stained for 1 hour in 0.5% Amido Black in 7% acetic acid, then destained electrophoretically in the Canalco Quick Gel Destainer and stored in 7% acetic acid.

Method 2:

High pH method of Davis.<sup>84</sup>

Gels were prepared as above except that the separating gel buffer was .375M Tris-HCl, pH 8.9, the stacking gel buffer was .0625M Tris-HCl, pH 6.7, and the electrode buffer was .038M glycine-Tris, pH 8.3. The separatory gel catalyst was .07% persulfate. Protein entered the gel at an initial current of 1 mamp/gel and was then raised to higher values as described in the Results section. Running time was also variable. Staining and destaining was as above.

SDS Gel Electrophoresis:

Electrophoresis was performed according to the method of Weber and Osborn.<sup>85</sup> Protein samples were preincubated at 37°C for 2 hours in .01M sodium phosphate buffer, pH 7.0, 1 % in SDS and 1 % in mercaptoethanol. 10 x 6 cm gels containing 10% acrylamide, 0.1M Na phosphate, pH 7.1, 0.1% SDS, were polymerized with .075% persulfate. 3 to 15 µg of protein was applied to each gel in a solution containing 3 µl of .05% Bromophenol blue (tracking dye), 1 drop glycerol, 5 µl mercaptoethanol, and 50 µl of .01M phosphate, pH 7.0, containing 0.1% SDS and 0.1% mercaptoethanol. Electrode buffer was 0.1M phosphate, pH 7.1, with 0.1% SDS. A current of 8 mamp/gel was applied for 4-5 hours until the marker dye had moved about 4/5 down the gel. The distance was measured for each gel. The gels were then stained in a 0.25% solution of Coomassie brilliant blue in 45% methanol, 9.2% acetic acid, for 4-10 hours. The gels were destained in a solution of 25%

methanol, 7% acetic acid, overnight. After destaining, they were stored in 7% acetic acid and the positions of the blue protein zones recorded.

#### Analytical Gel Isoelectric Focusing:

Gel electrofocusing was performed essentially according to the photopolymerization method of Wrigley.<sup>86,87</sup> In each gel tube was mixed a) 0.42 ml of a concentrated gel mixture of the following composition: 0.2 ml of 1% TEMED, .014% riboflavin solution, 0.75 ml of a 30% acrylamide, 0.8% methylene bisacrylamide solution and .075 ml of a 40% solution of Ampholine (pH 3-10 or pH 7-9) b) 50-60  $\mu$ g protein in .02-.05 ml c) sufficient H<sub>2</sub>O to a total volume of 1.26 ml. The final acrylamide concentration was 7.5% and the Ampholine concentration was 1%. After water layering, the gels were photopolymerized for 30 minutes. The anode buffer was 0.2% sulfuric acid w/v and the cathode buffer was 0.4% w/v diethanolamine. Electrofocusing was carried out for 3 1/2 hours after gradually increasing the voltage to 275 volts over a 10-15 minute period. Afterwards, gels were stained for protein, according to the method of Vesterberg,<sup>88</sup> for 30-45 minutes at 60°C in the following solution: methanol, 75 ml, TCA, 30g, sulfosalicylic acid, 9g, H<sub>2</sub>O, 150 ml, and Coomassie brilliant blue at a final concentration of 0.1%. Destaining was carried out overnight against several changes of a solution containing 25% ethanol, 8% acetic acid. Gels were stored in 7% acetic acid.

Photopolymerization results in a rather soft gel, especially if it contains the pH 7-9 Ampholines, which must be handled carefully.

Preparative Sucrose Density Gradient Isoelectric Focusing:

The 110 ml electrofocusing column was filled exactly as described in the LKB instruction manual. A linear sucrose gradient of 0-40% was established using a Buchler polystaltic pump. When about half the column was filled, approximately 2 1/2 mgm of enzyme (in about 3 ml) was added to the concentrated sucrose reservoir and filling of the columns continued. The final concentration of Ampholines (pH 7-9) was 1%.\* The anode buffer was a 0.1N phosphoric acid solution and 0.1N sodium hydroxide filled the cathode compartment. The entire column was water jacketed and maintained at 4°-6°C. 600 volts was applied for 70 hours. Initially, 4.5 mamps current was recorded which dropped to 0.5 - 1.0 mamp at the end of the electrofocusing. After the current was disconnected, the column was drained slowly and 1.0 ml fractions collected. Fractions were measured for absorbance at 280 mμ in a Beckmann DU spectrophotometer and their pH recorded at 5°C with a temperature compensated Radiometer pH meter. Aliquots were removed for assay.

Sedimentation Coefficient:

Purified enzyme was dialyzed against .05M phosphate, .002M DTT, .001M EDTA, pH 7.5, and centrifuged at 60,000

---

\*The solution in the column also contained .0005M DTT.

RPM and 20°C in a Spinco Model E analytical ultracentrifuge with Schlieren optics. Photographs were taken every 16 minutes and the movement of the peak measured by a Nikon microcomparator. By plotting the logarithm of the peak displacement from the center of rotation against time, the sedimentation coefficient, S, was determined from the formula:

$$S_{\text{obs}} = \frac{d \ln x}{dt} \times \frac{1}{60\omega^2} \times 10^{13} \quad \text{where } x = \text{peak displacement} \\ \text{and } \omega = \text{angular velocity}$$

Corrections for the density and viscosity of the solution were made from the following relationship:

$$S_{20^\circ;w} = S_{\text{obs}} \frac{(\eta_t)}{\eta_{20^\circ}} \frac{(\eta_{\text{sol}})}{\eta_w} \frac{(1 - \bar{v}\rho_{20^\circ,w})}{1 - \bar{v}\rho_{t,\text{sol}}} \quad \text{where } \eta = \text{viscosity of the liquid} \\ \text{where } \rho = \text{density of the liquid}$$

and  $\bar{v}$  = partial specific volume of the solute.

Centrifugations were done at several protein concentrations and extrapolated back to zero to determine the concentration independent sedimentation coefficient,  $S^0_{20^\circ,w}$ .

#### Molecular Weight:

The molecular weight was determined by equilibrium centrifugation in the analytical ultracentrifuge according to the Spinco instruction manual using the high speed meniscus depletion method of Yphantis.<sup>89</sup> Enzyme was dialyzed against the phosphate buffer described above and centrifuged at several concentrations between 0.25 and 0.50mg/ml at 16,000 RPM and 20°C. After 15-20 hours, photographs were taken

using the Raleigh interference optics system. Fringe displacement was measured in the microcomparator. By plotting the logarithm of the fringe displacement versus the square of the distance from the center of the rotor, the molecular weight can be determined from the following formula:

$$MW = \frac{2RT}{(1-\bar{v}\rho)\omega^2} \times \frac{d \ln(Y_r - Y_o)}{d(r^2)}$$

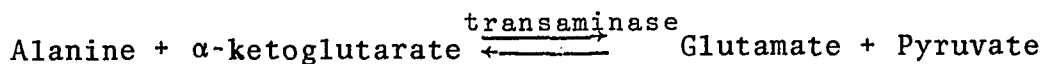
where R is the gas constant, T is the absolute temperature,  $\bar{v}$  is the partial specific volume of the solute (assumed to be 0.74),  $\rho$  is the solution density (1.008 for this solution),  $Y_r - Y_o$  is the fringe displacement, and r is the distance from the center of the rotor. The fringe displacement is proportional to the change in refractive index across the cell, which in turn is proportional to the concentration gradient. A plot which shows no deviation from linearity is indicative of a homogeneous system in which only a single polymeric species of one molecular weight is present in solution.

#### Enzyme Assay:

The standard assay mixture contained the following components, unless otherwise specified:

0.2M L-alanine, 0.01M  $\alpha$ -ketoglutarate, approximately  $2 \times 10^{-4}$ M DPNH, 0.6 to 1.0 unit of beef heart LDH, 1.5 to 2.1mg albumin, appropriately diluted enzyme, and 0.1M  $K_2HPO_4$ , pH 7.5, in a total volume of 3.0 ml. Assays were performed at 30°C in a water jacketed Beckmann DU spectrophotometer with Gilford

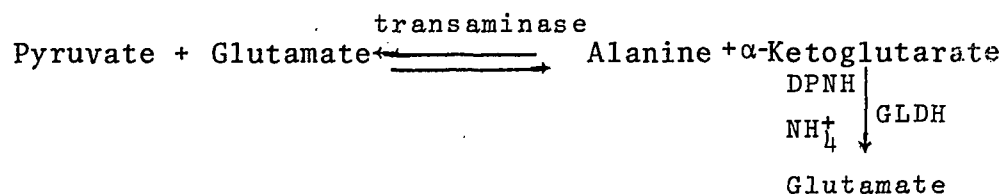
attachment by following the decrease in absorbance at 340 mu resulting from the oxidation of DPNH via the following reaction:



Assays generally were started by adding the ketoglutarate at zero time. Excess LDH ensures that the rate of DPNH oxidation is equal to the rate of pyruvate formation. After an initial lag period, the rate becomes linear with time until 80-90% of the limiting reagent (DPNH) has reacted. Specific activity is defined as the number of micromoles of pyruvate formed per minute per mg of protein at 30°C. The highly purified enzyme is stable when diluted to the  $\mu\text{g/ml}$  range in 0.1M phosphate, pH 7.5, containing 1 mg/ml albumin, for at least 20 minutes at room temperature and several hours at 0°C. In the absence of albumin, the diluted enzyme rapidly loses activity after a stable period of a few minutes at either temperature and activity is not restored even if the assay is performed in the presence of albumin. If the enzyme is diluted in the absence of albumin, and immediately assayed, also in the absence of albumin, the rate is only about 50% that when both dilution and assay occur with albumin present. This difference is taken into account, and dilution and assays performed rapidly, in those experiments in which albumin was not present. Crude enzyme preparations do not require albumin for stability. Variation of albumin concentration over the range described in the standard assay did not affect the rate. In the experiments described in the Results

section, substrate and buffer ion concentrations as well as pH and temperature are varied as noted with each experiment.

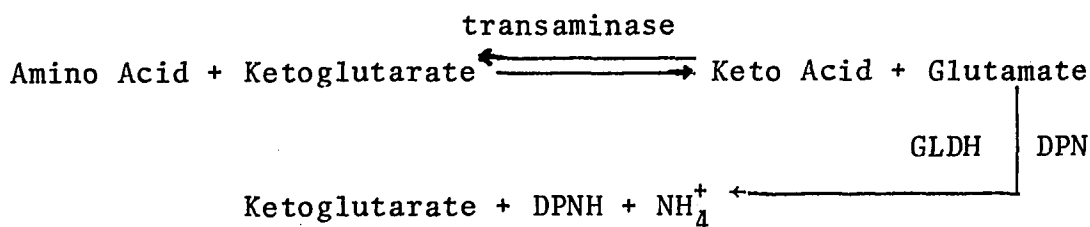
Assays were performed in the reverse direction in a mixture containing glutamate and pyruvate at varying concentrations, .033M  $(\text{NH}_4)_2\text{SO}_4$ ,  $2 \times 10^{-4}$ M DPN, 0.2 - 0.4 units of glutamate dehydrogenase and transaminase in the same phosphate-albumin buffer at 30°C. The glutamate dehydrogenase present is in sufficient excess to aminate the ketoglutarate as fast as it forms:



The reaction is followed by measuring the decrease in absorbance at 340mu. Since glutamate is a product of the GLDH reaction as well as a substrate of the transaminase reaction, glutamate concentration was not raised above 22.5mM, to minimize product inhibition. Specific activity is defined as the number of micromoles of ketoglutarate formed per minute per mg enzyme at 30°C.

To test the specificity of alanine aminotransferase, alanine was replaced by a series of other amino acids in an assay mixture containing ketoglutarate, GLDH and DPN, and measuring the increase in absorbance at 340 mu. The rate in the presence of alanine served as control. The reaction

would proceed as follows:



To test the keto acid specificity, ketoglutarate was replaced by a series of keto acids in the forward direction assay. Mixtures in which transaminase was not present served as controls for those keto acids which were substrates for LDH. In the reverse direction, pyruvate was replaced by this same series of keto acids. Transaminase-free controls served to subtract the contribution to the observed rate obtained from the reaction of those keto acids which were substrates of GLDH.

To test for inhibitory action, amino, keto, mono and dicarboxylic acids were present in both the forward and reverse assays, with both inhibitors and substrates at varying concentrations, as described in the Results section. Specific activity is readily calculated from the following formula:

$$\text{Sp. Act} = \frac{\Delta \text{O.D. units/min} \times 3 \times 1000}{6.22 \times 10^3 \times \frac{\text{mg protein}}{\text{ml}} \times \text{ml diluted enzyme}} \times \frac{1}{\text{dilution factor}}$$

Enzyme Purification: All procedures done at room temperature unless otherwise specified.

1. Twenty four pounds of rabbit muscle, in 3 pound batches, are ground once in a meat grinder and then suspended with occasional stirring for 10 minutes in an equal volume of .002M EDTA, .02M mercaptoethanol, pH 7.2 (Buffer A). The suspension is poured through two layers of cheesecloth and the extract collected. The cheesecloth is folded into a bag and the bag squeezed to near dryness. The hash is then reextracted with another volume of Buffer A and the extracts combined. The liquid is then heated in a 85°-90°C water bath to 56°-57°C, held there for 5-7 minutes, and then chilled rapidly to room temperature or below in an ice-water bath. After the heavy denatured protein settles to the bottom, the upper liquid is poured through a large funnel in which glass wool is packed. The heavy bottom suspension is poured into centrifuge cups and centrifuged at 12,000 RPM in a Sorval RC2-B for 20-30 minutes. The supernatant is poured off through the glass wool packed funnel and combined with the earlier extract. The clear, pink liquid can be stored at this point for several days in the cold. Generally, 12 pounds of tissue can be conveniently brought to this stage in one working day.
2. To the total, clear extract is added 270 mg/ml of ammonium sulfate at 0°-4°C. The lightly turbid suspension is centrifuged

at 16,000 RPM using a Szent-Gyorgi-Blum continuous flow attachment with high speed lift assembly. Flow rate should be about 125 ml/min. Over the 3-4 hours required for the procedure, the temperature of the suspension should not be allowed to rise above 10°C, as more protein precipitates at the higher temperatures with no increase in the yield of transaminase. The packed precipitates (about 2-3 ml in each tube) are taken up in 100-150 ml .02M Tris-HCl, .001M EDTA, .01M mercaptoethanol, pH 8.5-8.6 (Buffer B). Insoluble material is spun down and reextracted with an additional 50-100 ml of Buffer B. Insoluble material is spun out and discarded and the clear supernatants combined. The supernatant is dialyzed against several changes of 3 liters of Buffer B. Any turbidity that develops is spun out.

3. Sufficient DEAE-Sephadex A-50 is swelled and equilibrated with Buffer B to make 1 liter of gel. This is poured onto a 2 liter sintered disc funnel and suction applied until the liquid drops just to the top of the gel. The dialyzed supernatant from step 2 is carefully poured over the gel and drawn into it with suction. Two 300 ml portions of Buffer B are poured over the gel and sucked into it in a similar manner. The liquid filtrate is discarded. Then 5 to 8 300 ml portions of .02M Tris, .001M EDTA, .01M mercaptoethanol, .06M NaCl, pH 8.5-8.6 (Buffer B) are poured over the gel with suction. The filtrates are collected separately and assayed. The active filtrates are combined and 270 mg/ml ammonium

sulfate added. The lightly turbid suspension is spun down at 12,000 RPM in large centrifuge cups for 20-30 minutes. The supernatant is discarded and the precipitate is taken up in a minimum volume of Buffer B, and it is dialyzed against several changes of this buffer. The liquid is yellow.

4. A 2.5 x 40 cm column of DEAE-Sephadex A-50 is equilibrated against Buffer B. The dialyzed enzyme from step 3 is applied to the top of the column and washed in with 2-3 column volumes (350-500 ml) of Buffer B. A portion of the yellow material moves slowly through the column about  $1/3 - 2/3$  the way down.\* A linear gradient is then established between Buffer B and Buffer B' (total volume=450 ml), and 5-10 ml fractions are collected at a flow rate of 50-75 ml/hr and assayed. Fig. 1 shows the elution pattern. The active fractions are pooled and chilled to 0°C. 200-205 mg/ml of ammonium sulfate are added and the very light suspension is spun down at 0°C. The precipitate is discarded. After allowing the supernatant to warm up to room temperature, an additional 50 mg/ml (relative to the initial volume of the liquid) is added and the suspension spun down at room temperature. The precipitate is taken up in a minimum volume of .001M phosphate, .002M DTT, pH 7.0, (Buffer C) and dialyzed against several changes of this buffer. The solution is intensely yellow.

---

\*Yellow material that stays at the top is impurity.

5. A 1.5 x 27 cm column of hydroxylapatite is prepared and equilibrated with Buffer C. The dialyzed enzyme is applied to the column and washed in with 1-1 1/2 column volumes of Buffer C. The yellow material sticks to the upper 1-2 cm of the hydroxylapatite. The buffer is then changed to .012M, phosphate, .002M DTT, pH 7.0 (Buffer D), and 1-1 1/2 column volumes is washed in at 15-20 ml/hr. Yellow material begins to spread slowly down the column. Before it reaches the bottom, the buffer is changed to .028M phosphate, .002M DTT, pH 7.0 (Buffer E), and 1-2 column volumes washed in. Two ml fractions are collected. As the buffer front moves down the column, the yellow material begins to concentrate and move down the column with the buffer front. Some of the yellow enzyme leaves the column before this front. Because of this, the enzyme elutes in two peaks, the first broad and shallow, as shown in Fig. 2. This procedure minimizes contamination by material that elutes just before and just after the enzyme. The active fractions are combined and the volume is reduced by placing in a dialysis bag surrounded with dry G-150 or G-200. The enzyme is then transferred to another bag and dialyzed against .05M phosphate, .001M EDTA, .002M DTT, pH 7.5 (Buffer F). The enzyme is 95-99% pure at this stage as shown by disc gel electrophoresis at pH 4.3. An alternate procedure is to elute the enzyme with .020M phosphate, .002M DTT, pH 7.5, after the wash with Buffer C.

Approximately 50% of the enzyme elutes in a broad shallow peak just after a small peak of impurity. The remainder can be eluted with .035M phosphate, .002M DTT, pH 7.0, but it is considerably more impure. The enzyme eluted in the shallow peak is pure or very nearly so as shown by disc gel. The enzyme is concentrated as described above and dialyzed against Buffer F.

6. If electrophoresis indicates any impurity in the enzyme after step 5, it can be removed by one of two methods:

a) The enzyme is dialyzed vs Buffer C and hydroxylapatite chromatography repeated as described in step 5.

b) Gel filtration on a 1.5 x 85 cm column of G-200 equilibrated with Buffer F is performed. The sample is applied in a total volume of 1-2 ml and eluted with Buffer F at 20-30 ml/hr. The impurity is heavier than the enzyme and elutes somewhat ahead of it. The enzyme can be readily followed because of its yellow color. The active fractions are pooled, the volume reduced with dry G-200, and the enzyme dialyzed against Buffer F. The enzyme is stored at 4°C and is stable for months if dialyzed against fresh Buffer F every few weeks.

RESULTS

A summary of a typical purification procedure is given in Table I. Several facets of this purification procedure require comment:

1. The specific activity of the initial extract will vary between .025 and .070 with different batches of muscle tissue. The specific activity of the heated extract will also vary accordingly. Total activity of the heated extract will generally vary between 15,000 and 25,000 units for 24 pounds. Specific activity of the heated extract will, at times, increase slightly (10-20%) over that of the initial extract. Heating may act to destroy a naturally occurring inhibitor in the initial extract of some batches of muscle tissue.
2. Specific activity of the first ammonium sulfate precipitate generally varies between 1.0 and 3.5. Residual transaminase activity remaining in the supernatant is qualitatively different from that which precipitates out. Two phenomena illustrate this difference. By working up small quantities of muscle tissue, additional ammonium sulfate fractionation of the heated extract can be conveniently carried out. Adding an additional 100-125 mg/ml of ammonium sulfate to the first ammonium sulfate supernatant results in a precipitate containing about 10-20% of the residual transaminase. Adding another 200-250 mg/ml results in a third precipitate containing most of the remaining transaminase. Thus, this third precipitate contains a transaminase that precipitates at an ammonium sulfate concentration significantly removed from the major transaminase fraction. In addition, the activity of the former, when assayed in the presence of 0.4M D,L-alanine is

90-95% inhibited compared to its activity with 0.2M L-alanine, whereas little or no inhibition occurs when the latter is assayed with D,L-alanine. This differential sensitivity to D-alanine further distinguishes the two transaminases. Because of the low yield, the sensitive transaminase was not investigated further.

3. Specific activity of the 3rd ammonium sulfate precipitate generally varies between 60 and 120, depending upon the somewhat variable capacity of the DEAE-Sephadex column chromatography to separate the enzyme from impurities.

4. The specific activity of the purified enzyme varies between 270 and 350. Therefore, disc gel electrophoresis and not specific activity is the only useful criterion for enzyme purity. This variability in specific activity may be accounted for by enzyme aging or oxidation over the course of the purification. Alternately, the isozymic composition of different preparations may differ. As discussed later, the purified enzyme is a heterogeneous mixture of many isozymes, each of which may have a different specific activity, so that the observed activity is an average, dependent on the isozymic composition of the preparation.

5. The purified enzyme is in all probability of cytoplasmic origin. Studies with other tissues have shown a mitochondrial alanine transaminase to be present, but it represents no more than 10% of the total activity. In addition, it is difficultly solubilized from the mitochondria and is quite heat labile.

Centrifugation of the heated extract removes the mitochondria in the rabbit muscle preparation and leaves most of the activity in the clarified supernatant. Furthermore, experiments with small quantities of rabbit muscle in which care was taken to preserve mitochondria intact (extraction of freshly butchered rabbit muscle in .025M sucrose at 0°C), followed by centrifugation at 0°C to remove the mitochondria, showed that only about 10% of the activity is in the mitochondrial fraction. Workup of the mitochondrial-free extract gave relative yields in the various fractions that were essentially the same as preparations using the harsher extraction procedure described above. The isozymic heterogeneity described later is, therefore, probably not the result of the mixing of cytoplasmic and mitochondrial enzymes, but rather is cytoplasmic in origin.

#### Disc Gel Electrophoresis:

a) Low pH - The purity of the enzyme recovered from the hydroxylapatite column was determined by subjecting it to analytical disc gel electrophoresis at pH 4.3. As shown in Fig. 3, a single, sharp band of protein with only the slightest traces of slower moving impurity can be seen. These impurity bands, plus others, stain significantly more intensely when preparations from earlier stages of the purification are examined (not shown). The impurities in the highly purified sample account for no more than 1-2% of the

total stainable material. Based on this single criterion, the enzyme is essentially purified by the procedure outlined.

b) High pH - In order to further examine the state of purity of the enzyme, electrophoresis at pH 9.5 was performed. As shown in Fig. 4a<sub>1</sub>, a rather broad slow moving band results, which upon electrophoresis for longer periods, diffuses in a manner which seems to indicate heterogeneity, as seen in Fig. 4a<sub>2</sub> and 4a<sub>3</sub>. Applying four times as much protein results in a broad, unresolved band (Fig. 4b). Slicing of corresponding unstained gels and assaying indicated that the activity was spread over the same broad region.

#### Analytical Isoelectric Focusing:

The apparent conflict between the results of low and high pH disc gel prompted the use of isoelectric focusing to determine if further heterogeneity could be detected. Fig. 5 shows the band pattern obtained using a gradient of pH from 3-10. A cluster of 10-12 bands can be seen, with isoelectric points between pH 7.5-9. A more dramatic and clearly resolved band pattern is observed when the gradient is narrowed to pH 7-9, as seen in Fig. 6. Approximately 12-14 bands can be resolved, with isoelectric points between pH 7.5-8.5. This multiplicity of bands stands in striking contrast to the results obtained at low pH with disc gel electrophoresis, where only one band is observed. Since disc gel separates molecules on the basis of both size and charge, whereas

focusing only distinguishes between molecules with different isoelectric points, the results seem to indicate that a mixture of proteins of the same or similar molecular dimensions but with variable charge is present in the "purified" enzyme. Since the isoelectric points are spread over only 1 pH unit, it is conceivable that electrophoresis at low pH could not distinguish between molecules that had roughly similar net charges 4-5 pH units below their isoelectric points. In order to determine whether these multiple bands represent heretofore unrecognized impurity in the preparation or are instead, the result of extensive isozymic heterogeneity, unstained gels subjected to isoelectric focusing were sliced and assayed for enzymatic activity. These results are shown in Fig. 7. It is clear that activity is spread throughout the gel, with 4-5 peaks of activity detectable. The fact that fewer activity peaks are detectable than protein bands is probably due to the inability to slice the gel thin enough to detect them.

#### Prep. Isoelectric Focusing:

In an attempt to obtain better resolution of the enzymatic activity and to correlate this activity with zones of protein, preparative sucrose density gradient isoelectric was undertaken. Approximately 2 1/2 mg of 95% purified transaminase (based on low pH analytical disc gel electrophoresis) was applied to a 110 ml column and focusing performed for 70

hours at 4°C. The elution profile is shown in Fig. 8. The results clearly demonstrate the close correlation of peaks of activity with peaks of 280 m $\mu$  absorbance. Only one protein peak is present, at pH 7.1, which does not correspond to a peak of enzyme activity. This probably corresponds to the 5% impurity present in that particular sample. Approximately 8-10 activity peaks can be resolved, which although less than can be detected visually on analytical gels, is clearly indicative of isozymic multiplicity in the purified enzyme and negates the possibility that the band pattern observed on the gel is artifactual. Although multiple enzymic subforms are not unique, as has already been discussed with regard to aspartate transaminase, the degree of this multiplicity is quite extraordinary. Other purified alanine transaminases, described earlier, were not shown to contain any significant degree of heterogeneity. Although this may have been due to the failure to utilize sufficiently sensitive characterization procedures, the presence of this remarkable multiplicity of isozymes in the rabbit muscle preparation is not made any less significant thereby. Mechanisms whereby such heterogeneity may arise is discussed in some detail in the Discussion.

#### SDS Gel Electrophoresis:

The subunit structure of the enzyme was examined by SDS gel electrophoresis. Fig. 9 shows only a single band of

protein present in the 99+% purified preparation. This single band is further evidence of enzyme purity. No evidence of subunit heterogeneity exists, thereby eliminating different molecular weight subunits as a possible reason for the multiple band pattern seen in isoelectric focusing. This was to be expected, since resolution of the isozymes occurs only in a system that separates on the basis of net charge, not molecular size and shape. The molecular weight of the subunit was determined by plotting the logarithm of the molecular weight of the enzyme and a series of marker proteins against the relative mobilities of these proteins in a series of SDS gels. Fig. 10 indicates the molecular weight of the minimum alanine transaminase subunit to be 55,000  $\pm$  2000.

Sedimentation Coefficient:

The purified enzyme was examined in a series of sedimentation velocity runs in the analytical ultracentrifuge. Fig. 11 shows the sedimenting peak to be symmetrical with no trace of faster or slower moving components, which is further evidence for the molecular homogeneity of the purified enzyme. The sedimentation coefficients were calculated according to procedures outlined in the Methods. A typical plot of  $\ln$  (peak distance) vs time is shown in Fig. 12. Plotting the apparent S values vs concentrations and extrapolating to zero concentration gave a perfectly fitted straight line and an

$S_{20,w}^{\circ}$  of 6.45, as shown in Fig. 13.

#### Molecular Weight:

The molecular weight of the purified enzyme was determined by analytical ultracentrifugation using the high speed meniscus depletion method as described in Methods. Runs at four different concentrations were performed and the results averaged. The molecular weight was found to be  $110,000 \pm 4000$ .\* All plots of  $\ln(\text{fringe displacement})$  vs  $(\text{distance})^2$  were linear with no hint of upward curvature near the bottom of the cell. This is further indication of the homogeneity of the sample as far as molecular dimensions are concerned. Upward curvature would point to a polydisperse system in which more than one molecular species were present. A typical plot is shown in Fig. 14. The molecular weight of the native enzyme is twice that of the minimum subunit as determined by SDS electrophoresis. The native enzyme is, therefore, composed of polypeptide chains of similar or identical molecular weight which are readily ruptured by incubation in SDS and mercaptoethanol.

#### Tryptophan and Tyrosine Content:

By solving the 2 simultaneous equations of Edelhoch as described in Methods, the number of moles of tryptophan

---

\*This value agrees closely with the molecular weights of pig heart and rat liver enzymes described earlier in the Introduction.

$N_{\text{TRYP}}$ , per mole of enzyme may be determined. This solution gives

$$N_{\text{TRYP}} = \left( \frac{\text{O.D. } 288 \text{ m}\mu}{(\text{Enz})_{\text{molar}}} \times .332 - \frac{\text{O.D. } 280 \text{ m}\mu}{(\text{Enz})_{\text{molar}}} \times .097 \right) 10^{-3}$$

Enzyme was diluted to a final concentration of  $0.292 \times 10^{-5} \text{M}$  in 6M guanidine HCl and O.D.'s of .180 and .105 at 280 m $\mu$  and 288 m $\mu$  respectively, were determined. Solving the equation gives  $N_{\text{TRYP}} = 6.0$

Solving the 2 simultaneous equations for tyrosine gives

$$M_{\text{TYR}} = \left( \frac{\text{O.D. } 280 \text{ m}\mu}{(\text{Enz})_{\text{molar}}} \times 1.21 - \frac{\text{O.D. } 288 \text{ m}\mu}{(\text{Enz})_{\text{molar}}} \times 1.43 \right) 10^{-3}$$

Using the above mentioned values, the equation reduces to

$$M_{\text{TYR}} = 23.2$$

Assuming identical subunits, each polypeptide chain, therefore, contains 3 tryptophan and 11-12 tyrosine residues.

#### PLP Content:

The pyridoxal-5<sup>phosphate</sup> content of the purified enzyme was determined spectrofluorometrically as described in Methods. A standard curve of fluorescence intensity vs PLP is presented in Fig. 15. Points are plotted on the graph for  $3.27 \times 10^{-8} \text{M}$  and  $6.54 \times 10^{-8} \text{M}$  enzyme. From these data, an average of 1.85 moles of PLP per mole enzyme (110,000 molecular weight) is calculated. This value in-

dicates that the enzyme contains one molecule of PLP per subunit. The close agreement between theory and experiment is further indication of the purity of the enzyme preparation - if the many bands seen in isoelectric focusing represented impurity, then the measured PLP content would be significantly less than 2 moles PLP/mole enzyme.

#### Sodium Borohydride Reduction:

Enzyme was treated with  $\text{NaBH}_4$  as described in Methods and assayed. 99% of the activity was lost within one minute with no further change after 5 minutes more. Borohydride acts to reduce the aldimine bond to a secondary amine in PLP enzymes. The loss of activity with this reduction demonstrates the absolute requirement for an aldimine group in the transamination reaction.

#### Removal of PLP from the Holoenzyme:

##### Method 1:

After treatment of the enzyme with PCMB and  $(\text{NH}_4)_2\text{SO}_4$  followed by DTT treatment, the specific activity dropped from 260 to 71, a loss of 73%. In the case of the rat liver enzyme, a 98% loss occurred. Apparently, either PLP is incompletely removed or irreversible modification of essential -SH groups occurs, with resultant loss of activity. Attempts at reconstitution with PLP resulted in only a small increase in specific activity from 27% of the control, to 36%.

Method 2:

Treatment with imidazole-citrate-cysteine resulted in a drop of only 30% in the specific activity of the enzyme. Because of this small effect, no reconstitution with PLP was attempted.

These preliminary results indicate that PLP is tightly bound to the enzyme and is not readily removed by conventional means.

PCMB Titration:

Purified enzyme at a specific activity of 280 units/mg was treated with PCMB as described in Methods. Fig. 16 shows the relative loss of activity with respect to the number of moles of PCMB incorporated per mole of enzyme. The results indicate that the activity decreases in a roughly linear fashion to about 5% initial activity after 6-7 SH groups have reacted. In contrast, no loss of activity occurs when the 1st 7-8 -SH group of the rat liver enzyme has reacted with either PCMB or DTNB.<sup>41</sup> Only after the next 6-9 groups are titrated is activity reduced by 90-95%. Attempts to measure the total number of titratable SH groups in both the presence and absence of 6M guanidine-HCl failed because of the development of turbidity under both conditions after 7-10 moles of PCMB had reacted.

### Spectra:

Spectra of the pyridoxal and pyridoxamine forms of the enzyme at pH 7.0 over the range 250  $m\mu$  to 500  $m\mu$  are shown in Fig. 17. In A, the buffer is .05M phosphate, .001M DTT, .001M EDTA. In B, the buffer is the same plus 0.2M L-alanine. Wavelengths of the respective peaks are given in the figure. The peak positions are nearly identical with the corresponding peaks of the rat liver and pig heart enzymes. The purified enzyme, as isolated, is in the pyridoxal form.

The effect of pH on the spectrum of the pyridoxal enzyme is shown in Fig. 18. The pH was changed by successive additions of small aliquots of 1M  $\text{Na}_2\text{CO}_3$  or 1M acetic acid, and the spectra determined after each change, corrected for dilution. As can be seen, the change in absorbance of the 330-335  $m\mu$  peak over the pH range examined is small. The change in absorbance of the 410-420  $m\mu$  peak is more significant, with absorbance increasing as the pH decreases. An isosbestic point at 380  $m\mu$  can be seen. As discussed in the introduction, the peak at 420  $m\mu$  is associated with the protonated aldimine form of the enzyme-bound PLP. The pKa of this group can, therefore, be determined by plotting the change of absorbance against pH as shown in Fig. 19. A pKa value of 7.4 - 7.5 can be estimated from the inflection point of this plot. This value is close to that reported for the rat liver and pig heart enzymes.<sup>40,41</sup>

In the presence of  $1 \times 10^{-5}M$  of the potent enzyme inhibitor, aminooxyacetate, the peak at 420  $m\mu$  disappears and is replaced by one at 375  $m\mu$ . With 0.1M proline, a weak competitive inhibitor of alanine, a peak at 365  $m\mu$  replaces the 420  $m\mu$  peak. Formation of inhibitor - PLP Schiff bases, described earlier in the Introduction, adequately accounts for these spectral changes. These spectra are shown in Fig. 20 (A & B).

Effect of pH on enzyme activity:

Enzyme activity was assayed over the pH range of 6.0-9.0 at constant phosphate concentration and constant ionic strength (these 2 parameters affect activity as will be shown in the next section). If it is assumed that enzyme activity is controlled by the reversible protonation of a titratable group in the enzyme, then the midpoint of the ascending limb of the activity vs pH curve would be equal to the pKa of that group. This pKa, under the present assay conditions, equals pH 6.6 - 6.8. Maximal activity occurs between pH 7.5 - 8.1. Activity vs pH was also determined in the presence of 3 different inhibitors, aminooxyacetate, proline, and phenylpyruvate at the same phosphate and ionic strength conditions. The results are plotted in Fig. 21. The pH optimum for inhibition by aminooxyacetate is 6.5 - 7.0, whereas the inhibition optimum for proline is 8.0 - 8.5. Inhibition is maximal for phenylpyruvate at pH 6.0, but it declines continuously as the pH is raised. Plots of %

inhibition vs pH for these compounds are presented in Figs. 22-24. Since none of the inhibitors have pKa's in the pH range considered, the midpoints of either the ascending or descending limbs of the % inhibition vs pH curves of these compounds are probably equal to the pKa's of groups on the enzyme that either bind to or are modified by these inhibitors. These pKa's are:

- a) for aminoxyacetate - pH 7.9-8.1    b) for proline - pH 7.1-7.3    c) for phenylpyruvate - pH 7.4-7.6

The experiments with aminoxyacetate yield curves which strongly resemble curves obtained from similar experiments performed with the rat liver enzyme.<sup>45</sup>

#### Ionic Strength Effects:

The activity of alanine aminotransferase is strongly inhibited by increasing ionic strength of the reaction mixture. Fig. 25a shows the effect of increasing ionic strength on enzyme activity at low phosphate buffer concentration. If the data is replotted for log activity vs the square root of the ionic strength a straight line relationship is obtained, as seen in Fig. 25b. Multiplying by the appropriate factors gives the corresponding second order rate constants at each ionic strength. Fig. 25c is a logarithmic plot of the rate constants vs the square root of the ionic strength. The slope, -2.2, which is reasonably close to the integral value of -2, is approximately equal to

the product of the charges of the bi-molecular enzyme-substrate complex in the transition state of the reaction pathway. This interpretation derives from the Bronstead equation:

$$\log k_2 = B + 1.03 Z_a Z_b I^{1/2} \text{ at } 30^\circ\text{C}$$

which describes the primary kinetic salt effect, where  $Z_a$  and  $Z_b$  are the ionic charges of the reacting species in the activated complex. The above mentioned slope is, therefore, equal to  $1.03 Z_a Z_b$ .

The relationship between log activity and  $\sqrt{\text{ionic strength}}$  in a high phosphate concentration buffer was examined and was also found to be linear as shown in Fig. 26. However, by comparing the rates in Fig. 25b and Fig. 26, it can be seen that at equivalent ionic strengths, the rate is greater when the phosphate concentration is greater. In both experimental series, the same quantity of enzyme was used. Phosphate, therefore, activates the enzyme in some manner even as it deactivates by virtue of its contribution to the ionic strength. This is more clearly demonstrated in Fig. 27 which plots log activity vs the square root of the ionic strength for a series of reaction mixtures containing increasing concentrations of phosphate. The measured slope is considerably less severe than those of Fig. 25b and Fig. 26, illustrating thereby the activating effect of phosphate by dampening the loss of activity with increasing ionic strength.

Effect of Temperature on Enzyme Activity:

The effect of temperature on a chemical reaction is given by the Arrhenius equation:

$$\frac{d \log \text{ rate}}{d \left(\frac{1}{T}\right)} = \frac{-E_a}{2.3R}$$

where  $E_a$  is the activation energy. Fig. 28 is an Arrhenius plot over the range 12°C to 42°C. Two bends occur, at 16°C and at 35°C. Three activation energies can, therefore, be calculated from the graph for this enzymatic reaction. They are:

Below 16°C;  $E_a = 27,400$  cal/mole

16°C - 35°C;  $E_a = 13,300$  cal/mole

Above 35°C;  $E_a = 7,850$  cal/mole

Possible explanations for this unusual occurrence will be considered in the Discussion.

Enzyme Specificity:

The ability of alanine aminotransferase to utilize amino acids other than its normal substrates was tested as described in Methods. The reaction mixtures contained  $8.7 \times 10^{-4}$ M ketoglutarate and .04-.05M of the following amino acids: L-valine, L-leucine, L-isoleucine, L-proline, L-tryptophan, D-L-phenylalanine, L-methionine, glycine, L-serine, L-threonine, L-asparagine, L-glutamine, L-cysteine, L-aspartic acid, L-lysine, L-arginine, L-histidine, L-hydroxyproline,  $\alpha$ -aminoisobutyric acid, D,L, $\alpha$ -aminovaleric acid,  $\beta$ -alanine, .004M L-tyrosine, .0025M cysteine.\* Of all these, only the  $\alpha$ -aminovaleric acid had weak substrate activity of about 3% the rate with .05M L-alanine.

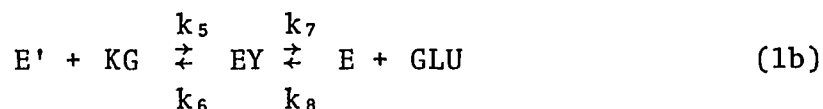
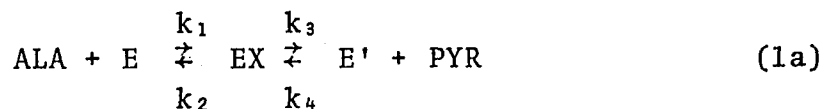
The following keto acids were tested for their ability to replace ketoglutarate in the forward direction assay: ketovalerate, ketoisocaproate, ketocaprylate, phenylpyruvate, ketobutyrate, oxaloacetate and mesoxalate. All were tested at a concentration of 4mM except ketobutyrate which was at 0.5mM. Alanine was at .05M. Only mesoxalate reacted at about 5% of the rate with ketoglutarate. In the reverse direction, the same keto acids were tested replacing pyruvate at a concentration of 2mM. Glutamate was at 15mM. Mesoxalate gave about 5% activity in this assay as well. In addition, ketobutyrate was also slightly active, with about 2% of the activity with pyruvate. All others were inactive.

---

\*Albumin was present in all assays.

Kinetic Theory and Parameters:

The simplest minimal formulation to describe the trans-aminase shuttle mechanism in which the enzyme reacts with one substrate at a time is given by:<sup>17</sup>



where E and E' are the PLP and PMP enzymes, respectively, and EX and EY represent sequences of intermediates over the course of the reaction. The reciprocals of the Michaelis-Menten rate equations derived from this reaction mechanism are:

$$\frac{1}{v_f} = \frac{1}{V_{mf}} \left( \frac{K_{\text{ALA}}}{(\text{ALA})} + \frac{K_{\text{KG}}}{(\text{KG})} + 1 \right) \quad (2a)$$

$$\frac{1}{v_r} = \frac{1}{V_{mr}} \left( \frac{K_{\text{GLU}}}{(\text{GLU})} + \frac{K_{\text{PYR}}}{(\text{PYR})} + 1 \right) \quad (2b)$$

where  $v$  and  $V$  are initial and maximal velocities, the subscripts  $f$  and  $r$  refer to forward and reverse reaction directions, and the  $K$ 's are Michaelis constants. According to equation 2, double reciprocal Lineweaver-Burke plots of initial velocity vs concentration of one substrate, alanine for example, at a series of fixed concentrations of the second substrate, keto-glutarate, should yield a set of parallel lines, one for each concentration of ketoglutarate. The same is true of the reverse reaction.

In addition, sets of parallel lines from the same data are obtained when either substrate is considered as the independent variable. Fig. 29 shows the results obtained with alanine as the variable substrate. Fig. 30 shows the plots with pyruvate as the variable substrate. Plots with keto-glutarate and glutamate as the variable substrates can be derived from the data of Figs. 29 and 30, respectively. The intercepts on the ordinates are reciprocals of apparent maximal velocities,  $\frac{1}{V'_m}$ , dependent on the cosubstrate concentration, and the intercepts on the abscissas are negative reciprocals of apparent Michaelis constants,  $\frac{1}{K'}$ 's. These are related to the concentration independent constants by equations 3 and 4:

$$(3) \quad \frac{1}{V'_m} = \frac{1}{S_2} \left( \frac{K_{S2}}{V_m} \right) + \frac{1}{V_m}; \quad \frac{1}{K'_{S1}} = \frac{1}{S_2} \left( \frac{K_{S2}}{K_{S1}} \right) + \frac{1}{K_{S1}}$$

$$(4) \quad \frac{1}{V'_m} = \frac{1}{S_1} \left( \frac{K_{S1}}{V_m} \right) + \frac{1}{V_m}; \quad \frac{1}{K'_{S2}} = \frac{1}{S_1} \left( \frac{K_{S1}}{K_{S2}} \right) + \frac{1}{K_{S2}}$$

Therefore, from Eq. 3, plotting  $\frac{1}{V'_m}$  vs  $\frac{1}{S_2}$  yields  $V_m$  and  $K_{S2}$  and a plot of  $\frac{1}{K'_{S1}}$  against  $\frac{1}{S_2}$  yields  $K_{S1}$  and  $K_{S2}$ . As a check, one can plot from Eq. 4.  $\frac{1}{V'_m}$  vs  $\frac{1}{S_1}$  and obtain  $V_m$  and  $K_{S1}$ , and from a plot of  $\frac{1}{K'_{S2}}$  vs  $1/S_1$ ,  $K_{S2}$  and  $K_{S1}$  are obtained. Data for all four substrates from these so called "secondary plots"

are averaged and summarized in Table II. Secondary plots derived from Figs. 29 and 30 are shown in Figs. 31 and 32 respectively. It can be seen that the reaction rate with alanine and ketoglutarate is more rapid than with glutamate and pyruvate. In addition, the Michaelis constants for the keto acids are 1-2 orders of magnitude lower than those for the amino acids. The fact that the graphical plots are in accord with the predictions of equation 2 is strong evidence for the correctness of the mechanism described by equation 1. Rate equations containing terms such as  $\frac{Ks_1Ks_2}{S_1S_2}$  would be required if ternary rather than binary complexes between enzyme and substrate formed, and the plots would not be sets of parallel lines, but sets of lines that intersected in the upper left quadrant of the graph.

#### Inhibitors:

A wide series of amino, keto, mono and dicarboxylic acids were tested for their ability to inhibit both the forward and reverse enzymatic reactions. Tables III-V summarizes these experiments. Comparing Tables III and IV reveals the following; 1) the extent of inhibition by nearly all the compounds is roughly the same in both reaction directions. 2) keto acids are better inhibitors than their carboxylic acid analogues. 3) except for mesoxalate, which is also a weak substrate, dicarboxylic acids are poor inhibitors. 4) inhibition increases with increasing chain length of monocarboxylic acids, a result qualitatively similar to that obtained with the pig heart

enzyme.<sup>40</sup> 5) Intermediate and long chain fatty acids inhibit better in the absence of albumin than in its presence (experiments not shown indicated that short chain acids are not affected by albumin), a not unexpected result, considering the fact that albumin binds fatty acids.<sup>91</sup>

Table V indicates that alanine aminotransferase is inhibited to varying degrees by most of the natural amino acids, with proline, tryptophan and cysteine being especially inhibitory. Proline inhibition has also been demonstrated with the rat liver enzyme,<sup>47</sup> and has been ascribed to PLP-proline Schiff base formation. Inhibition by cysteine has been shown with other PLP enzymes<sup>92</sup> and has been explained as the result of thiazolidine ring formation between cysteine and PLP.<sup>93</sup>

The nature of the inhibition by certain of these compounds was investigated more fully via inhibition kinetics. Linear competitive inhibitions kinetics for alanine aminotransferase in the forward direction is described by equation 5.<sup>17</sup>

$$\frac{1}{v_f} = \frac{1}{V_{mf}} \left( \frac{K_{ALA}}{(ALA)} \times \frac{1}{K_I} + \frac{K_{KG}}{(KG)} \times \frac{1}{K'_I} \right) + \frac{1}{V_{mf}} \left( \frac{K_{ALA}}{(ALA)} + \frac{K_{KG}}{(KG)} + 1 \right)$$

where  $K_I$  = dissociation constant of EI from  $E + I \rightleftharpoons EI$

and  $K'_I$  = dissociation constant of E'I from  $E' + I \rightleftharpoons E'I$

All other terms have been defined. By plotting  $\frac{1}{v}$  against  $I$  at a fixed concentration of one substrate and several different concentrations of the second, a series of lines which intersect in the upper left quadrant result. Solving equation 5 for the intersection point, projected on the  $-I$  axis, yields  $K_I$  when alanine is the varied substrate and  $K'_I$  when ketoglutarate is the varied substrate. This is the so called Dixon plot.<sup>94</sup> For other types of inhibition, more complex equations are involved which when treated by a Dixon plot, give lines which intersect on the negative abscissa in the case of a non-competitive inhibitor, and a series of parallel non-intersecting lines in the case of an uncompetitive inhibitor. Kinetic treatment of the reverse reaction yields exactly the same patterns of lines. Several of the inhibitory fatty acids were examined by these methods and a typical plot with lauric acid as inhibitor, is shown in Fig. 33. Where the lines cross in the upper left hand quadrant, an inhibition constant competitive with pyruvate of  $0.21\text{mM}$  can be measured. Where the lines cross on the horizontal axis, an inhibition constant non competitive with glutamate of  $0.34\text{mM}$  can be seen. When phenylpyruvic acid was the inhibitor, only competitive inhibition against both pyruvate and glutamate could be demonstrated, as shown by the dual intersections in the upper left quadrant of Fig. 34. Similar results were obtained when alanine and ketoglutarate were the variable substrates. With cysteine, non-competitive inhibition against the amino acid substrates was seen,

whereas uncompetitive inhibition against the keto acid substrates resulted, as shown in Fig. 35 for the forward reaction substrates. With proline, inhibition was competitive against the amino acid substrates and uncompetitive against the keto acid substrates, as shown in Fig. 36 for the reverse reaction substrates. All of these inhibition studies are summarized in Table VI.

To say that a substance is a competitive inhibitor of an amino acid substrate is another way of saying that it reacts with or binds to the PLP enzyme, whereas if the substance is competitive with the keto acid substrates, it means that it reacts with or binds to the PMP enzyme. Conversely, if a substance is uncompetitive with the amino or keto acid substrates, then it doesn't react with or bind to the PLP or PMP enzyme, respectively. Cysteine inhibition, therefore, is curious since it would be expected to inhibit competitively with the amino acid substrates, rather than noncompetitively, as it does.

Finally, inhibition by aminooxyacetate was examined via Lineweaver-Burke reciprocal velocity vs substrate concentration plots. By varying one substrate concentration while keeping the second constant in the presence and absence of a fixed concentration of inhibitor, competitive, uncompetitive and noncompetitive inhibition can be distinguished. For the case of a two-substrate shuttle mechanism of which this transaminase is an example, competitive inhibition results either in lines that intersect on the  $\frac{1}{V}$

axis, as is the case with a simple one-substrate enzyme, or in lines with both slope and vertical intercepts different.<sup>17</sup> For an uncompetitive inhibitor, Lineweaver-Burke plots of reaction rates in both the absence and presence of inhibitor result in a set of parallel lines. Fig. 37 shows amino-oxyacetate inhibition of the forward reaction. The inhibitor is competitive with alanine, with a  $K_I$  of  $3 \times 10^{-8}$ M. Since the inhibitor can only react with the PLP enzyme, competitive inhibition with the amino acid substrate is to be expected. When assayed in the reverse direction, aminooxyacetate also competitively inhibits glutamate with the same inhibition constant. Inhibition of the keto acid substrate is uncompetitive over a portion of the concentration range examined, followed by a break in the plotted line as keto-glutarate concentration increases. The same phenomenon is observed in the reverse assay. This anomolous change may be tentatively explained by assuming that at high concentrations the keto acid begins binding to the PLP enzyme, thereby preventing its interaction with aminooxyacetate. The net effect would be to increase the reaction rate over what would be expected if no binding took place, since less enzyme is subjected to aminooxyacetate inhibition. Binding of pyruvate to the PLP form of the pig heart alanine transaminase has already been described in the Introduction.

Phosphorylase - Transaminase Complex:

In an attempt to study the nature of the phosphorylase-transaminase complex described by Bailin and Lukton,<sup>73</sup> phosphorylase was prepared from frozen rabbit muscle tissue as described and tested for protein-protein allosterism by assaying for phosphorylase activity both in the presence and absence of all four transaminase substrates. Transaminase activity was assayed in the presence and absence of the phosphorylase substrates, glycogen and glucose-1-phosphate. Not only was no effect on activity found in all cases examined, but the amount of transaminase activity obtained in the purified phosphorylase preparations was at least twenty times less than reported. Further recrystallization of the phosphorylase only succeeded in reducing the transaminase activity to negligible values. Other preparations, using tissue obtained from freshly killed rabbits in different physiological conditions (young, old, pregnant, starved overnight) gave the same negative results. One experiment involved injecting an alloxan-diabetic rabbit for six days with 5 mg/kg of prednisolone. Food was removed on the fifth day and the animal killed 3 hours after the last injection. Again, no protein-protein interaction could be detected. In addition, there was no significant change in the total quantity of transaminase in the initial extract, indicating that this treatment, which had previously been shown to increase the level of alanine aminotransferase in liver,

had no effect on the muscle enzyme. After purified transaminase was obtained, it was mixed with both purified phosphorylase a and b over a range of molar ratios, from 1:10 to 10:1, at various temperatures, in various buffers (pH 7.5-8.0) and assayed for transaminase activity in both the forward and reverse direction at various substrate concentrations in the presence and absence of 20mM glucose-1-phosphate. Some of these experiments were performed with an aliquot of initial muscle extract added, to cover the possibility that some factor in this extract might cause the two enzymes to interact. In no case was any protein-protein allosterism detected. At most, transaminase activity was depressed about 10% in the presence of glucose-1-phosphate. Even this effect can be readily ascribed to the increased ionic strength in the assay mixture containing the glucose-1-phosphate which has been shown to depress transaminase activity.

DISCUSSION

DISCUSSION

The discovery of heterogeneity in muscle alanine aminotransferase is not surprising, considering the large number of enzymes and other proteins which have been shown to consist of several subforms. Although numerous examples can be cited, a few will suffice to illustrate this widespread phenomenon. Lactate dehydrogenase, the most thoroughly studied isozymic system, consists of five electrophoretically distinguishable fractions, composed of two primary subunits, designated M and H, which are combined together randomly in groups of four to form the active tetrameric structures.<sup>95</sup> The subunits are structurally and immunologically distinct and arise from different genetic alleles. Considerable differences in enzymatic activity as a function of substrate concentration, pH, temperature and other variables exist between the various isozymes. The distribution of these isozymes in the various tissues is consistent with the biochemical pathways and metabolic conditions existing in each tissue so that efficient utilization of each isozyme occurs.

The functionality of other isozymic systems is less well understood. Plasminogen, the zymogen that is converted to plasmin, the clot lysing enzyme, can be separated by affinity chromatography into two fractions that migrate as single but distinct bands on gel electrophoresis at pH 4.3.<sup>96</sup> When

examined by gel electrophoresis at pH 9.5 or by isoelectric focusing, however, each fraction separates into five isozymes with a distinct isoelectric pH range. All other physical and chemical criteria indicate complete identity of the two fractions. The amino acid compositions and number of amides in each original fraction were also indistinguishable, allowing no straightforward explanation for the isozymic variability, nor can any physiological function be ascribed to this multiplicity. This inexplicability is in fact the case for most isozymes, LDH not withstanding.

Rat red cell hemoglobin can be separated on pH 9.5 gel electrophoresis and isoelectric focusing into six fractions, each of which has the same molecular weight and amino acid composition.<sup>97</sup> However, in this case, the differences in the isoelectric points are ascribed to the difference in the number of "surface" carboxyl groups in each isozyme which can be esterified. The source of the variability is not identified, but blockage by amide or ester groups can be imagined as well as the more subtle variability in carboxyl group accessibility due to conformational differences in the isozymes. In other systems, carbamylation or acetylation of amino groups may play a role in isozyme generation.

The great sensitivity of isoelectric focusing in distinguishing closely related molecular species is highlighted in the work of Susor et al,<sup>98</sup> who showed that a number of presumably purified enzymes were in fact hetero-

geneous mixture of several isozymes. These enzymes included aldolase A, glyceraldehyde-3-phosphate dehydrogenase, yeast aldolase, yeast enolase, and pyruvate kinase. All other criteria of purity had indicated that these preparations were pure. That the generation of artifacts was not a result of the isofocusing process was clearly demonstrated by the presence of only one protein band in a sample of LDHM<sub>4</sub>, which by definition should be homogeneous.

Although no attempt was made to investigate the basis for the multiple electrophoretic forms of alanine aminotransferase, principally because of the difficulty of preparatively resolving them, a simple model which accounts for the known facts can be proposed. If it is assumed that five polypeptide chains of the same molecular weight, but slightly different ratios of cationic to anionic groups exist and combine randomly into dimers, then 15 possible variants can arise. This would more than account for the 12-14 observable bands on gel isoelectric focusing. Amino acid content need not differ among any of the polypeptide chains; charge differences may arise by any of the mechanisms described above. Obviously, purification of the various isozymes is necessary for any conclusions to be drawn. The various subforms of aspartate transaminase discussed in the Introduction, may also be explained by a similar model.

Enzyme heterogeneity may also explain the curious Arrhenius plot described earlier, in which 3 activation energies were obtained over the range of 12° to 42°C. Different sets of isozymes may become the dominant active forms within different temperature ranges, each set having its own characteristic activation energy. In this regard, the kinetic parameters determined in this investigation could very likely be the result of an averaging of the various isozyme activities at the temperature of 30°C at which these parameters were studied. Individual isozymes, examined at various temperatures, may demonstrate unique kinetic parameters.

Inhibition by fatty acids requires some comment. The fact that inhibition increases with increasing chain length points to the possibility that the enzyme active site contains a hydrophobic pocket of considerable length which binds hydrocarbon chains with an efficiency proportional to their length. Negative control of transaminase activity by fatty acids can be reasonably postulated by these results. Alternately, the inhibition may be simply due to the detergent-like properties of the long chain molecules, which may act to disrupt the transaminase structure in a non-specific manner. Whatever the mechanism, the net effect is the same.

Finally, the inability to demonstrate protein-protein allosterism between alanine aminotransferase and phosphorylase under a variety of conditions calls the conclusions of Bailin

et al into doubt. If, in fact, the conditions which generate such a complex in muscle tissue are physiologically unique, then the outlook for bringing about or stumbling upon this physiological state in experimental animals is not very bright. However, a more intensive effort at ascertaining the possible existence of such a complex is still justified, considering the opportunities it would present for studying allosteric interactions transmitted through perturbations between two proteins.

TABLES AND FIGURES

TABLE I  
Summary of Enzyme Purification Procedure

<u>Step</u>	<u>Protein Conc. mg/ml</u>	<u>Sp. Activity units/mg</u>	<u>Total Units</u>	<u>Volume - mls.</u>	<u>% Yield</u>
1. Initial Extract	24.7	.0355	21,950	25,000	100
2. Heated and Filtered Extract	9.6	.082	18,200	21,700	83
3.a) Ammonium Sulfate Precipitate (1st)	10.4	2.7	10,400	370	47.5(100)*
b) 0-270 mg/ml Supernatant	-	-	2,900	25,000	-
4. DEAE-Sephadex Funnel Filtrate	0.85	7.4	9,100	1,450	41.5(87.3)
85 5. Ammonium Sulfate Precipitate (2nd) 0-270 mg/ml	19.3	17.0	7,400	22.3	33.8(71.2)
6. DEAE-Sephadex Chromatography Eluant	0.85	74.5	6,670	106	30.2(63.6)
7. Ammonium Sulfate Precipitate (3rd) 205-255 mg/ml	9.1	97.5	6,210	7.0	28.3(59.6)
8. Hydroxylapatite Chromatography, Reduced Volume	4.1	265	5,110	4.7	23.2(48.9)

\*The initial extract contains the D-alanine sensitive transaminase which is subsequently discarded. The first ammonium sulfate precipitate is the first step in the procedure to contain only the D-alanine insensitive transaminase. Yields in parentheses are, therefore, those of the D-alanine insensitive transaminase.

TABLE II

Michaelis Constants and Maximal Velocities Obtained in 0.1M Phosphate-Albumin, pH 7.5, 30°C

<u>K<sub>alanine</sub></u>	<u>K<sub>ketoglutarate</sub></u>	<u>K<sub>glutamate</sub></u>	<u>K<sub>pyruvate</sub></u>
(40)	(0.61)	(16.5)	(0.56)
43mM*(46)	0.64mM*(0.67)	17.5mM*(18.5)	0.64mM*(0.71)

V<sub>f</sub>  
 (318)  
 \*\*323 (328)

V<sub>r</sub>  
 (90)  
 \*\*93 (95)

\*Average value

\*\*Average value, in micromoles/minute.mg

Values in parenthesis were calculated from two different secondary plots described by equations 3 and 4.

TABLE III

Inhibition by Keto, Mono and Dicarboxylic Acids of the Forward Reaction. Alanine at 50mM, Ketoglutarate at 2mM. Acids at 20 mM unless otherwise indicated.

<u>Acid</u>	<u>% Inhibition</u>	<u>Albumin Present</u>
Ketovalerate	81	Yes
Ketoisocaproate	75	Yes
Ketocaprylate	100	Yes
Mesoxalate	62	Yes
Phenylpyruvate	99	Yes
Malonate	8	Yes
Succinate	9	Yes
Malate	11	Yes
Adipate	18	Yes
Citrate	8	Yes
Levulinate	18	Yes
Acrylate	20	Yes
Maleate	17	Yes
Phenylacetate	31	Yes
Acetate	0	Yes
Propionate	13	Yes
Butyrate	38	Yes
Valerate	56	Yes
Caproate	68	Yes
Caprylate (2mM)	38	Yes
Caprate (2mM)	72	Yes
Laurate (0.2mM)	48	No
Myristate (.05mM)	40	No

Controls for inhibition of the coupling enzyme, LDH, by the various acids, were necessary and the data above reflect compensation for any effect on the LDH. Certain carboxylic acids could not be tested because they were either potent inhibitors or good substrates of LDH.

TABLE IV

Inhibition by Keto, Mono and Dicarboxylic Acids of the Reverse Reaction. Glutamate at 15mM, Pyruvate at 2mM. Acids at 20mM Unless Otherwise Indicated.

<u>Acid</u>	<u>% Inhibition</u>	<u>Albumin Present</u>
Ketovalerate	79	Yes
Ketobutyrate	54	Yes
Ketoisocaproate	73	Yes
Mesoxalate	42	Yes
Ketocaprylate	99	Yes
Phenylpyruvate	93	Yes
Malonate	4	Yes
Succinate	*	-
Malate	*	-
Adipate	18	Yes
Citrate	8	Yes
Levulinate	11	Yes
Acrylate	21	Yes
Maleate	19	Yes
Phenylacetate	43	Yes
Acetate	1	Yes
Propionate	13	Yes
Butyrate	42	Yes
Valerate	57	Yes
Caproate	64	Yes
Oxaloacetate	19	Yes
Oxalate	9	Yes
Caprylate (2mM)	37	Yes
Caprate (2mM)	68	Yes
Laurate (0.2mM)	15	Yes
Myristate (0.2mM)	24	Yes
Laurate (0.2mM)	36	No
Myristate (0.05mM)	31	No

Controls for inhibition of activity with the coupling enzyme, GLDH, by the various acids were necessary and the data above reflect compensation for any effect on the GLDH.

---

\*Could not be measured because of strong inhibition of GLDH.

TABLE V

Inhibition by Amino Acids of the Forward Reaction. Alanine at 50mM, Ketoglutarate at 2mM. Albumin Present in All Reaction Mixtures. All Amino Acids at 50mM Unless Otherwise Indicated.

<u>Amino Acid</u>	<u>% Inhibition</u>
L-valine	24
L-leucine	19
L-isoleucine	27
L-proline	64
D-L-phenylalanine (20mM)	15
(40mM)	26
L-tryptophan (20mM)	36
(40mM)	55
glycine	0
L-serine	10
D-L-threonine (100mM)	4
L-cysteine	89
L-tyrosine (2mM)	2
L-asparagine	9
L-glutamine	13
L-aspartic acid	5
L-lysine	5
L-histidine	14
L-arginine	7
L-hydroxyproline	2
D-L-methionine (100mM)	33
$\alpha$ -aminoisobutyric acid	8
D-L- $\alpha$ -aminovaleric acid (100mM)	37
$\beta$ -alanine	0

TABLE VI

Inhibition Constants for Various Inhibitors of Alanine Aminotransferase. All Assays Performed in 0.1M Phosphate, pH 7.5, at 30°C.

<u>Inhibitor</u>	<u>Reaction Direction</u>	<u>Albumin Present</u>	<u>Type Of Inhibition</u>	<u>K<sub>I</sub></u>
Caprate	Reverse	No	Competitive with keto acid	0.42mM
Caprate	Reverse	No	Non-competitive with amino acid	0.93mM
Laurate	Reverse	No	Competitive with keto acid	0.21mM
Laurate	Reverse	No	Non-competitive with amino acid	0.34mM
Laurate	Forward	No	Competitive with keto acid	0.12mM
Laurate	Forward	No	Non-competitive with amino acid	0.26mM
Myristate	Reverse	No	Competitive with keto acid	0.03mM
Myristate	Reverse	No	Non-competitive with amino acid	0.10mM
Phenylpyruvate	Reverse	No	Competitive with keto acid	0.64mM
Phenylpyruvate	Reverse	No	Competitive with amino acid	1.19mM
Phenylpyruvate	Forward	No	Competitive with keto acid	0.40mM
Phenylpyruvate	Forward	No	Competitive with amino acid	1.05mM
Cysteine	Reverse	Yes	Non-competitive with amino acid	3.8mM
Cysteine	Reverse	Yes	Uncompetitive with keto acid	—
Cysteine	Forward	Yes	Non-competitive with amino acid	5.2mM
Cysteine	Forward	Yes	Uncompetitive with keto acid	—
Proline	Reverse	Yes	Competitive with amino acid	13mM
Proline	Reverse	Yes	Uncompetitive with keto acid	—
Proline	Forward	Yes	Competitive with amino acid	10.4mM
Proline	Forward	Yes	Uncompetitive with keto acid	—

Fig. 1 DEAE-Sephadex A-50 chromatography. Conditions as described in the text. 7.5 ml fractions were collected.

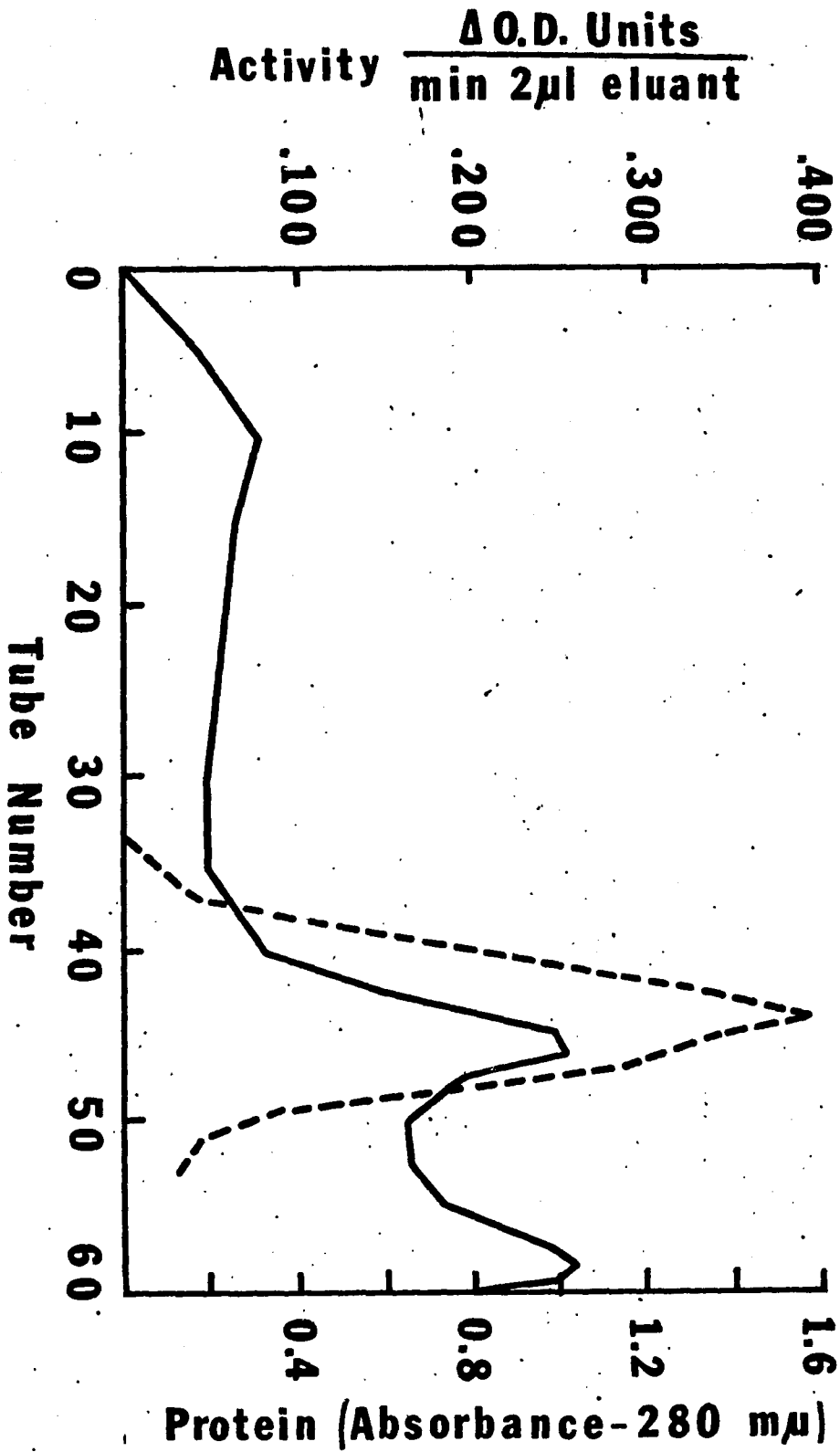
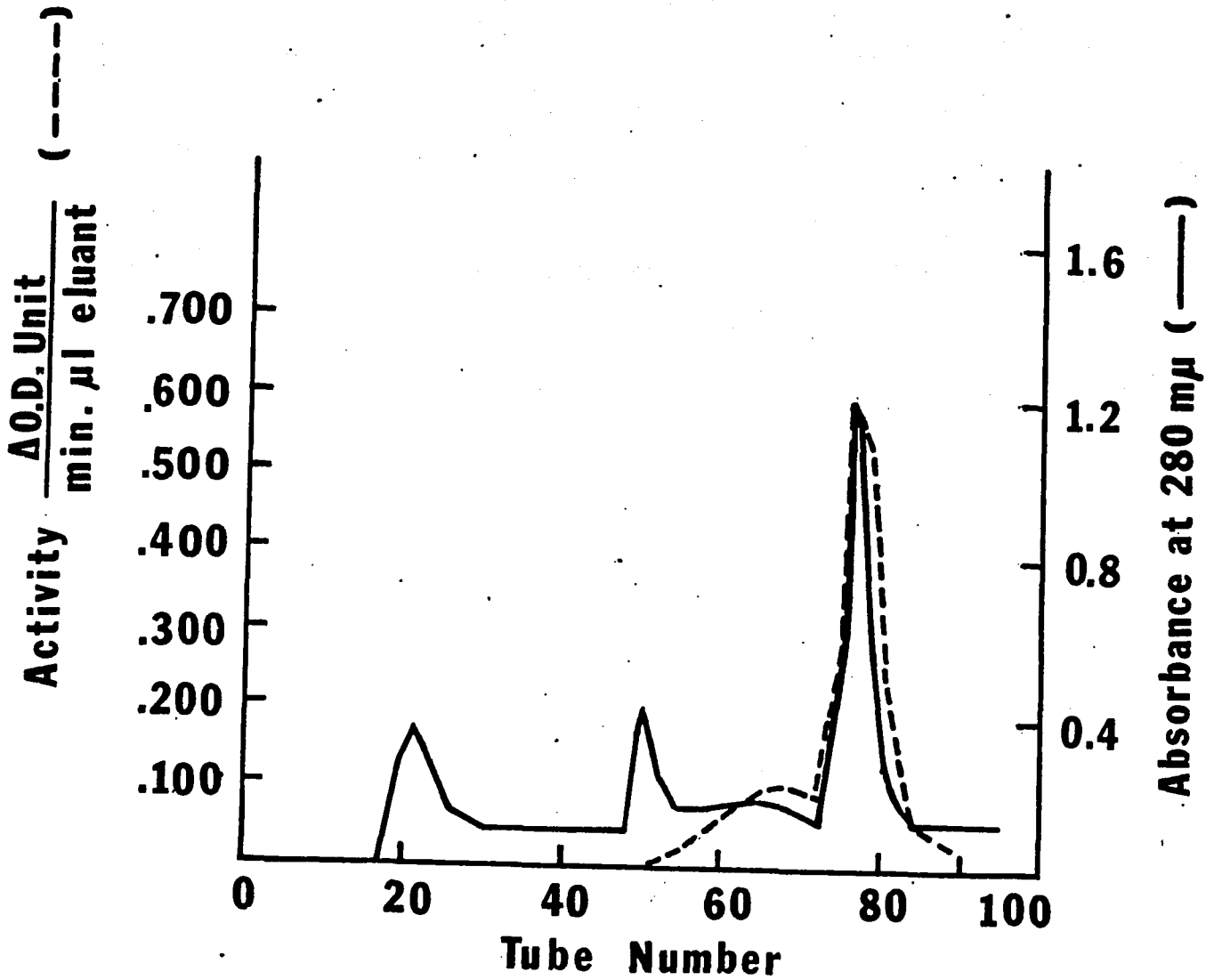


Fig. 2 Hydroxylapatite chromatography. Conditions as described in the text. Two ml fractions were collected. 1 microliter of column eluant was used in the standard assay.



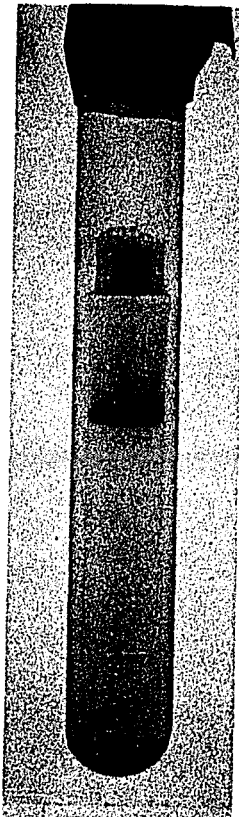
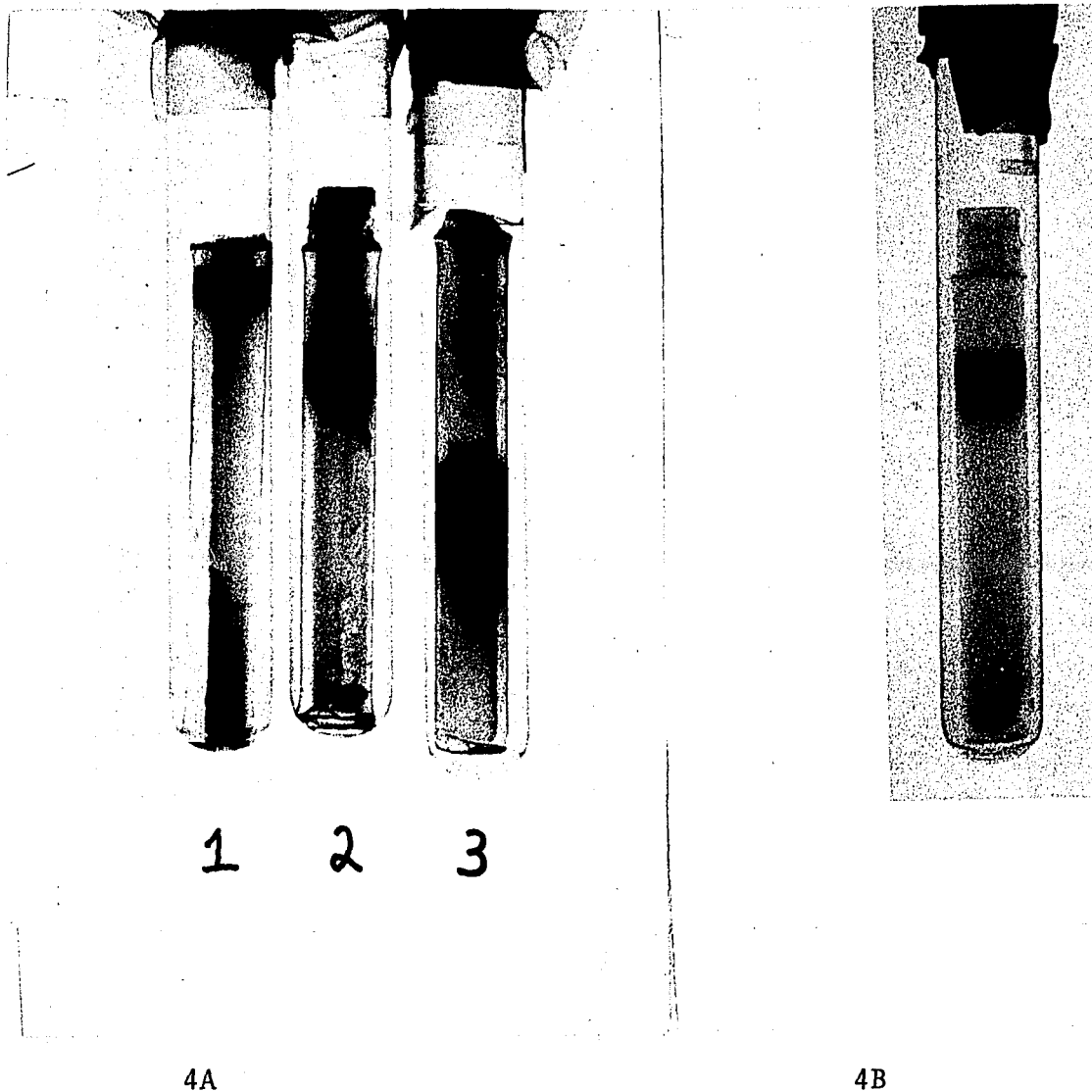


Fig. 3

Disc gel electrophoresis of hydroxylapatite purified enzyme (sp. act.-265) at pH 4.3. See Methods section for details. Approximately 30 ug of protein was applied. Stained with Amido Black. Electrophoresis performed at 4 mamp/gel for 1 hour.



4A

4B

Disc gel electrophoresis - pH 9.5. See Methods for details. Stained with Coomassie Blue.

- Fig. 4a
1. 9 ug. of protein applied. Electrophoresis was for 75 minutes at 2 mamps/gel.
  2. 9 ug. Electrophoresis for 6 hours at 1 mamp/gel.
  3. 9 ug. Electrophoresis for 15 hours at 1 mamp/gel.
- Fig. 4b
- 35 ug. applied. Electrophoresis for 3 hours at 2 mamps/gel.

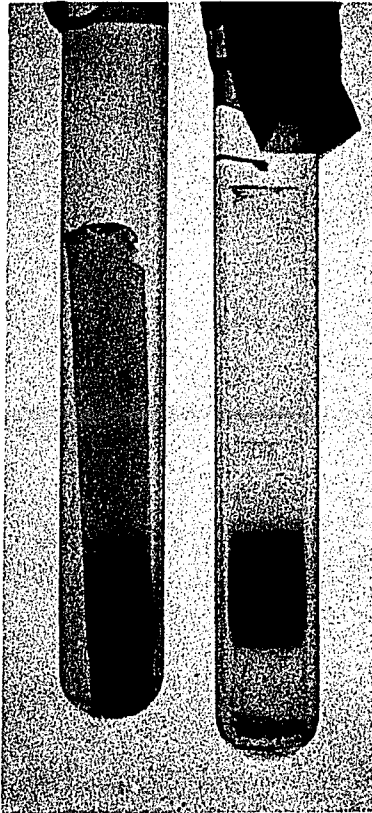


Fig. 5

Isoelectric focusing (pH 3-10) of hydroxylapatite purified enzyme (sp. act.-265) 60 ug protein applied to each gel. See Methods for details. Each gel contains enzyme isolated from a different preparation.

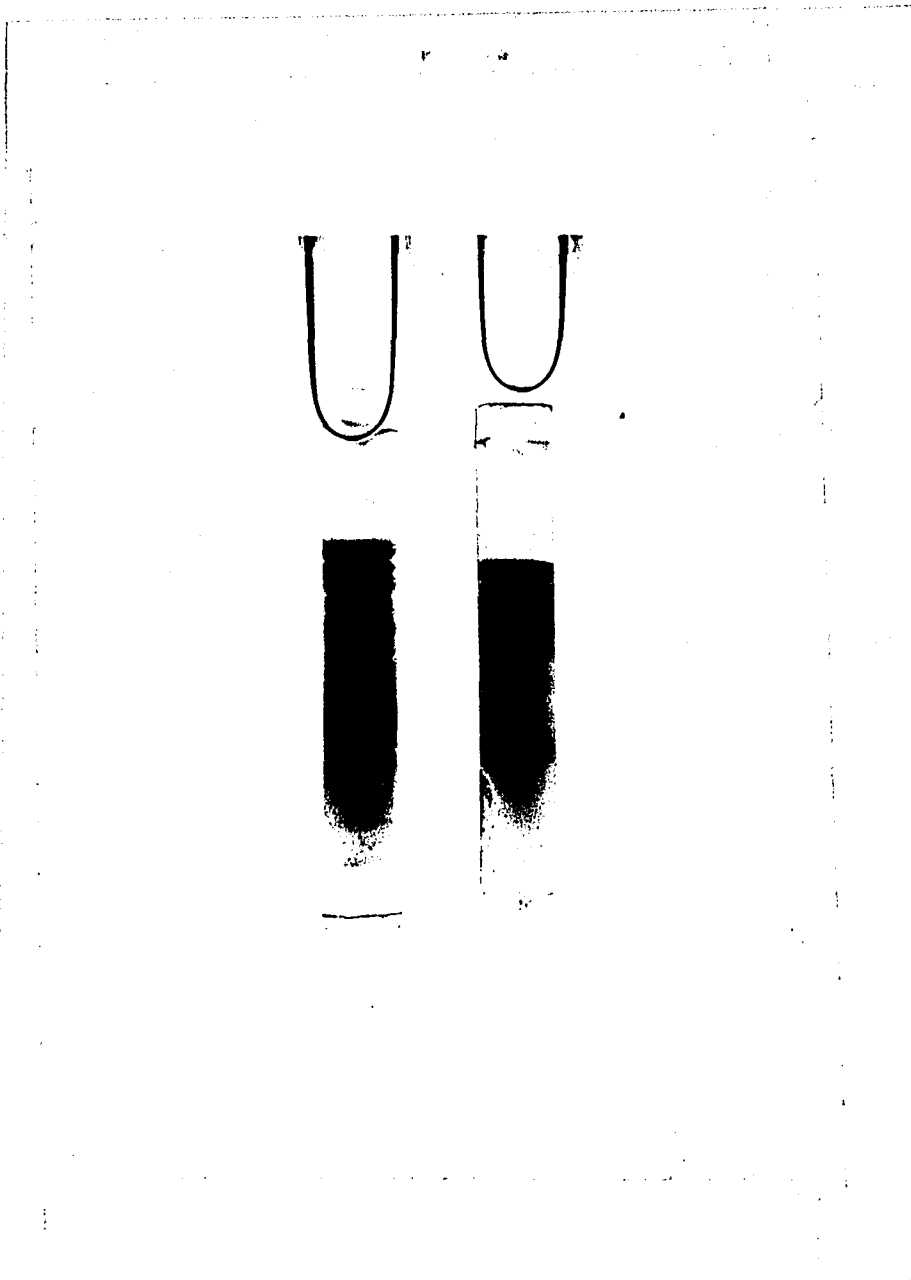


Fig. 6

Isoelectric focusing (pH 7-9) of hydroxylapatite purified enzyme (sp. act.-265). 60 ug protein applied to each gel. See Methods for details. Each gel contains enzyme isolated from a different preparation.

Fig. 7 Activity vs slice number for pH 7-9 isoelectric focusing gel.

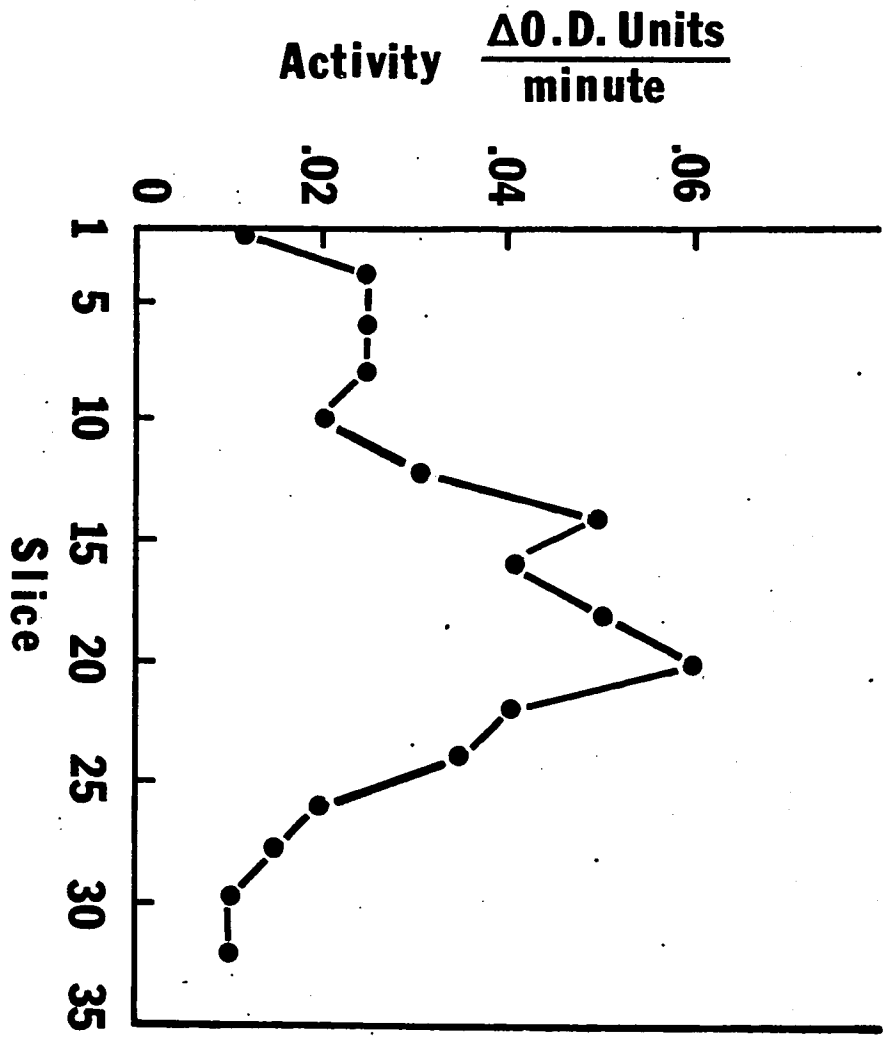
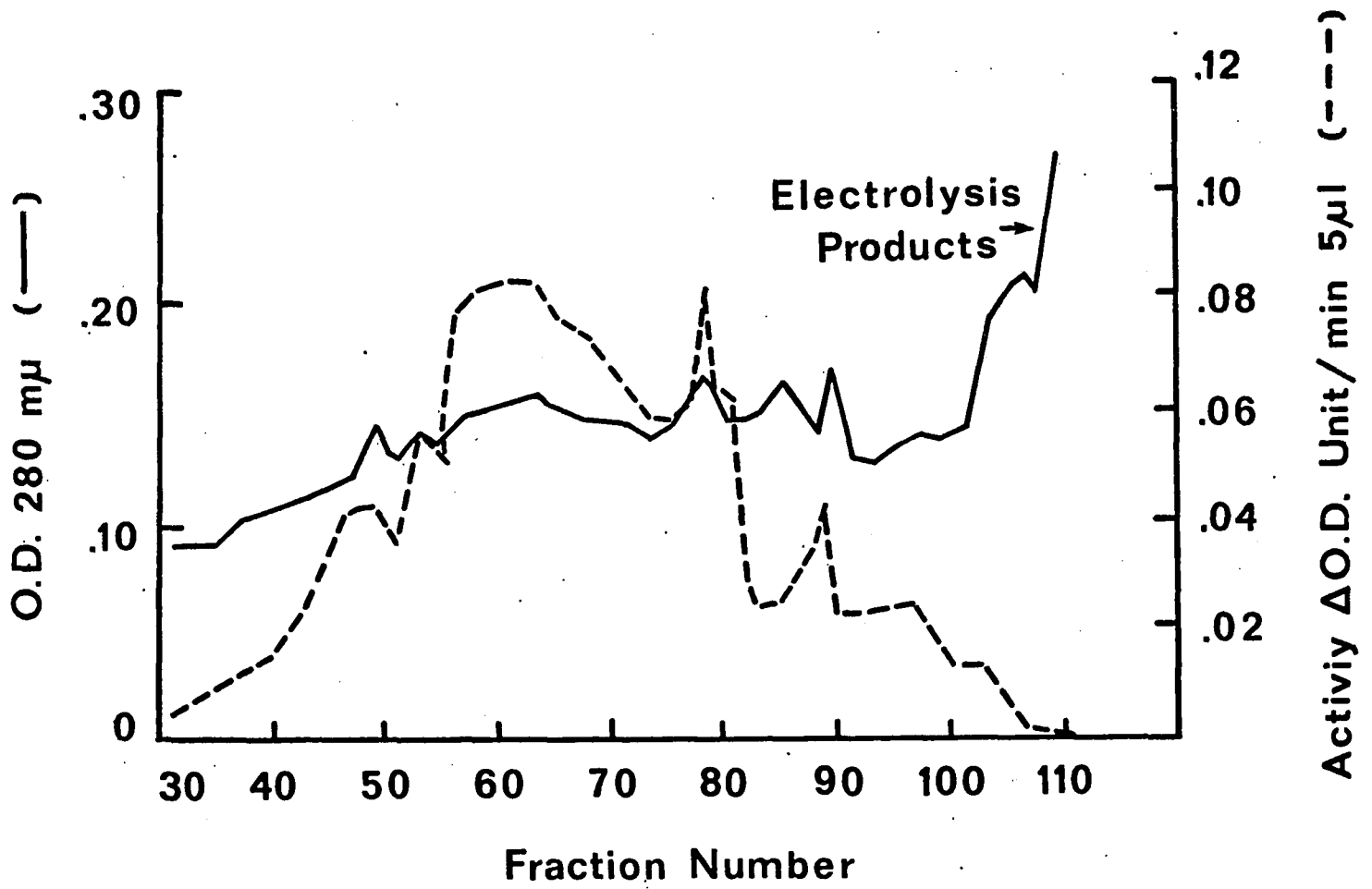


Fig. 8 Preparative isoelectric focusing (pH 7-9).  
pH increases from right to left, see Methods  
for details.



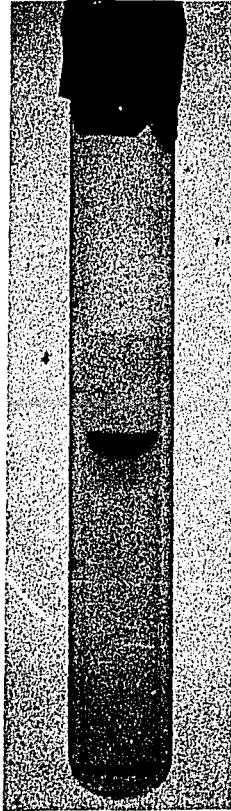
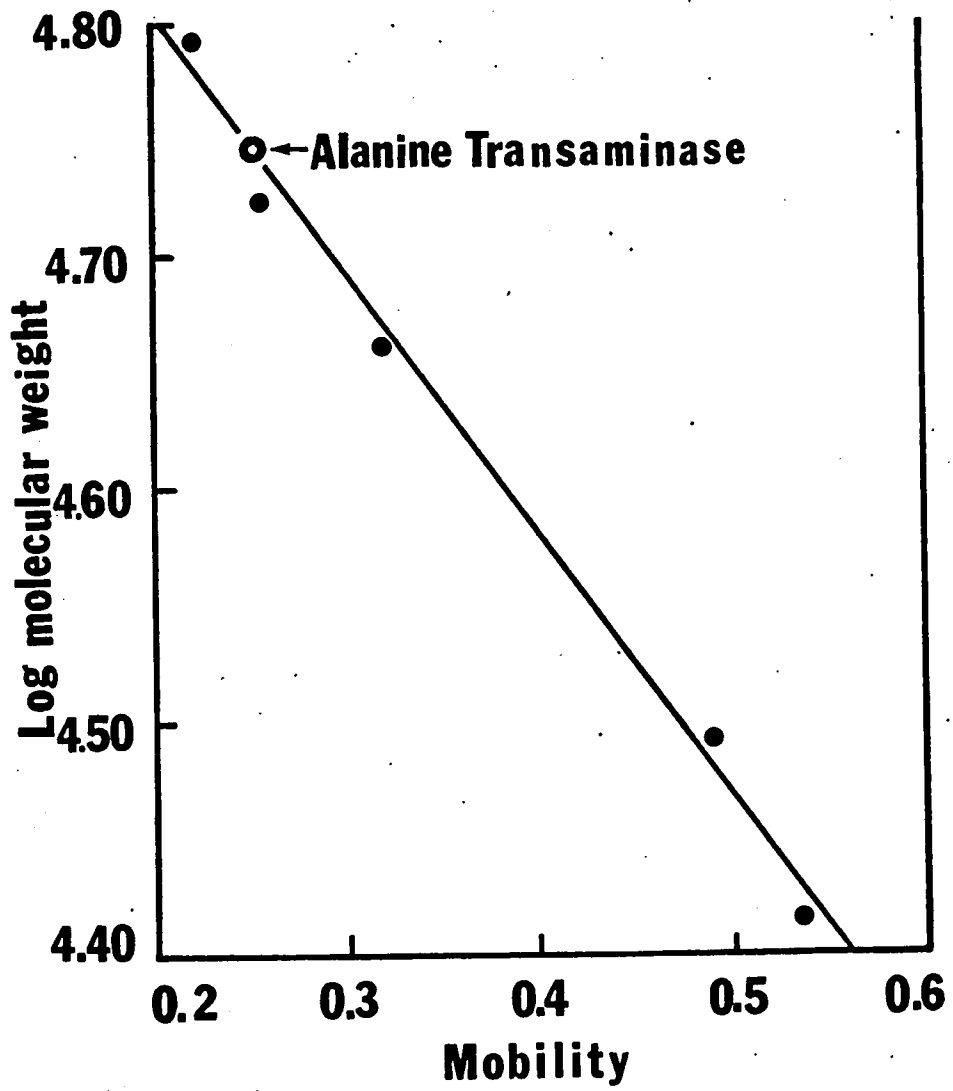


Fig. 9

SDS gel electrophoresis of hydroxylapatite purified enzyme (sp. act.-265). See Methods for procedure. 5 ug of protein applied. Stained with Coomassie Blue.

Fig. 10 Mobility of alanine aminotransferase and 5 marker proteins on 10% acrylamide - SDS gels. Markers - bovine albumin (67,000); glutamate dehydrogenase (53,000); ovalalbumin (46,000); pepsin (35,000) chymotrypsinogen (25,000). Corrected according to Dunker and Reuckert.<sup>90</sup>



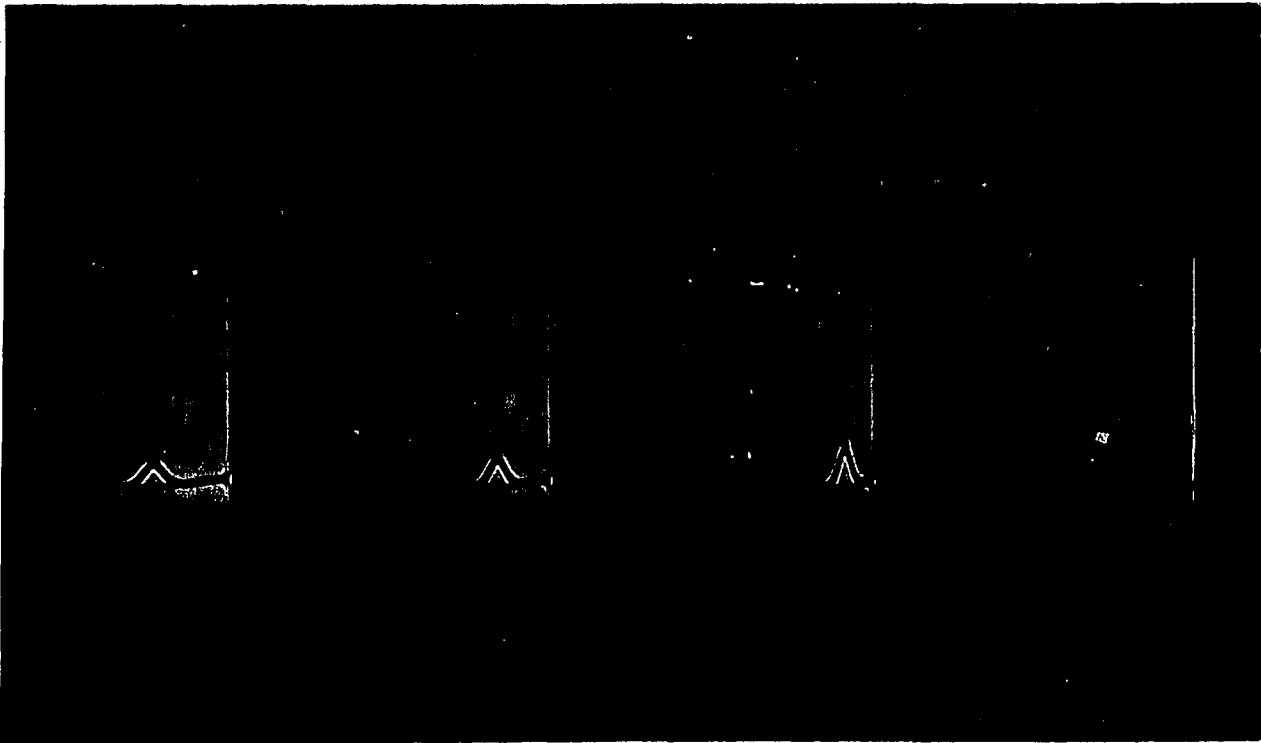


Fig. 11

Sedimentation velocity of hydroxylapatite purified enzyme. Enzyme at 2.5 mg/ml in .05M phosphate, .001M EDTA, .002M DTT, pH 7.5. Centrifugation at 60,000 RPM and 25°C. Sedimentation is from right to left. Photographs taken every 16 minutes.

Fig. 12 Plot of  $\ln$  (peak position) vs time for sedimentation velocity of purified enzyme at 2.35 mg/ml. Centrifugation at 60,000 RPM and 20°C.

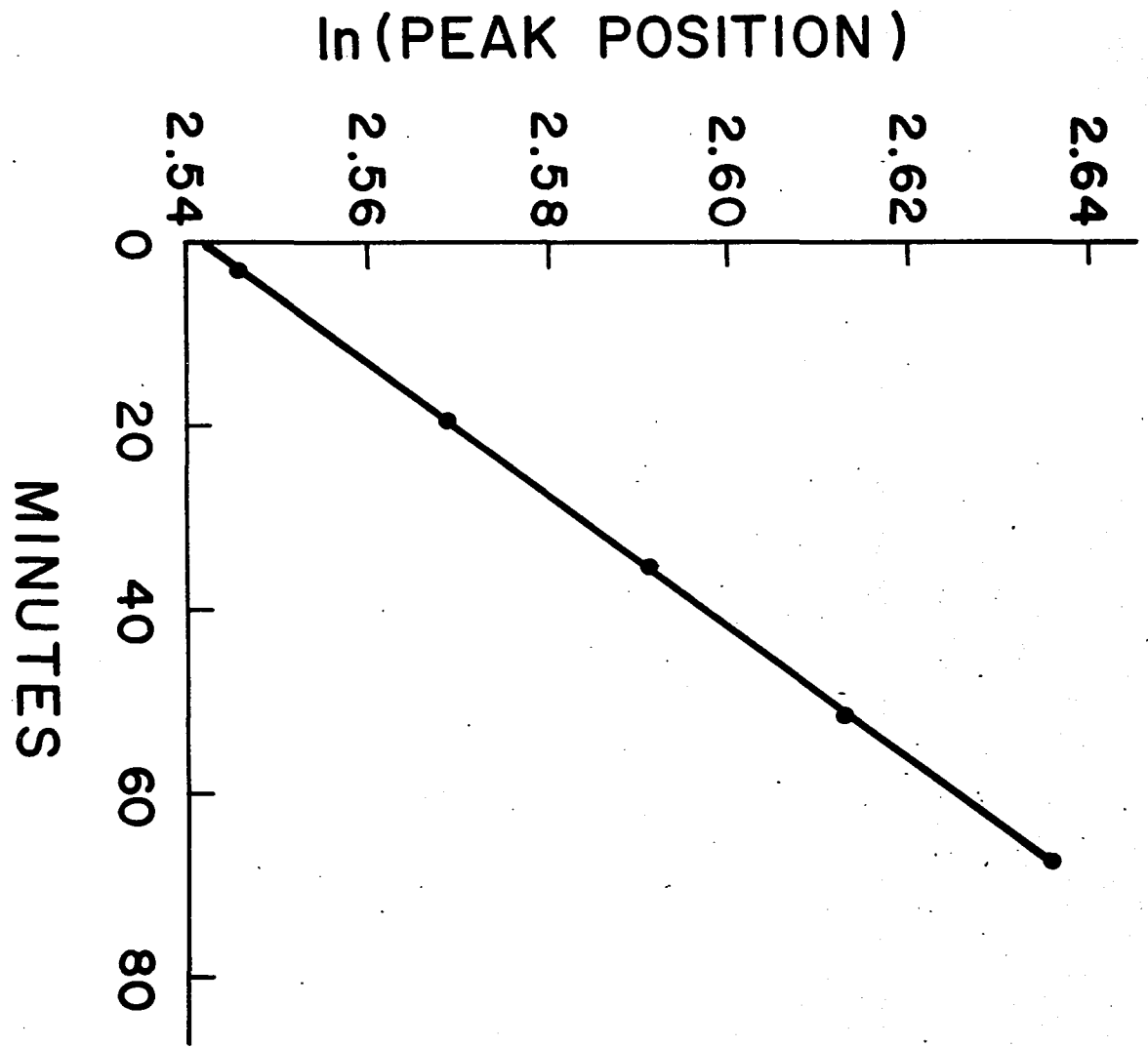


Fig. 13 Plot of  $S_{20}^{\circ,w}$  at several concentrations of protein.

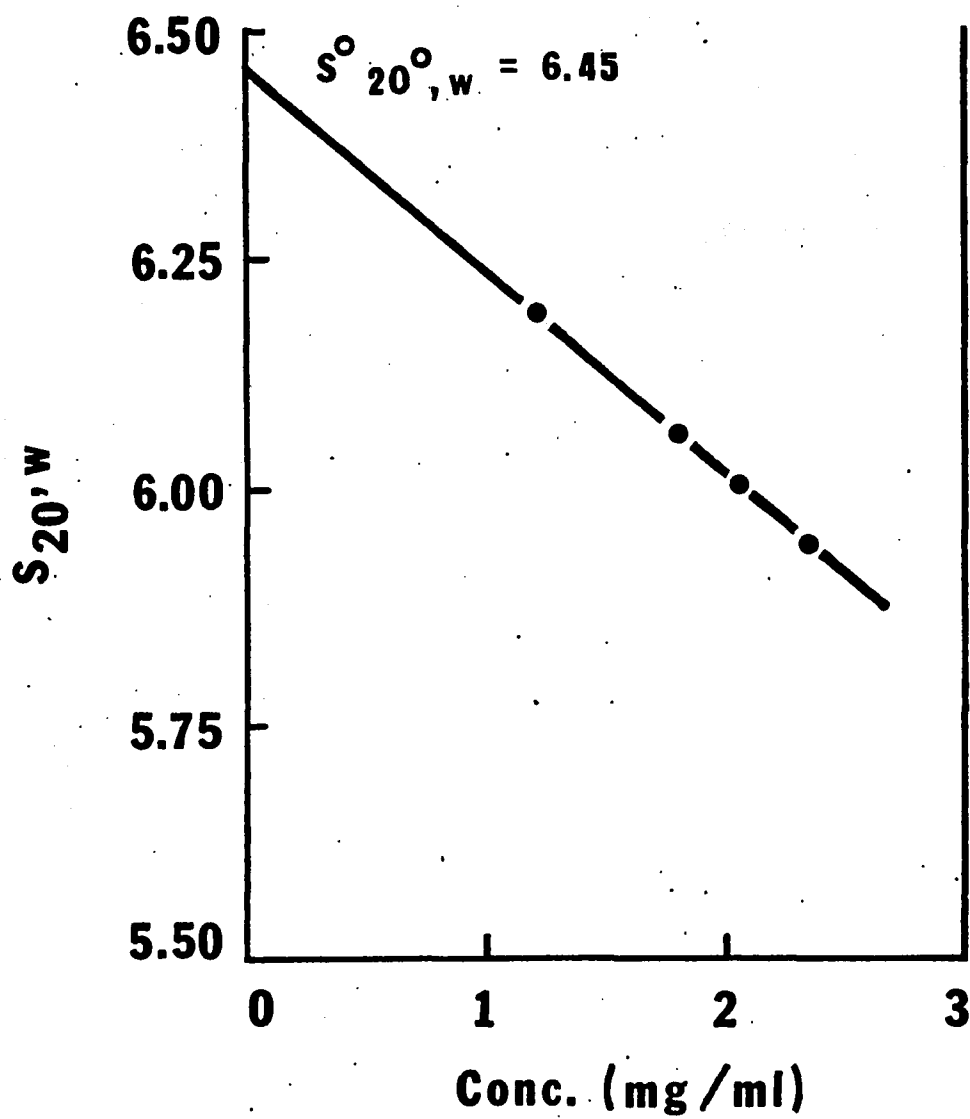


Fig. 14 Equilibrium sedimentation of 0.34 mg/ml purified alanine aminotransferase. Ordinate -  $\ln$  fringe displacement. Abscissa - (distance from center of rotor)<sup>2</sup>. Speed - 16,020 rpm. Temperature - 20.2°C. The molecular weight calculated from this determination is 108,200.

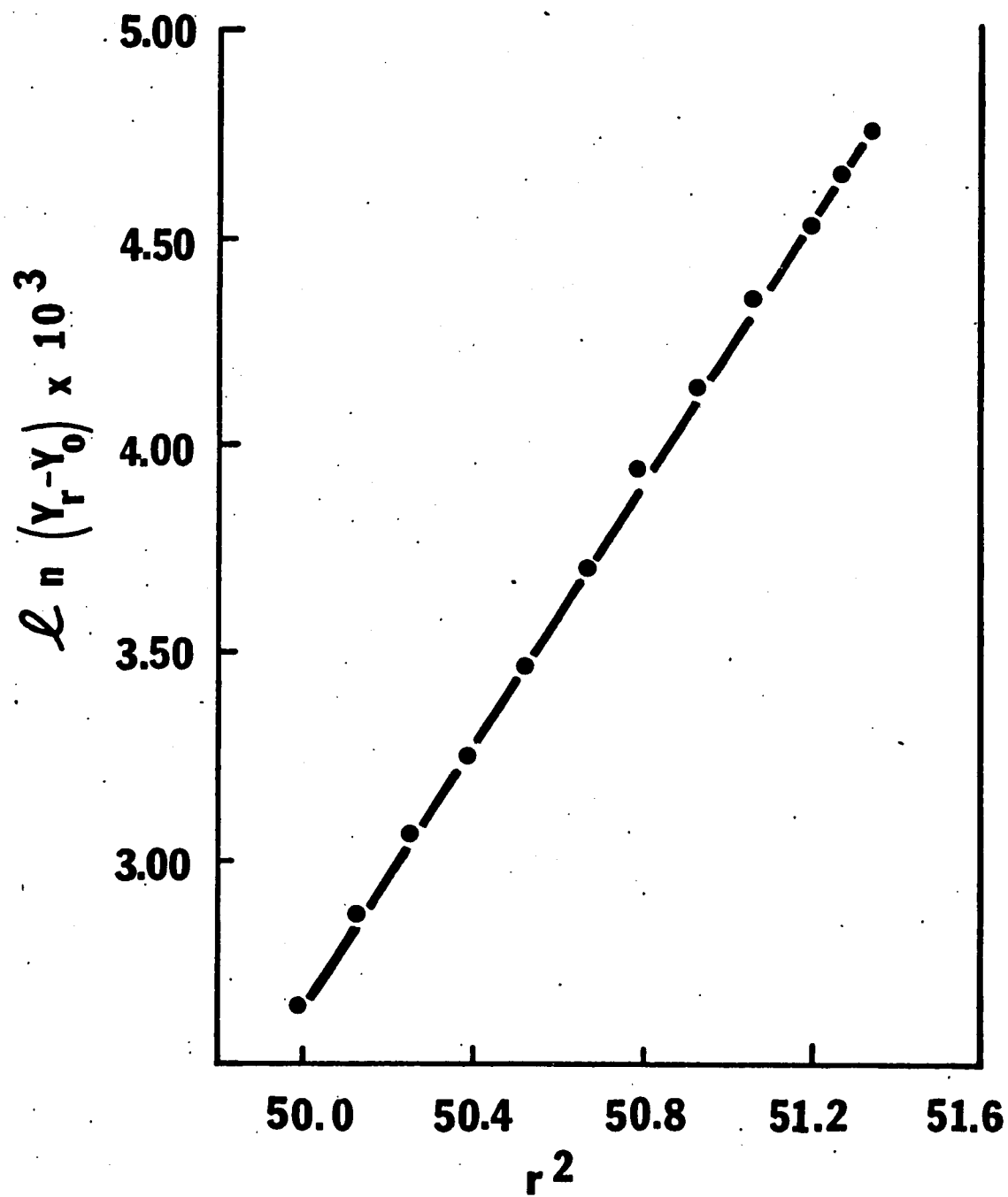


Fig. 15 Fluorescence Intensity vs PLP. See Methods for details.

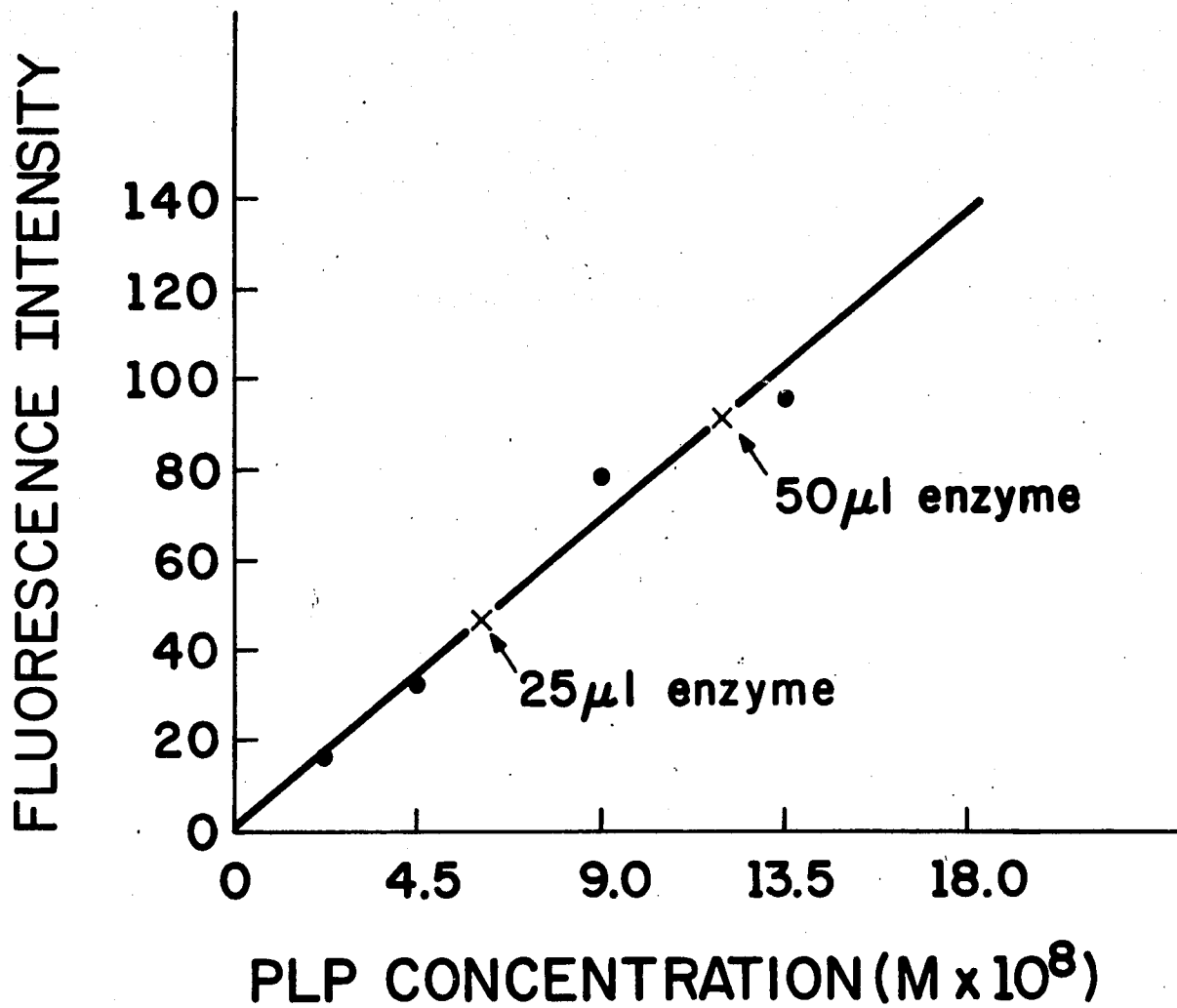


Fig. 16 Loss of enzyme activity with PCMB. See Methods for experimental details. The points are the average of 3 determinations.

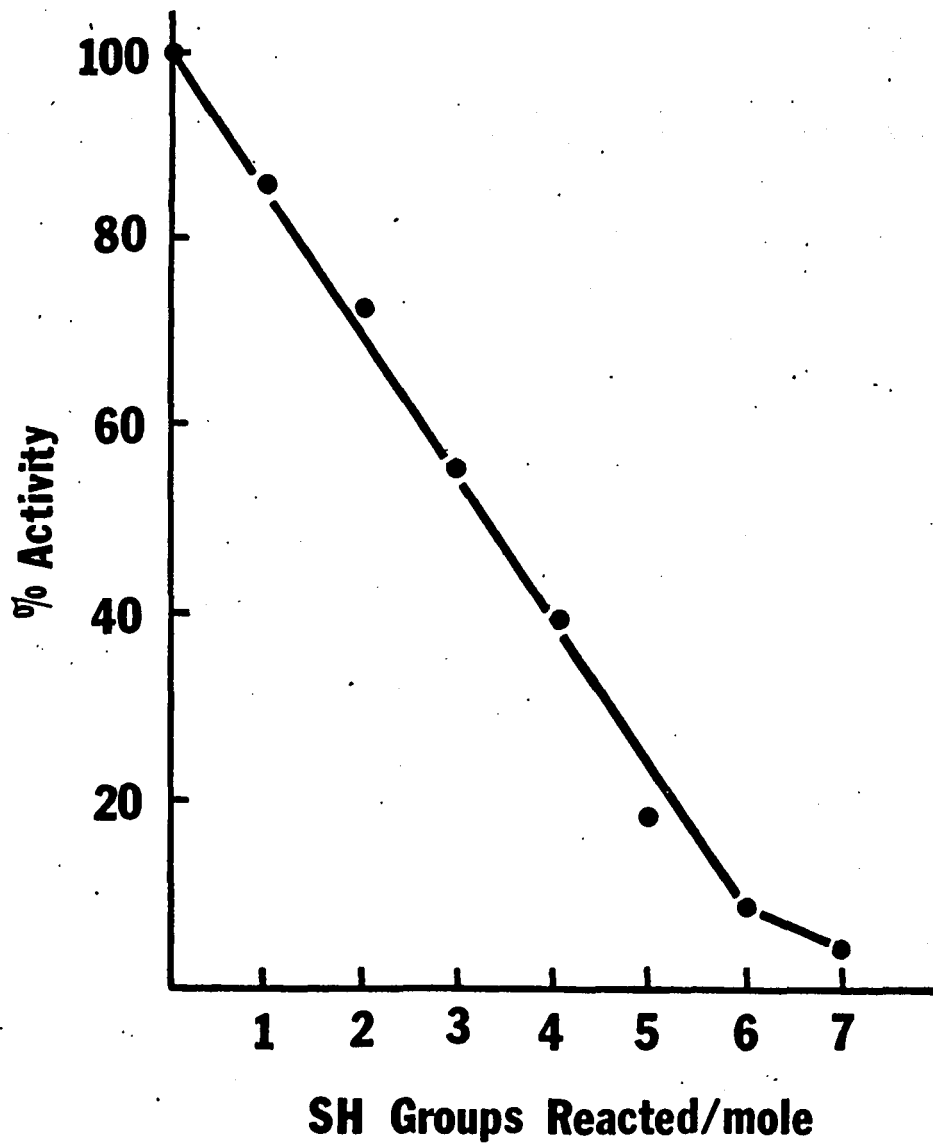


Fig. 17 Spectra of alanine aminotransferase

- A. .05M phosphate, .001M EDTA, .001M DTT,  
pH 7.0
- B. same as A + 0.2M L-alanine

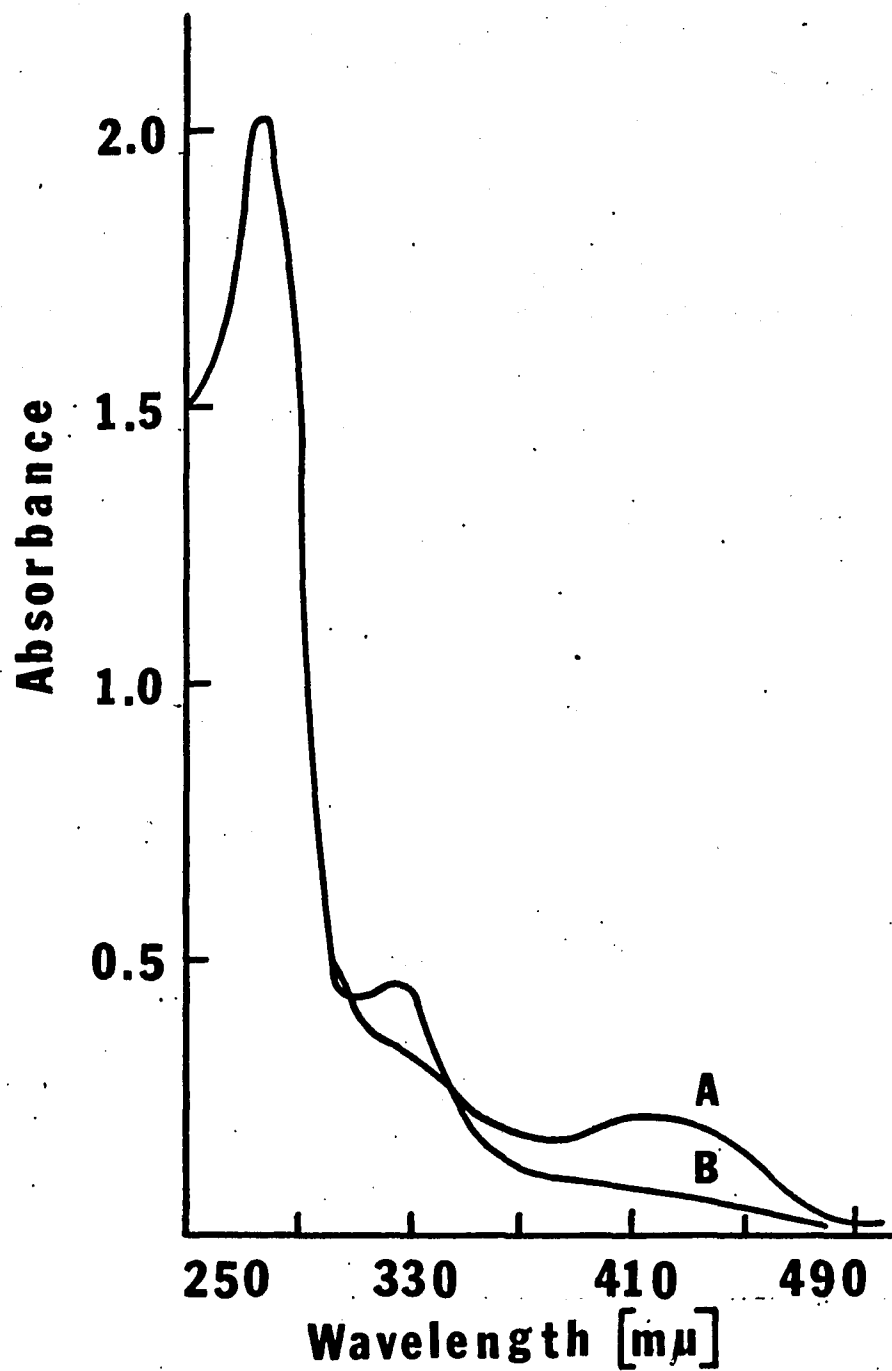


Fig. 18 Effect of pH on the spectrum of alanine aminotransferase  
Buffer - .05M phosphate, .001M EDTA, .001M DTT  
pH adjusted with 1M Na<sub>2</sub>CO<sub>3</sub> and 1M acetic acid

- A - pH 6.5
- B - pH 7.0
- C - pH 7.5
- D - pH 8.0
- E - pH 8.5

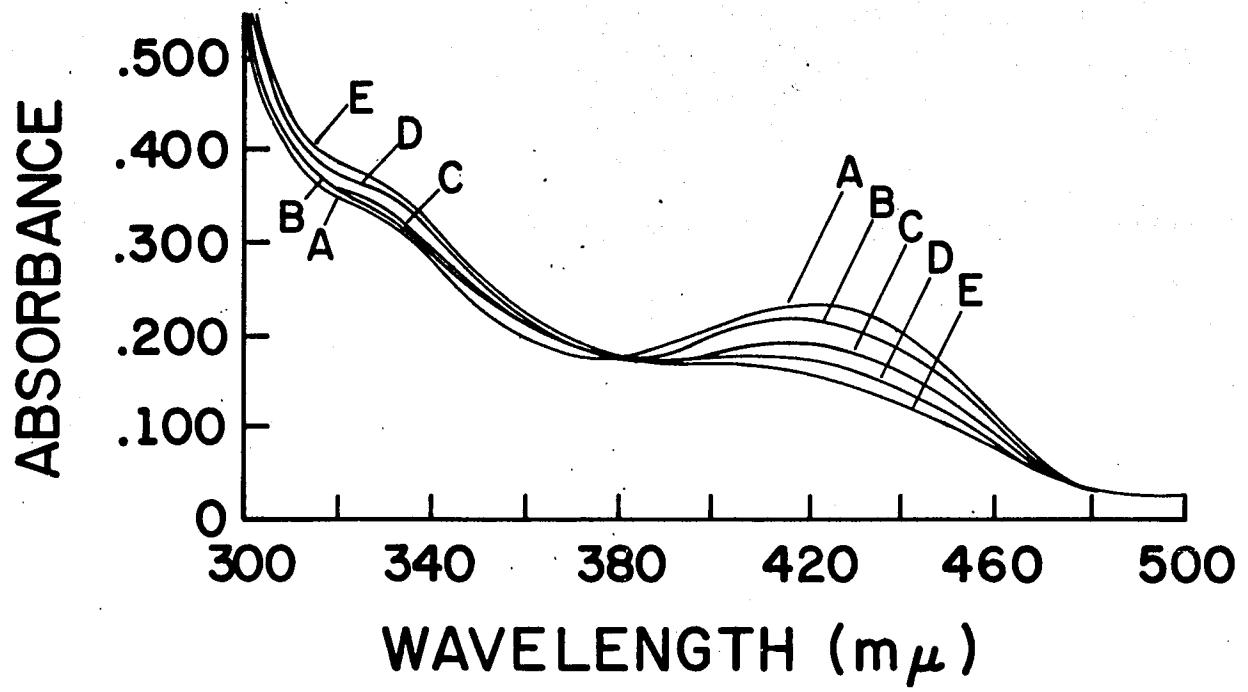
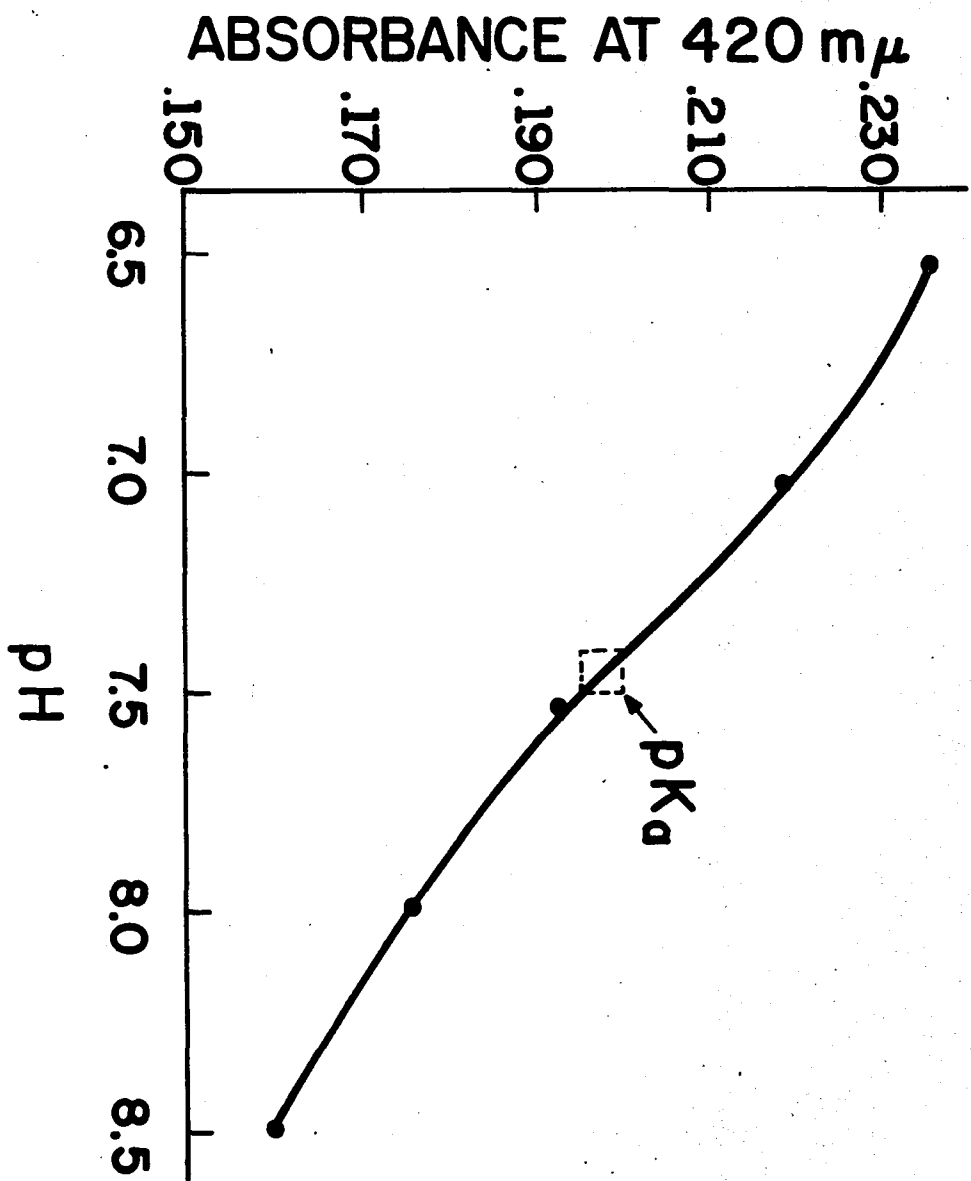
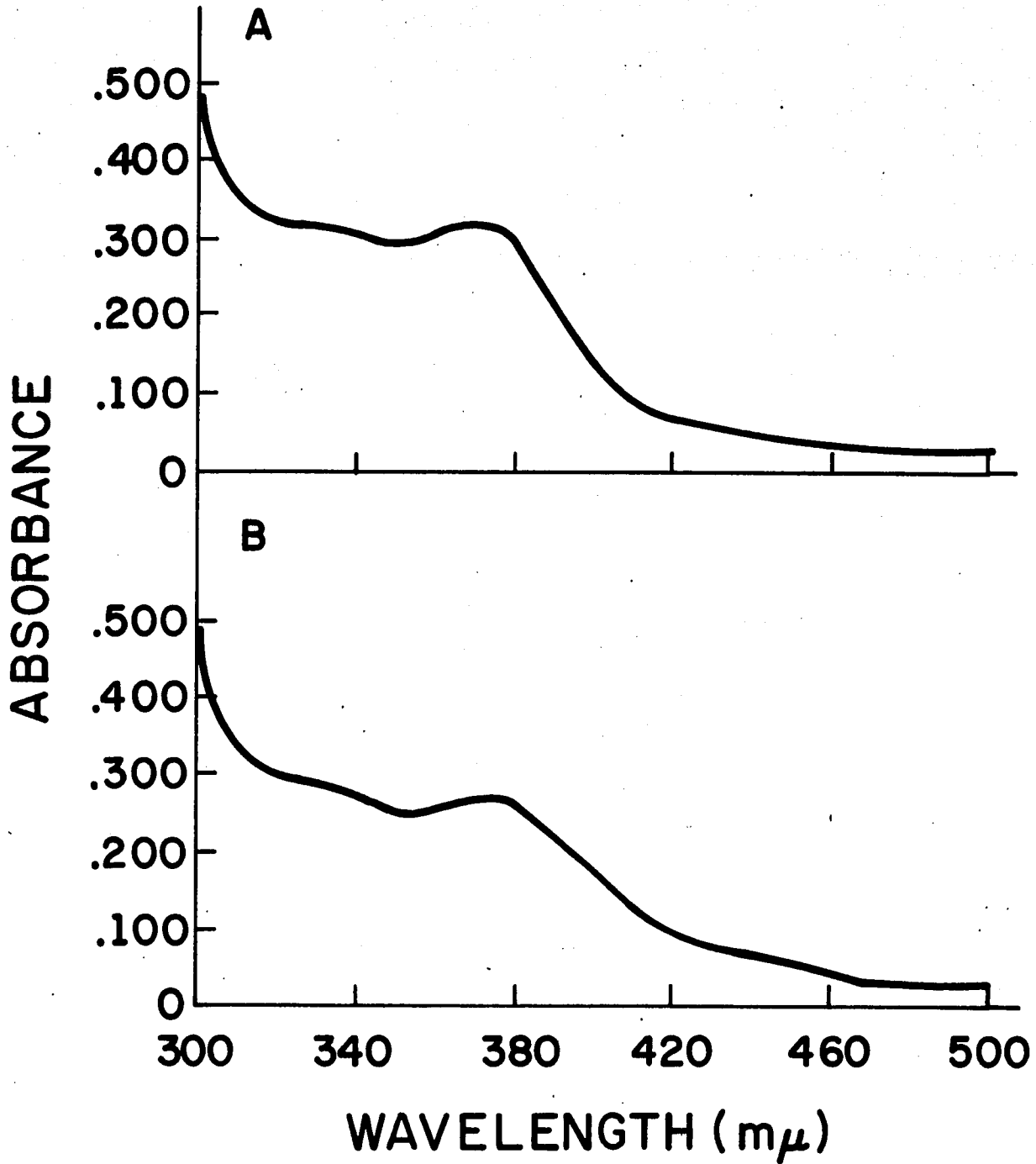


Fig. 19 pKa determination. Absorbancies at 420 m $\mu$  peak from Fig. 18 plotted vs pH.



- Fig. 20A Spectrum of alanine aminotransferase in the presence of  $1 \times 10^{-5}$  M aminooxyacetate. Buffer as in Fig. 17.
- Fig. 20B Spectrum of alanine aminotransferase in the presence of 0.1M L-proline. Buffer as in Fig. 17.



- Fig. 21 a) Enzyme activity vs pH. Assay conditions - .066M phosphate, 100mM alanine, 10mM ketoglutarate, with albumin.  $\mu=0.25$ , adjusted with KCl.
- b) same as a) +  $1 \times 10^{-7}$ M aminooxyacetate
- c) same as a) + 20mM L-proline
- d) same as a) + 1.5mM phenylpyruvate

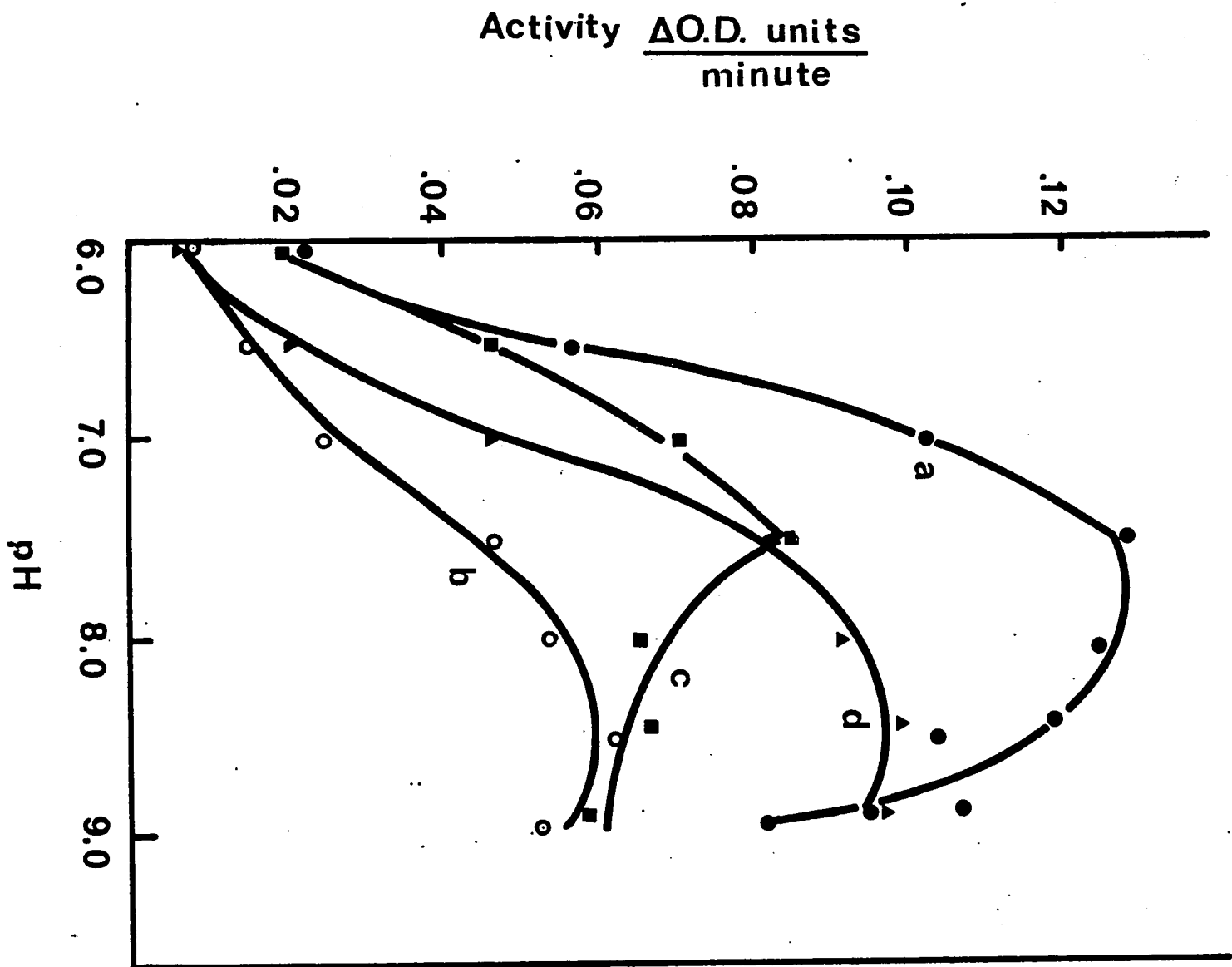


Fig. 22 Per cent inhibition by aminoxyacetate vs pH.  
Conditions as in Fig. 21.

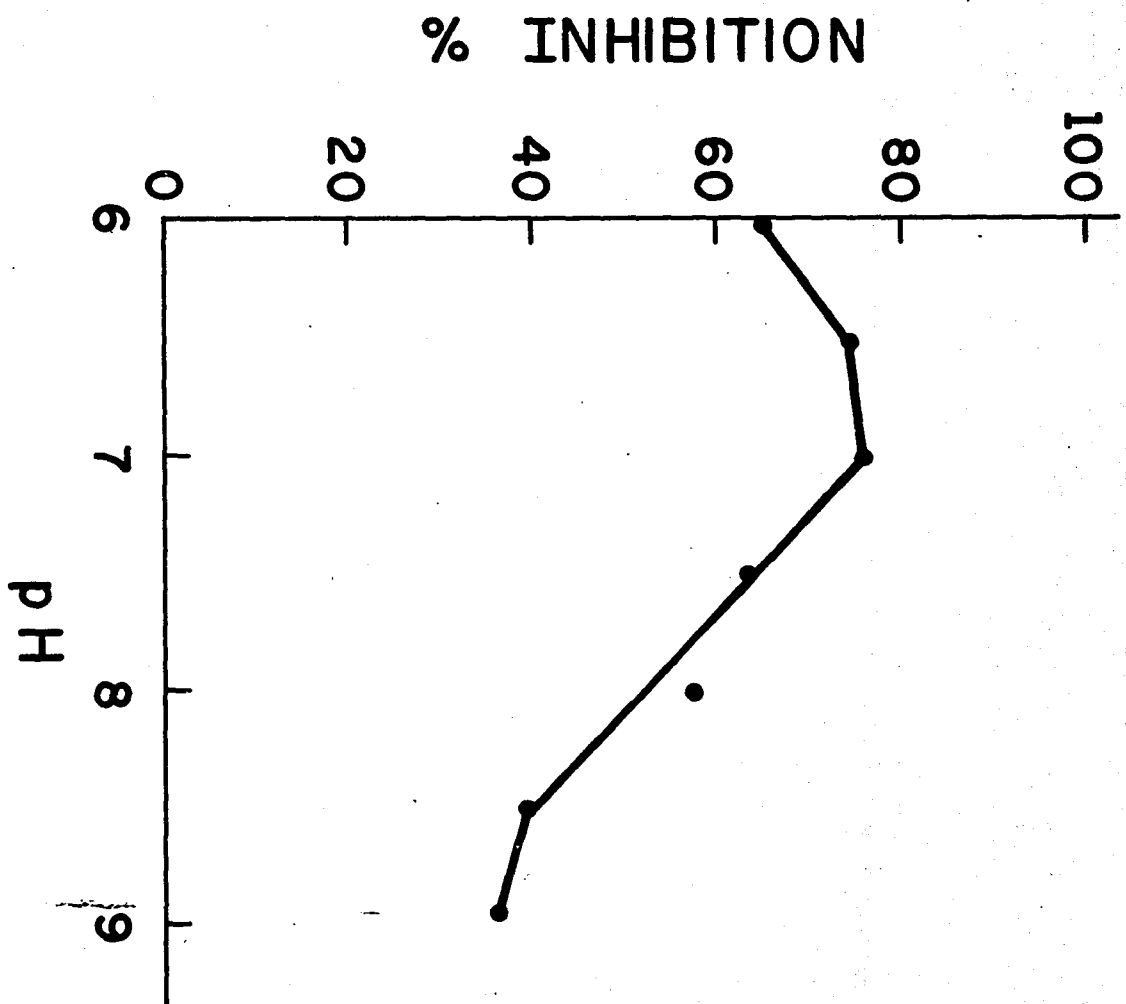


Fig. 23 Per cent inhibition by proline vs pH. Conditions as in Fig. 21.

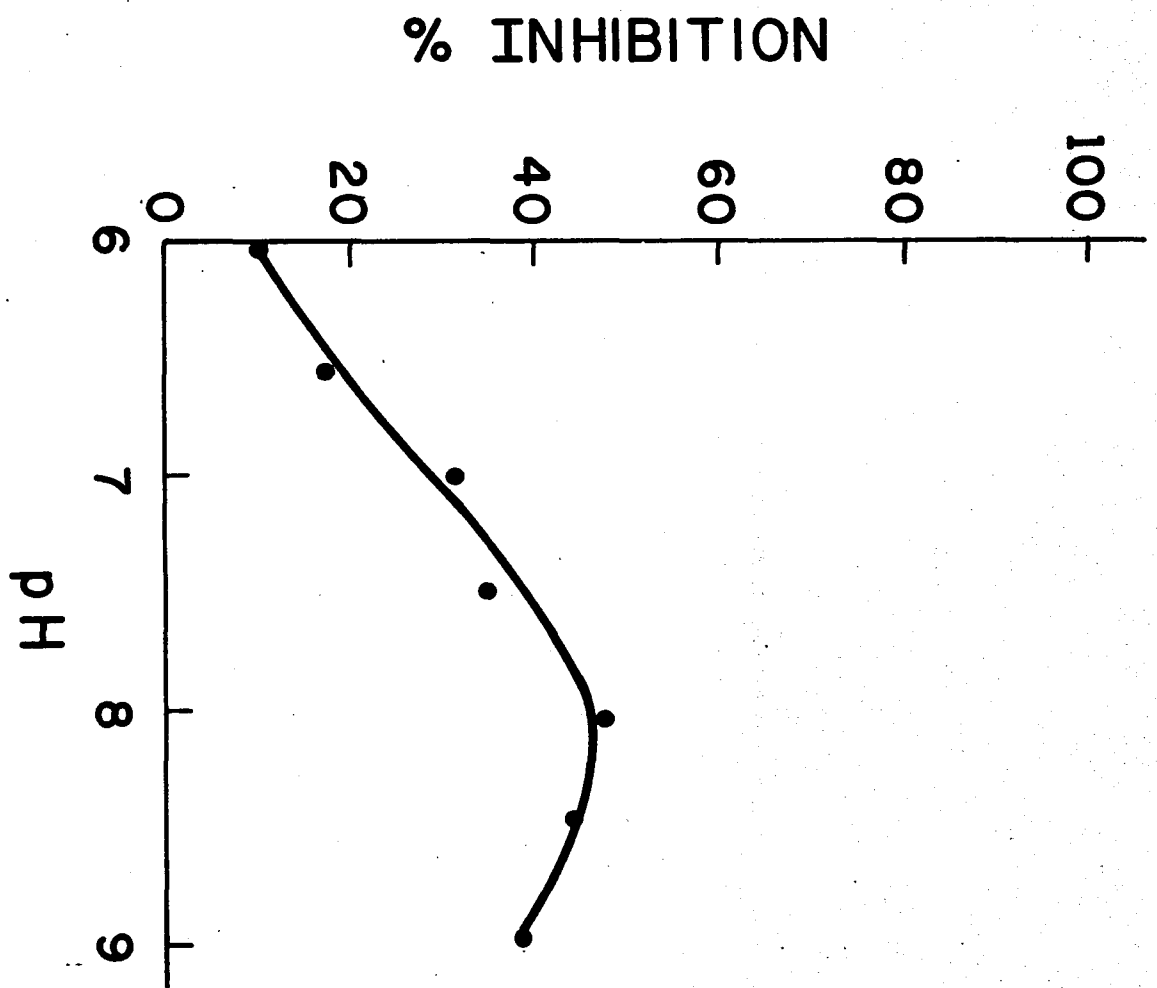


Fig. 24 Per cent inhibition by phenylpyruvate vs pH.  
Conditions as in Fig. 21.

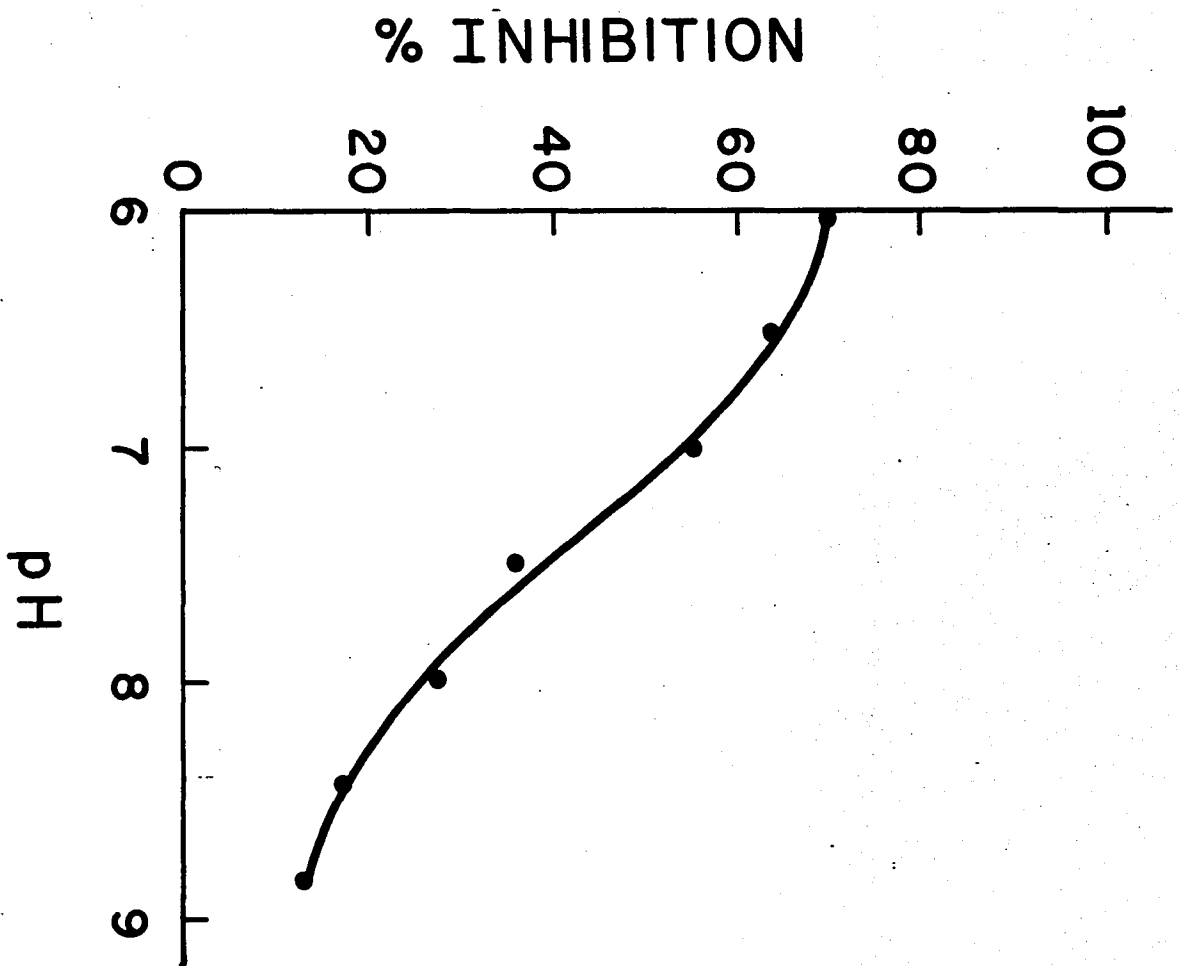


Fig. 25a Activity vs ionic strength. Reaction mixture contained .01M phosphate with albumin, 50mM alanine, 1mM ketoglutarate + KCl to adjust ionic strength to indicated values. Assays performed at 30°C and pH 7.5.

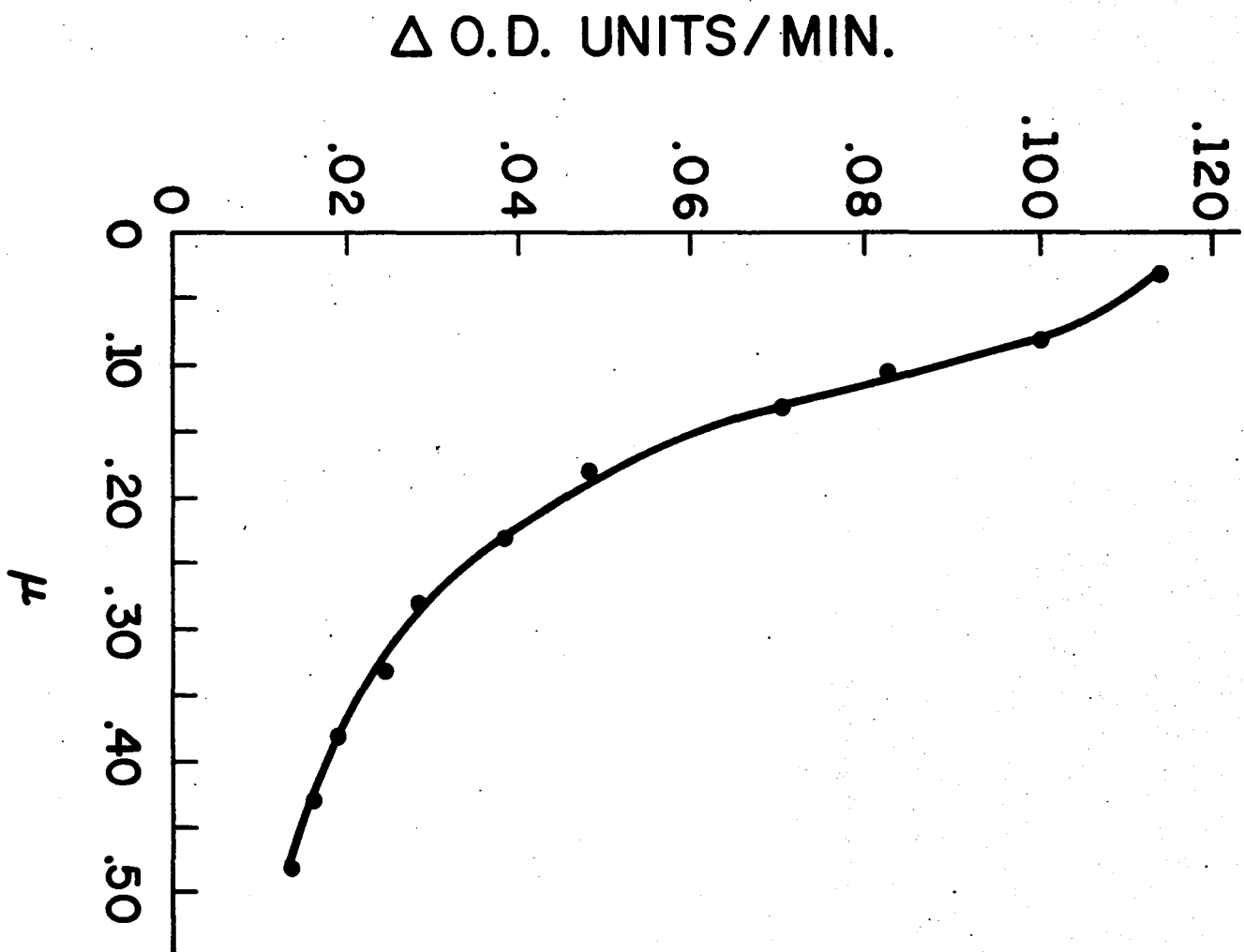


Fig. 25b Log activity vs the square root of the ionic strength.  
Data of Fig. 25a replotted.

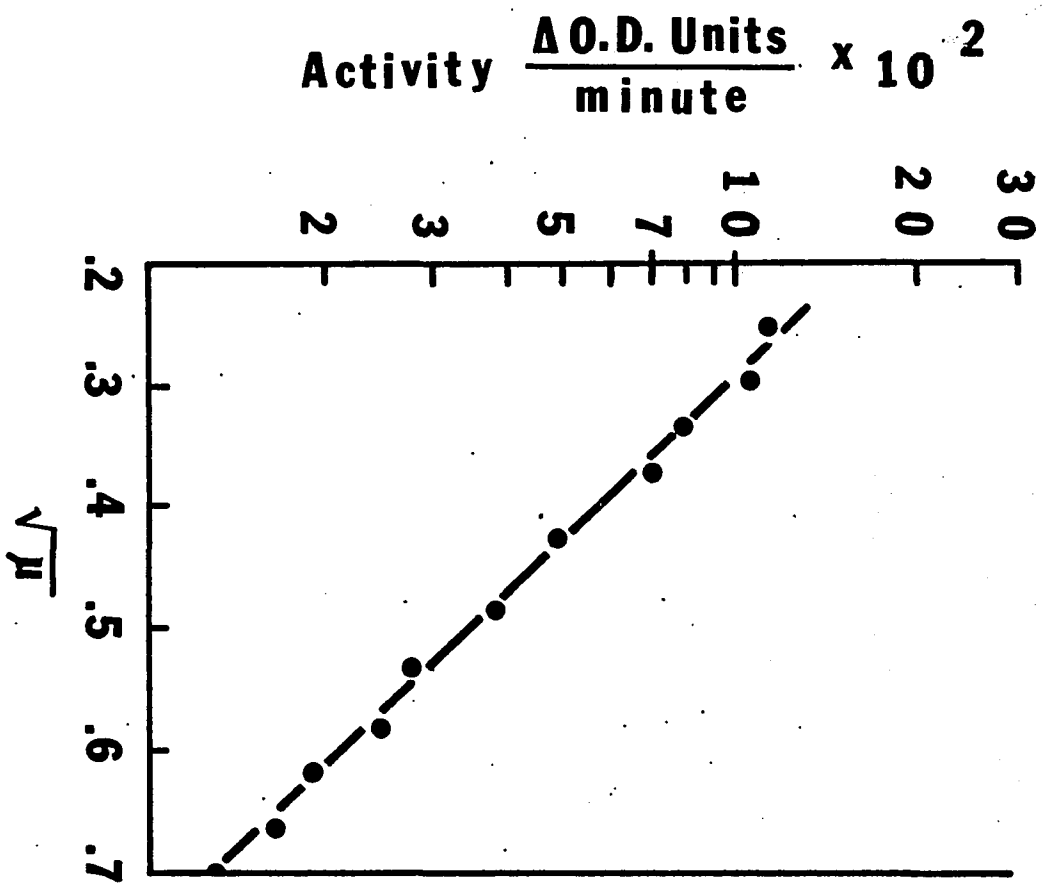


Fig. 25c Log rate vs the square root of the ionic strength.  
Data of Fig. 25a replotted.

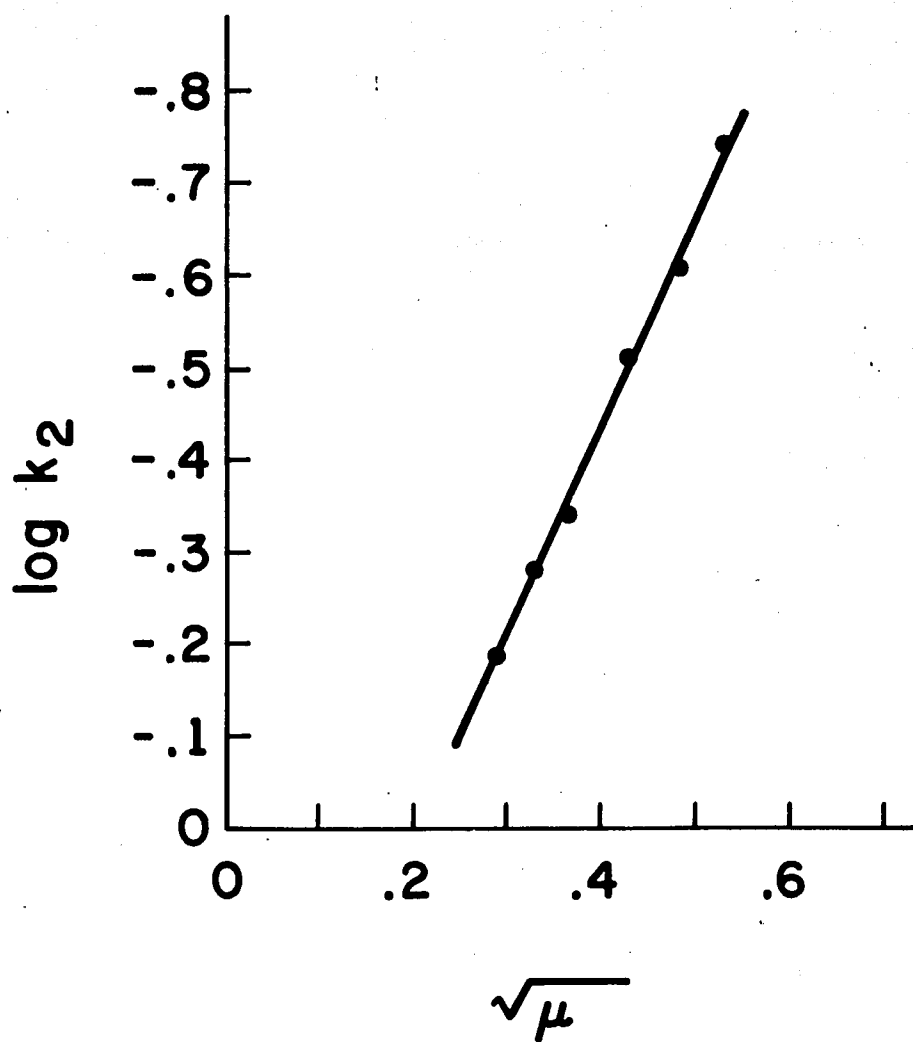


Fig. 26 Log activity vs the square root of the ionic strength. Conditions as in Fig. 25a except 0.1M phosphate is present.

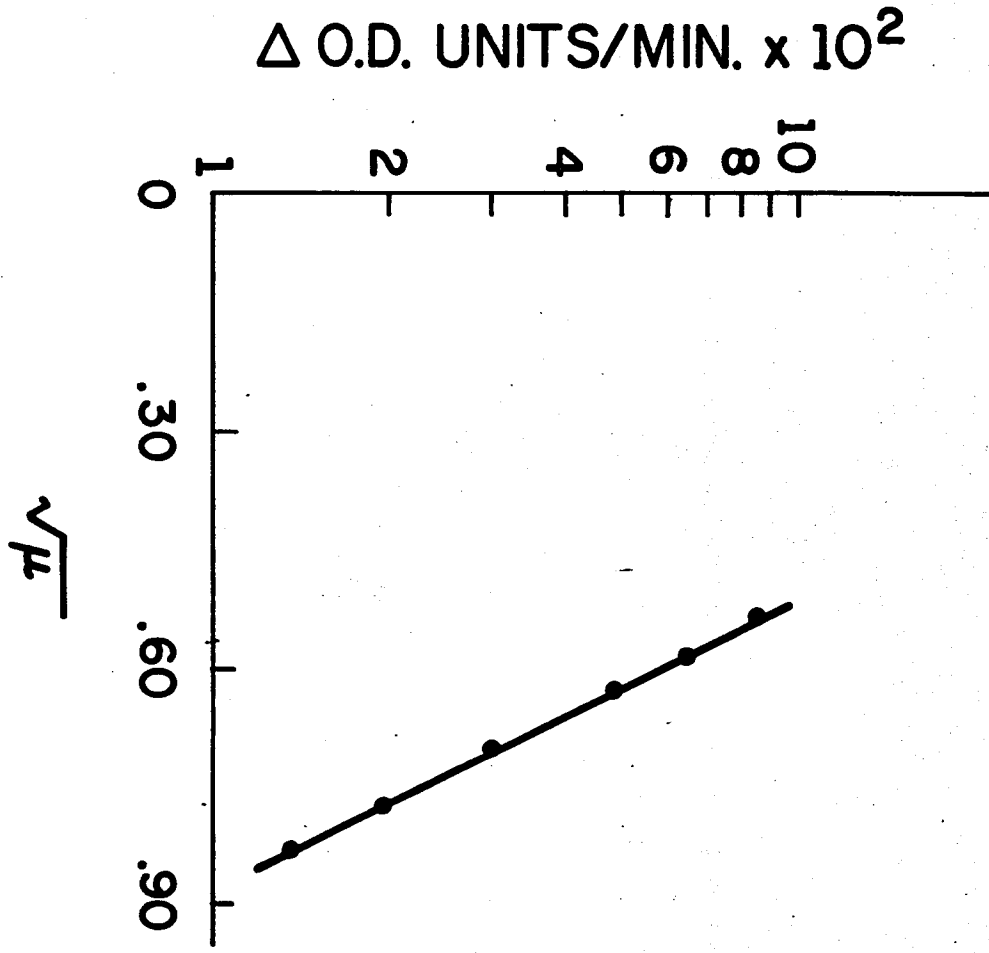


Fig. 27 Log activity vs the square root of the ionic strength. Conditions as in Fig. 25a except that ionic strength is a function of phosphate concentration. No KCl is added.

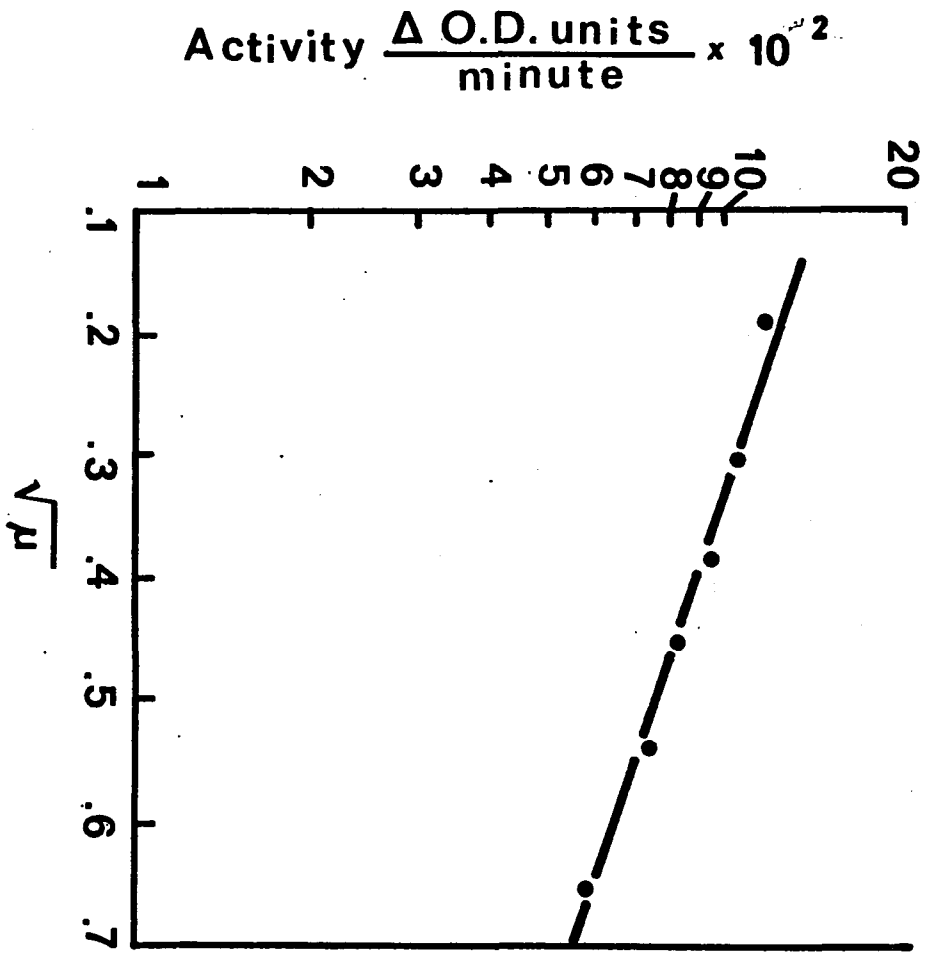


Fig. 28 Arrhenius plot. Log activity vs the reciprocal of the absolute temperature. Assay conditions - 0.1M phosphate with albumin, 0.2M alanine, 10mM ketoglutarate, pH 7.5.

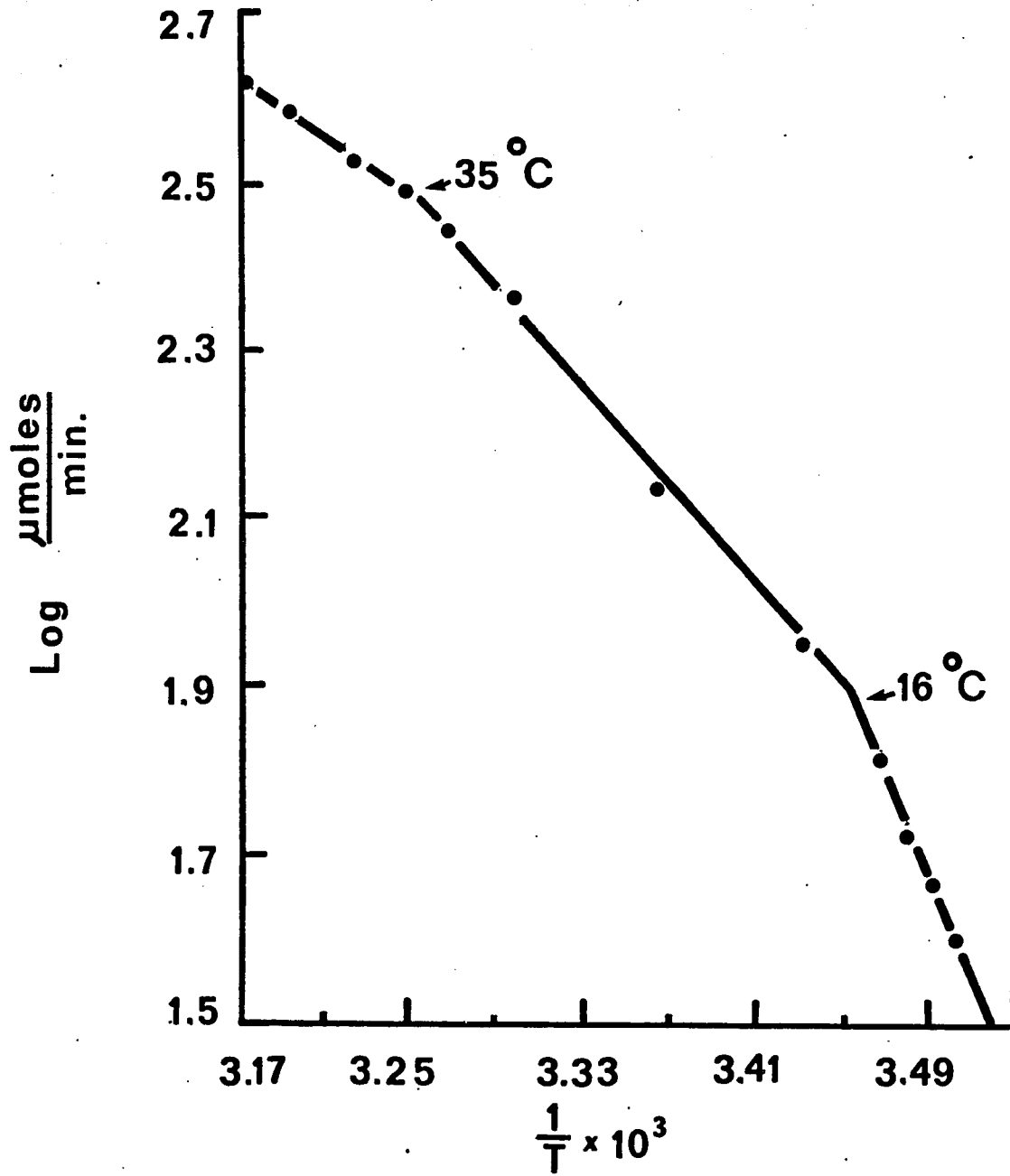


Fig. 29 Double reciprocal plot of initial velocity vs alanine concentration at a series of fixed ketoglutarate concentrations. Assays performed with 0.1M phosphate - albumin, pH 7.5 at 30°C. 3 ml assay mixture contained 0.24  $\mu$ g enzyme of specific activity = 265 units/mg. Ketoglutarate concentrations: A) 10mM B) 0.9mM C) 0.5mM D) 0.25mM E) 0.20mM

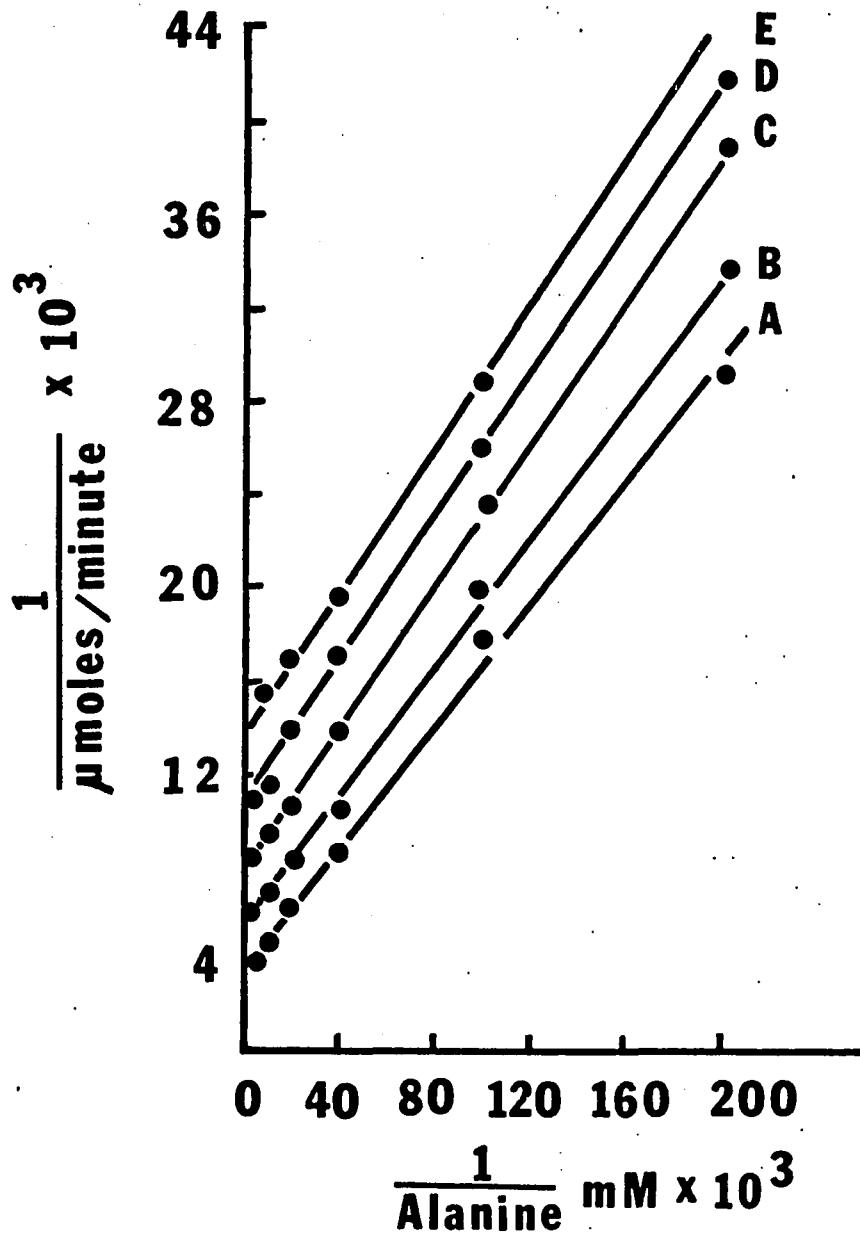


Fig. 30 Double reciprocal plot of initial velocity vs pyruvate concentration at a series of fixed glutamate concentrations. Conditions as in Fig. 29 except 0.48  $\mu$ g enzyme was used in each assay. Glutamate concentrations:

A) 22.5 mM	B) 15mM	C) 9mM
D) 6mM	E) 3mM	F) 1.8mM

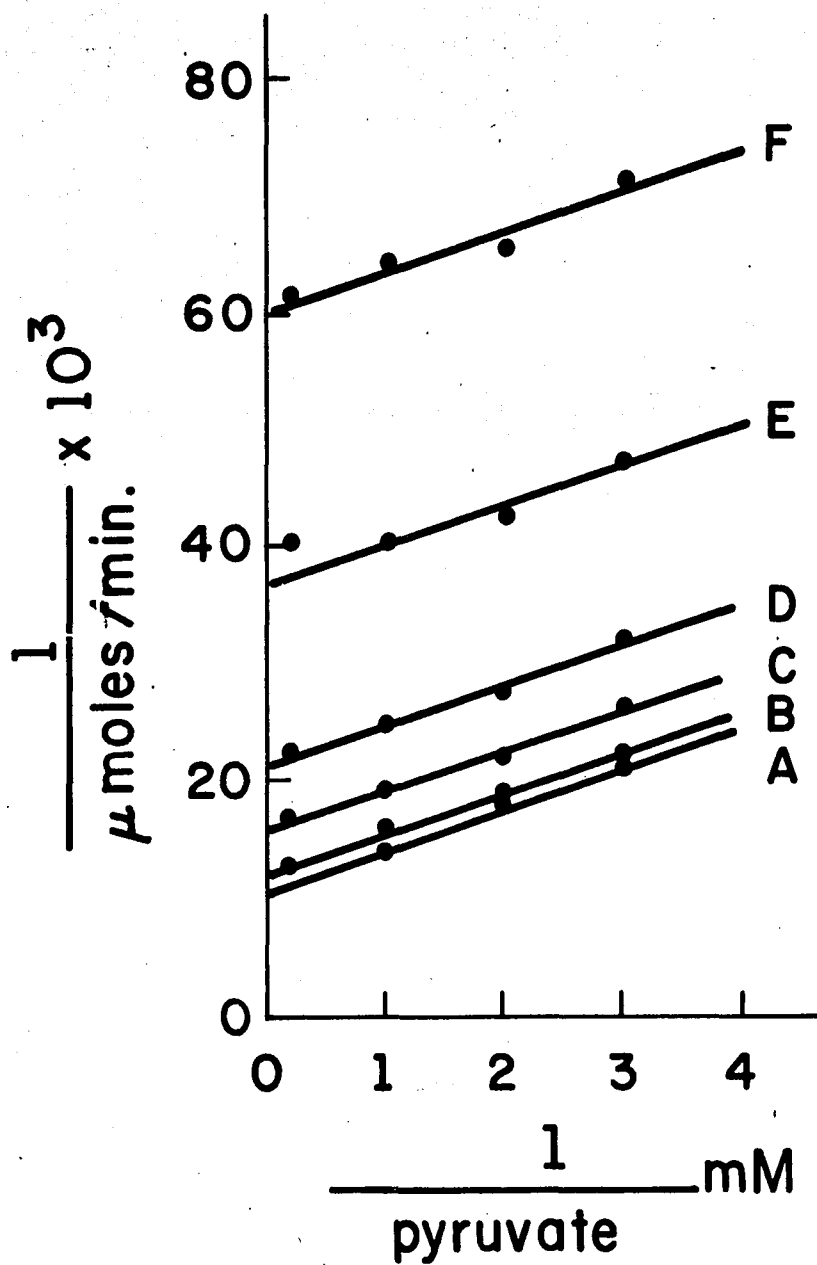


Fig. 31 Secondary plots from data of Fig. 29.

Upper line -  $\frac{1}{v_m}$  vs 1/ketoglutarate

Lower line -  $K'_{\text{alanine}}$  vs 1/ketoglutarate

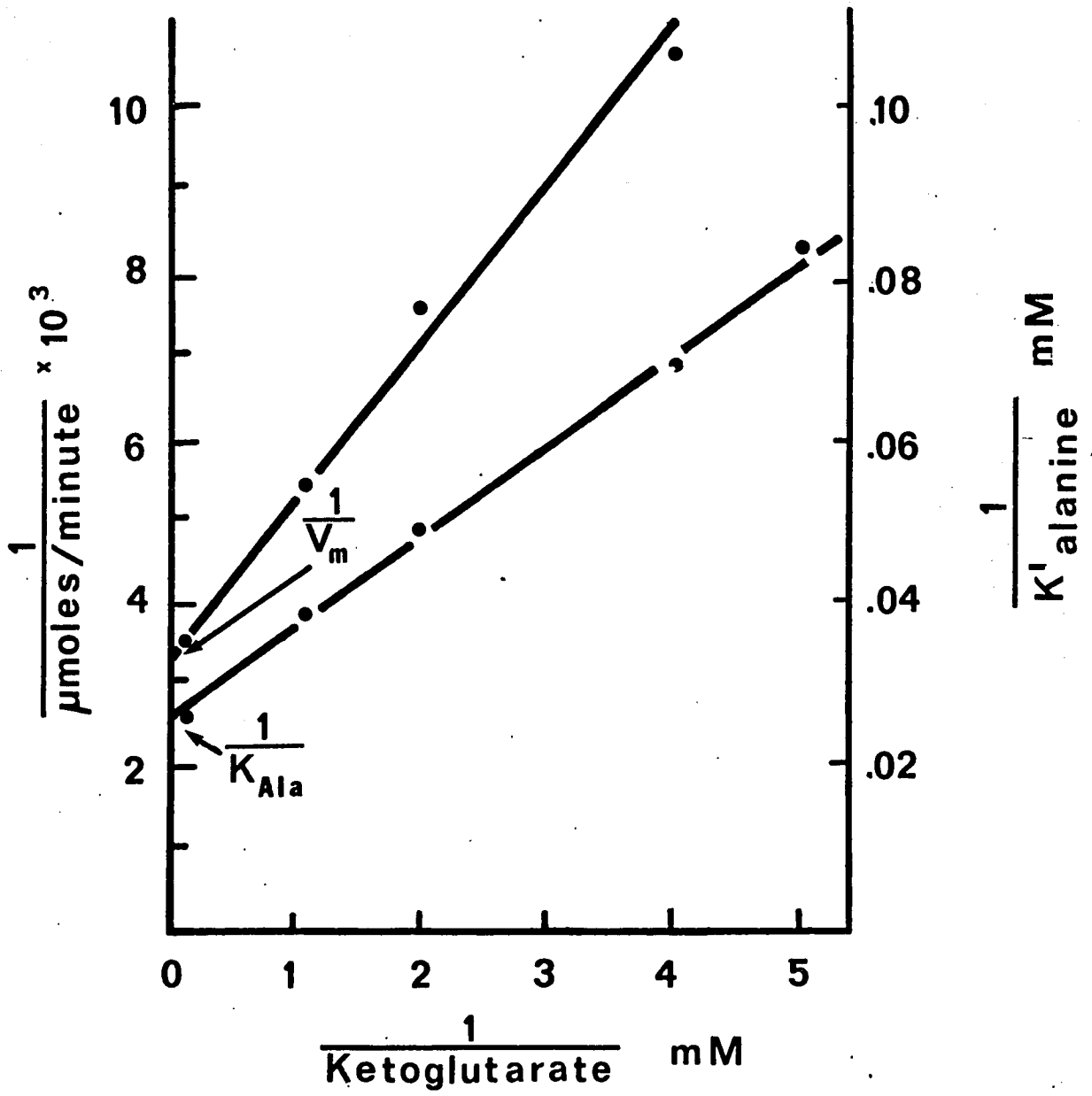


Fig. 32 Secondary plots from data of Fig. 30.

Upper line -  $1/K'_{\text{pyruvate}}$  vs  $1/\text{glutamate}$

Lower line -  $1/V'_m$  vs  $1/\text{glutamate}$

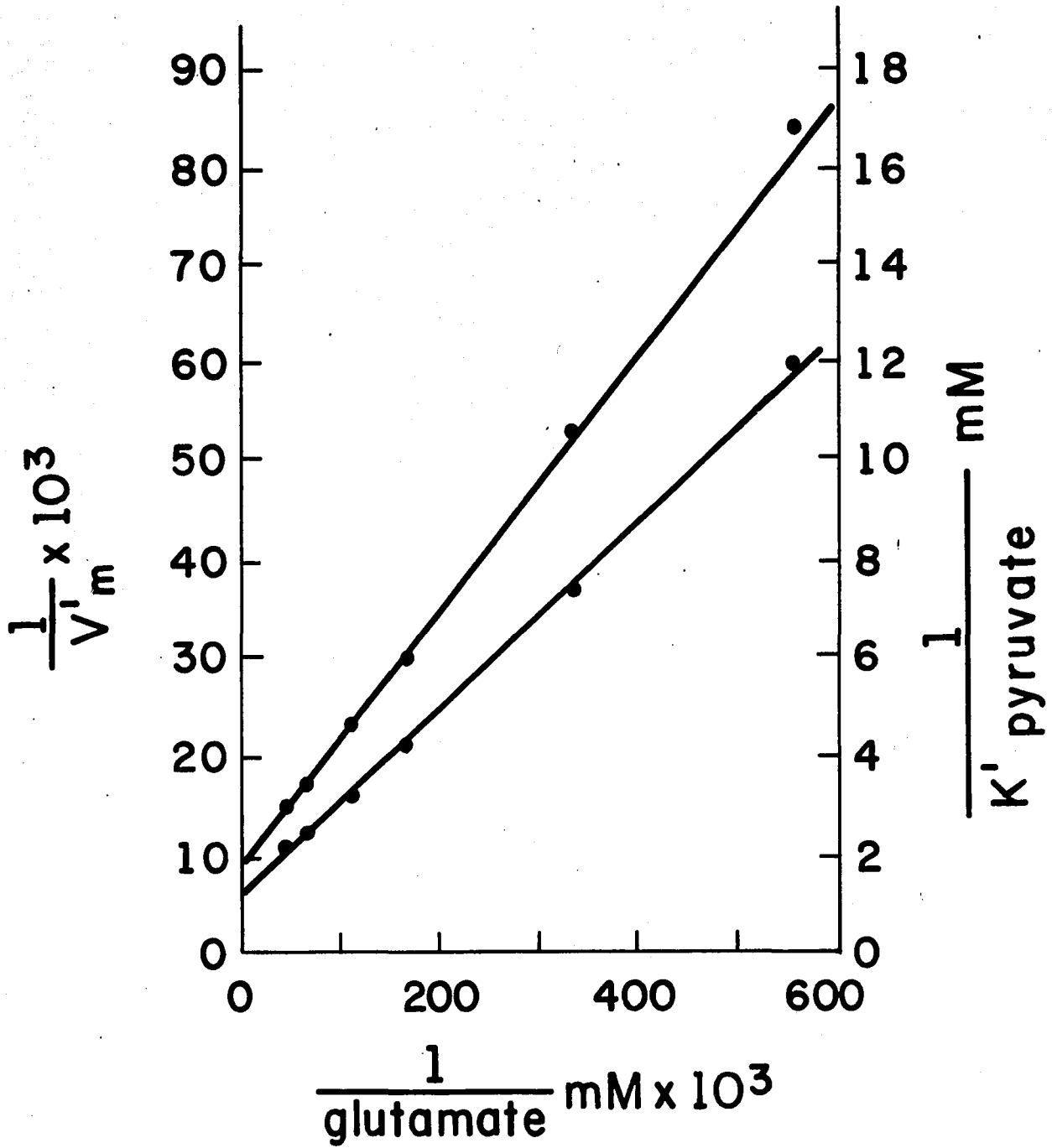


Fig. 33 Dixon plot of alanine aminotransferase inhibition by lauric acid. Assay for reverse reaction. Buffer - 0.1M phosphate, pH 7.5, 30°C. No albumin in assay mixture.

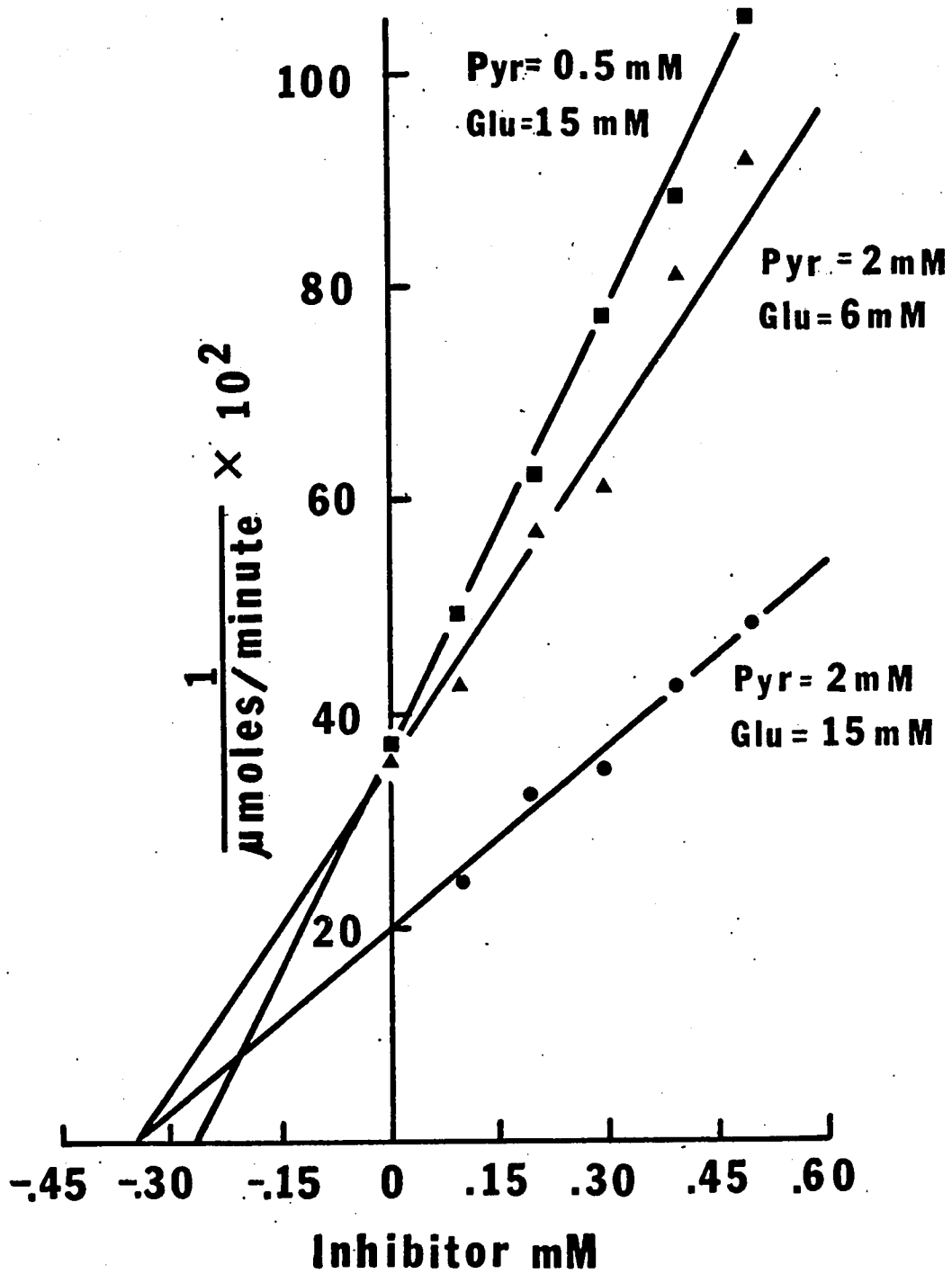


Fig. 34 Dixon Plot of alanine aminotransferase inhibition by phenylpyruvate. Assay for reverse direction. Buffer - 0.1M phosphate, pH 7.5, 30°C. No albumin in assay.

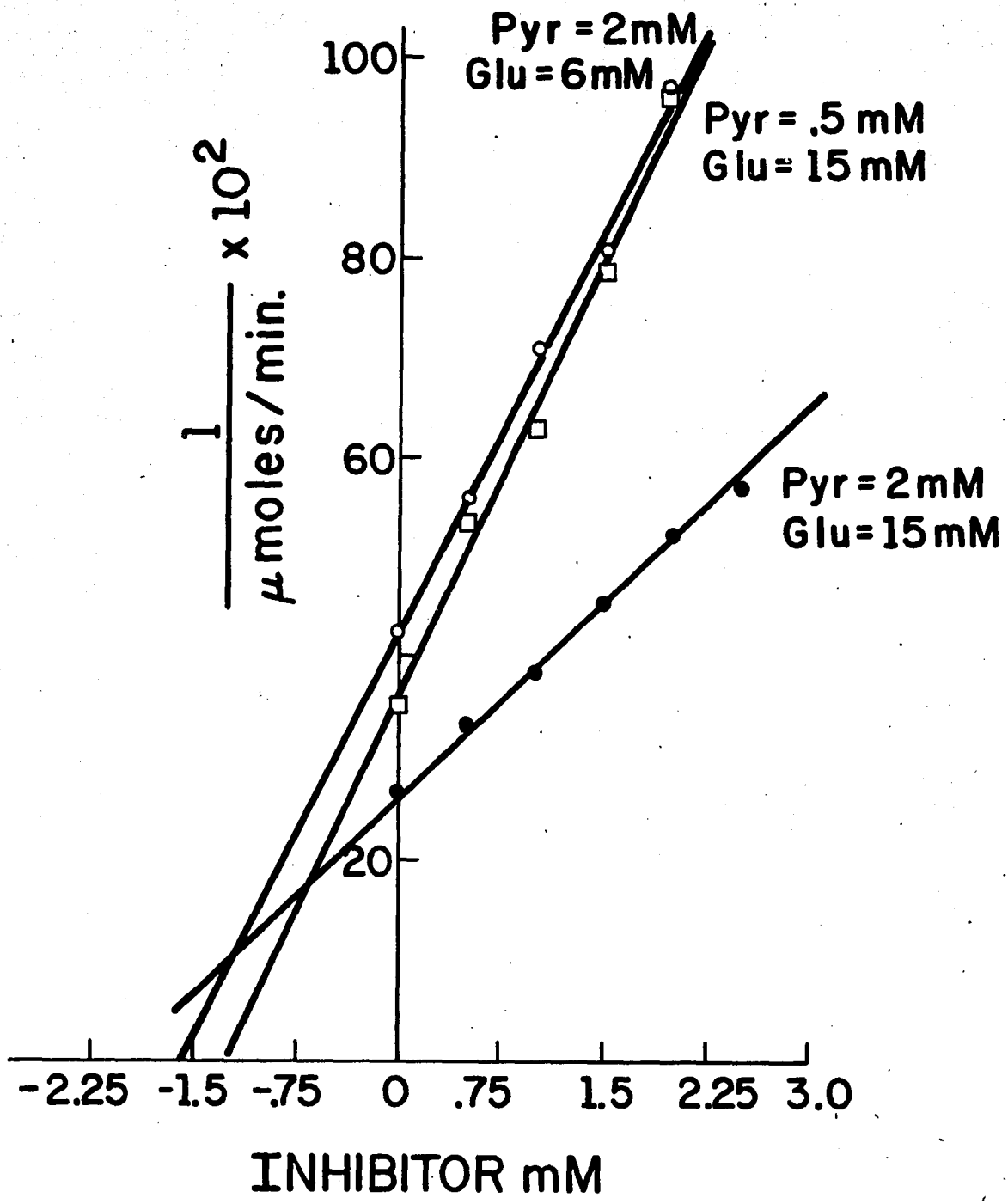


Fig. 35 Dixon plot of alanine aminotransferase inhibition by L-cysteine. Assay for forward reaction. Buffer - 0.1M phosphate, pH 7.5, 30°C. Albumin present in assay.

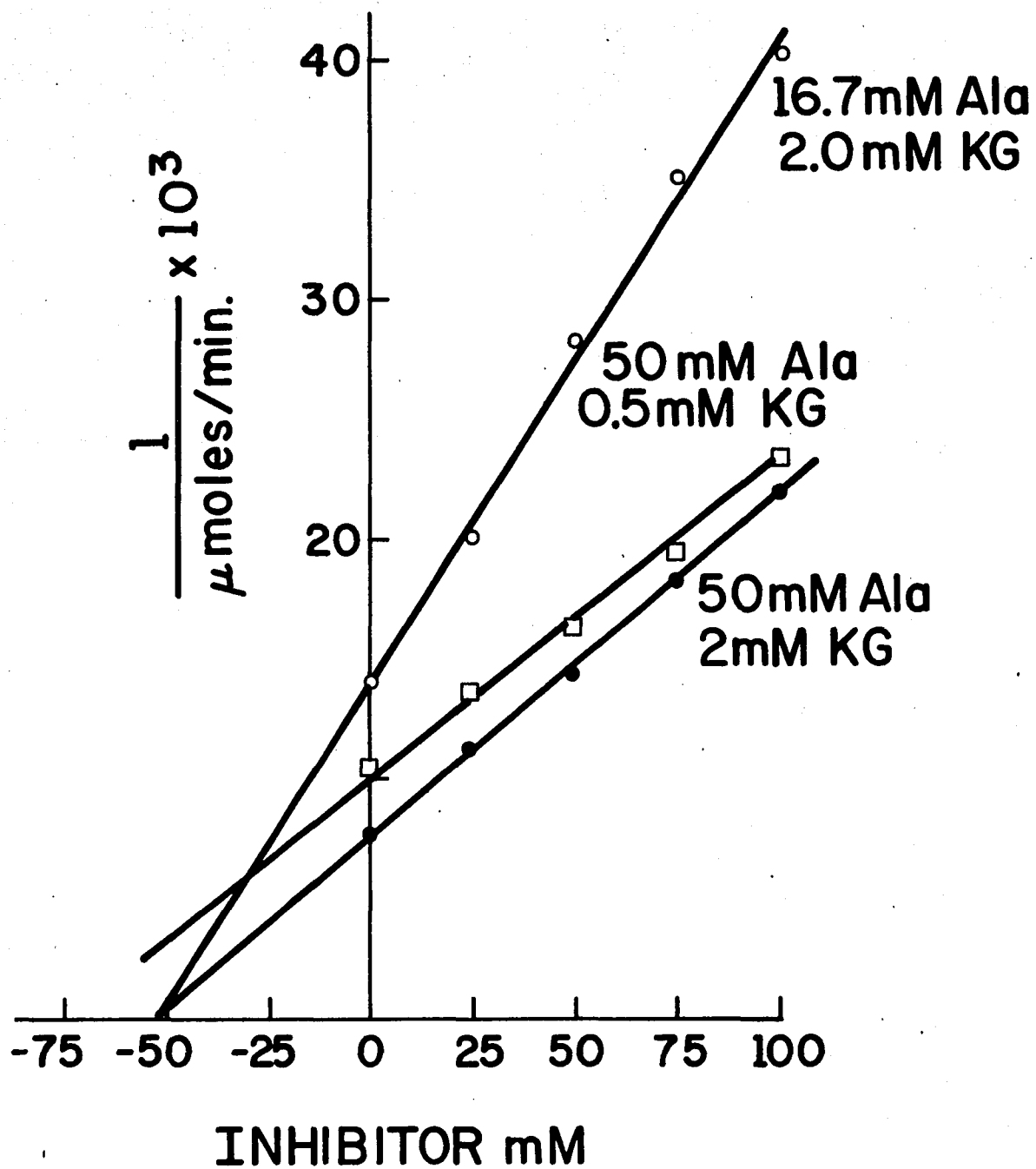


Fig. 36 Dixon plot of alanine aminotransferase inhibition by L-proline. Assay for reverse reaction. Buffer - 0.1M phosphate, pH 7.5, 30°C. Albumin present in assay.

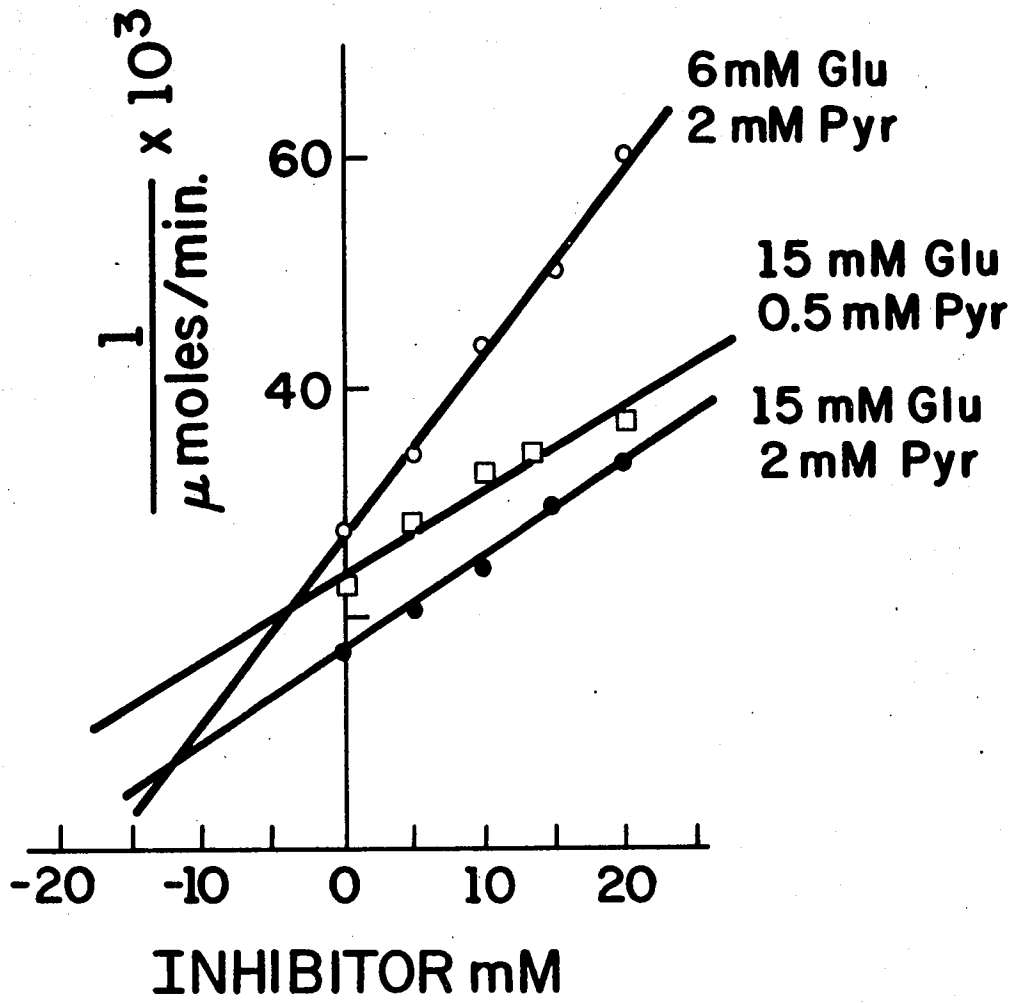
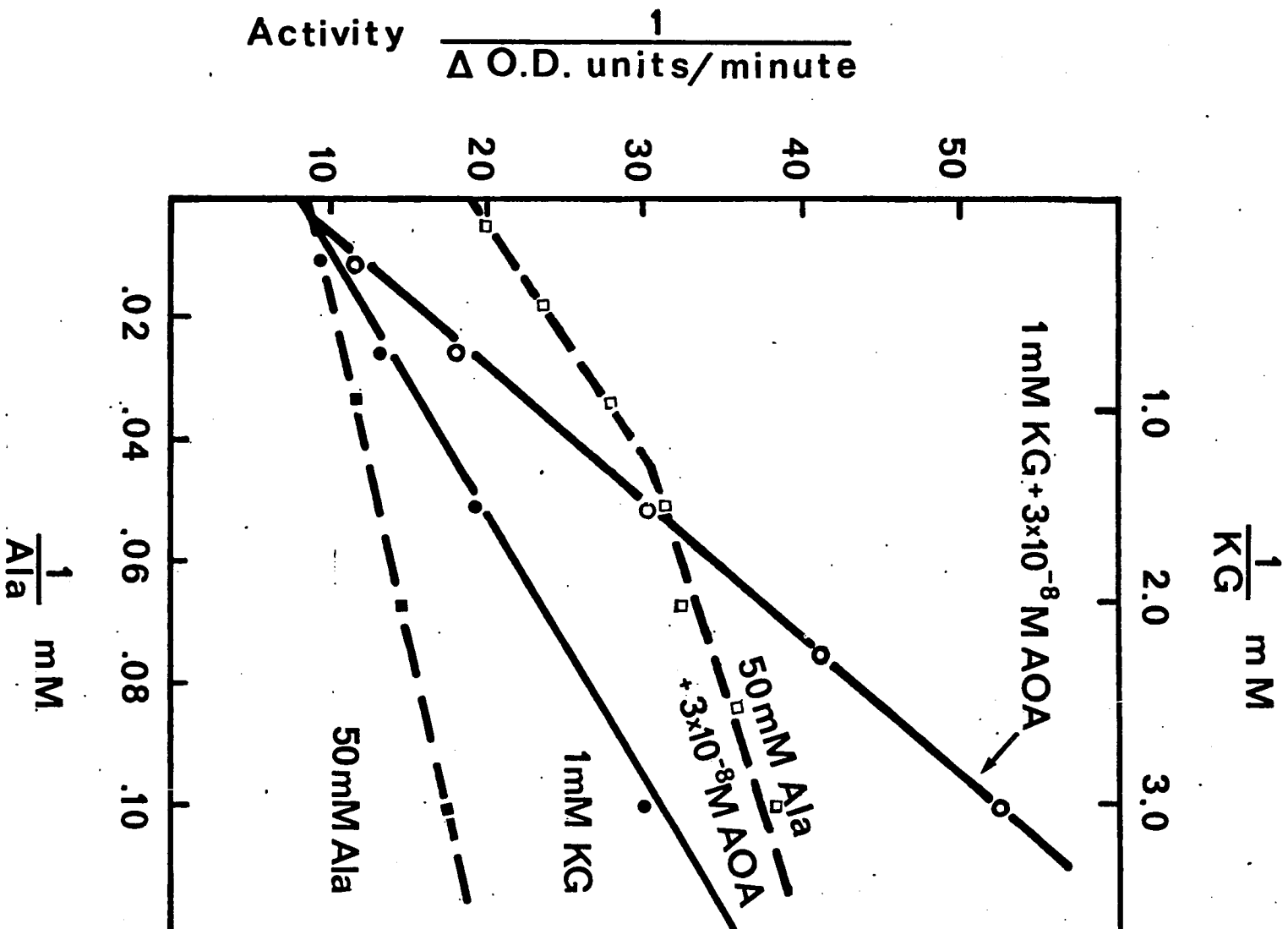


Fig. 37 Lineweaver-Burke plot of alanine aminotransferase inhibition by aminoxyacetate. Assay for forward reaction. Buffer - 0.1M phosphate, pH 7.5, 30°C. Albumin present in assay.



REFERENCES

REFERENCES

1. Snell, E. E. J. Am. Chem. Soc. 67, 194(1945).
2. Rabinowitz, J. C. and Snell, E. E. J. Biol. Chem. 169, 643(1947).
3. Baddiley, J. and Mathias, A. P. J. Chem. Soc. p. 2583 (1952).
4. Metzler, D. E. and Snell, E. E. J. Am. Chem. Soc. 74, 979(1952).
5. Metzler, D. E. J. Am. Chem. Soc. 79, 485(1957).
6. Metzler, D. E. and Snell, E. E. J. Biol. Chem. 198, 353, 363(1952).
7. Braunstein, A. E. and Shemyakin, M. M. Doklady Akad. Nauk. S.S.S.R. 85, 1115(1952).
8. Metzler, D. E., Ikawa, M., and Snell, E. E. J. Am. Chem. Soc. 76, 648(1954).
9. Ikawa, M. and Snell, E. E. J. Am. Chem. Soc. 76, 653(1954).
10. Snell, E. E. Vitamins and Hormones 16, 77(1958).
11. Braunstein, A. E. and Shemyakin, M. M. Biokimiya 18, 393(1953).
12. Jenecks, W. P. and Cordes, E. Chemical and Biological Aspects of Pyridoxal Catalysis (Snell, E. E., Fasella, P. M., Braunstein, A., Fanelli, A. R., eds.) The Macmillan Co., Pergamon Press, New York, p. 57 (1963).
13. Fasella, P. Pyridoxal Catalysis: Enzyme and Model Systems (Snell, E. E., Braunstein, A. E., Severin, E. S. and Torchinsky, Y. M., eds.) Interscience Publishers, John Wiley and Sons, New York, p. 1 (1968).
14. Hughes, R. C., Jenkins, W. T., and Fischer, E. H. Proc. Nat. Acad. Sci U.S.A. 48, 1615 (1962).
15. Snell, E. E. Brookhaven Symp. Biol. 15, 32(1962).
16. Banks, B. E. C., Diamantis, A. A. and Vernon, C. A. J. Chem. Soc. p. 4235 (1961).

17. Velick, S. F. and Vavra, J. J. Biol. Chem. 237, 2109(1962).
18. Bruice, T. C. and Topping, R. M. Chemical and Biological Aspects of Pyridoxal Catalysis (Snell, E. E., Fasella, P. M., Braunstein, A., Fanelli, A. R., eds.) The Macmillan Co., Pergamon Press, New York, p. 29 (1963).
19. Dunathan, H. C. Proc. Nat. Acad. Sci. U.S.A. 55, 712(1966).
20. Dunathan, H. C., Davis, L., and Kaplan, M. Pyridoxal Catalysis: Enzyme and Model Systems (Snell, E. E., Braunstein, A. E., Severin, E. S. and Torchinsky, Y. M., eds). Interscience Publishers, John Wiley and Sons, New York, p. 325 (1968).
21. Wada, H. and Morino, Y. Vitamins and Hormones 22, 441(1964).
22. Wada, H., Kasamiyama, H. and Watanabe, T. Pyridoxal Catalysis: Enzyme and Model Systems (Snell, E. E., Braunstein, A. E., Severin, E. S. and Torchinsky, Y. M., eds.) Interscience Publishers, John Wiley and Sons, New York, p. 111 (1968).
23. Morino, G., Paterno, M. and DeRosa, M. FEBS Letters 21, 53(1972).
24. Feliss, N. and Martinez-Carrion, M. Biochem. Biophys. Res. Commun. 40, 932(1970).
25. Krebs, E. G., and Fischer, E. H. Adv. Enzymol. 24, 263(1962).
26. Jenkins, W. T. and Sizer, I. W. J. Biol. Chem. 234, 51(1959).
27. Jenkins, W. T. and Sizer, I. W. J. Biol. Chem. 234, 1179(1959).
28. Jenkins, W. T. J. Biol. Chem. 239, 1742(1964).
29. Jenkins, W. T. and Taylor, R. T. J. Biol. Chem. 240, 2907(1965).
30. Jenkins, W. T. and D'Ari, L. J. Biol. Chem. 241, 2845(1966).
31. Fasella, P., Giartosio, A. and Hammes, G. G. Biochem. 5, 197(1966).
32. Braunstein, A. E. Vitamins and Hormones 22, 451(1964).
33. Martinez-Carrion, M., Turano, C., Riva, F. and Fasella, P. J. Biol. Chem. 242, 1426(1967).
34. Turano, C., Borri, C., Orlicchio, A., and Bossa, F. in Enzymes and Isoenzymes: Structure, Properties and Function Vol. 18 Ed. D. Shugar, Acad. Press, New York, p. 123 (1970).

35. Polyanovsky, O. L. and Keil, B. A. Biokhimiya 28, 373(1963).
36. Birchmeier, W., Wilson, K. J. and Christen, P. J. Biol. Chem. 248, 1751(1973).
37. Okamoto, M. and Morino, Y. J. Biol. Chem. 248, 82(1973).
38. Braunstein, A. E. Enzymes and Isoenzymes: Structure, Properties and Function Vol. 18 Ed. D. Shugar, Acad. Press, New York, p. 101 (1970).
39. Hopper, S. and Segal, H. L. Arch. Bioch. and Biophys. 105, 501(1964).
40. Saier, Jr., M. H. and Jenkins, W. T. J. Biol. Chem. 242, 91,101 (1967).
41. Matsuzawa, T. and Segal, H.L. J. Biol. Chem. 243, 5929(1968).
42. Bulos, B. and Handler, P. J. Biol. Chem. 240, 3283(1965).
43. Swick, R. W., Barnstein, P. L. and Stange, J. L. J. Biol. Chem. 240, 3334,3341(1965).
44. Segal, H. L., Beattie, D. S. and Hopper, S. J. Biol. Chem. 237, 1914(1962).
45. Hopper, S. and Segal, H.L. J. Biol. Chem. 237, 3189(1962).
46. Gatehouse, P. W., Hopper, S., Schatz, L. and Segal, H. L. J. Biol. Chem. 242, 2319(1967).
47. Segal, H. L., Abraham, G. J. and Matsuzawa, T. Biochem. Biophys. Res. Commun. 30, 63(1968).
48. Jenkins, W. T. Chemical and Biological Aspects of Pyridoxal Catalysis (Snell, E. E., Fasella, P. M., Braunstein, A., Fanelli, A. R., eds.) The Macmillan Co., Pergamon Press, New York, p. 139 (1963).
49. Park, C. R., Lewis, S. B., Wong, E., Mallette, L. E., Robison, G. A. and Exton, J. H. The Role of Adenyl Cyclase and Cyclic 3',5' -AMP in Biological Systems Fogarty International Center Proceedings No. 4, pgs. 137-151 (1969).
50. Mallette, L. E., Exton, J. H. and Park, C. R. J. Biol. Chem. 244, 5713(1969).
51. Felig, P., Pozetsky, T., Marliss, E., and Cahill, G. F. Science 167, 1003(1970).

52. Cori, C. F. Physiol. Rev. 11, 143(1931).
53. Adam, P. A. J., and Haynes, R. C. J. Biol. Chem. 244, 6444(1969).
54. Wicks, W. D., Kenney, F. T. and Lee, K. J. Biol. Chem. 244, 6008(1969).
55. Langan, T.A. J. Biol. Chem. 244, 5763(1969).
56. Langan, T.A. Proc. Nat. Acad. Sci. U.S.A. 64, 1276(1969).
57. Krebs, E. G., Delange, R. J., Kemp, R. G. and Riley, W. D. Pharmacol. Rev. 18, 163(1966).
58. Larner, J., Villar-Palasi, C., Goldberg, N. D., Bishop, J. S., Huijing, F., Wenger, J. I., Sasko, H. and Brown, N. B. Adv. Enz. Regul. 6, 409(1968).
59. Walsh, D. A., Perkins, J. P. and Krebs, E. G. J. Biol. Chem. 243, 3763(1968).
60. Reimann, E. M. and Walsh, D. A. Fed. Proc. 29, 601, Abst. (1970).
61. Lowry, O. H. and Passoneau, J. V. J. Biol. Chem. 241, 2268(1966).
62. Jost, J. P., Hsai, A., Hughes, S. D. and Ryan, L. J. Biol. Chem. 245, 351(1970).
63. Katunuma, N., Okada, M., Katsumuma, T., Fujino, A., and Matsuzawa, T. in Pyridoxal Catalysis: Enzyme and Model Systems (Snell, E. E., Braunstein, A. E., Severin, E. S. and Torchinsky, Y. M., eds.) Interscience Publishers, John Wiley and Sons, New York, p. 255 (1968).
64. Bitensky, M.W., Russel, V., and Blanco, M. Endocrinology 86, 154(1970).
65. Friedmann, N., Exton, J. H. and Park, C. R. Biochem. Biophys. Res. Commun. 29, 113(1967).
66. Rinard, G.A., Okuno, G. and Haynes, R. C. Endocrinology 84, 622(1969).
67. Dunn, A., Chenoweth, M. and Schaeffer, L. D. Biochem. Biophys. Res. Commun. 177, 11(1969).

68. Craig, J. W., Rall, T. W. and Larner, J. Biochim. Biophys. Acta. 177, 213(1969).
69. Jefferson, L. S., Exton, J. H., Butcher, R. W., Sutherland, E. W. and Park, C. R. J. Biol. Chem. 243, 1031(1968).
70. Menahan, L. A., Hepp, K. D. and Wieland, O. Eur. J. Biochem. 8, 435(1969).
71. Hepp, K. D., Menahan, L. A., Wieland, O. and Williams, R. H. Biochim. Biophys. Acta. 184, 554(1969).
72. Robison, G. A., Butcher, R. W. and Sutherland, E. W. eds. in "Cyclic AMP" Academ. Press, New York, p. 276 (1971).
73. Bailin, G. and Lukton, A. Biochim. Biophys. Acta. 128, 317(1969).
74. Krebs, E. G. and Fischer, E. H. Vitamins and Hormones 22, 399(1964).
75. Hedrick, J. L. and Fischer, E. H. Biochemistry 4, 1337(1965).
76. Fischer, E. H. and Krebs, E. G. Methods in Enzymology V, 369(1959).
77. Cori, G. T., Illingworth, B. and Keller, P. J. Methods in Enzymology I, 200(1955).
78. Edelhoeh, H. Biochemistry 6, 1948(1967).
79. Boyer, P. D. J. Am. Chem. Soc. 76, 4331(1954).
80. Yamada, M., Saito, A. and Tamura, Z. in Fluorescence Assay in Biology and Medicine ed., S. Udenfriend, Acad. Press, New York, II, 318(1969).
81. Schaltiel, S., Hedrick, J. L. and Fischer, E. H. Biochemistry 5, 2108(1966).
82. Zamenhof, S. Methods in Enzymology III, 696(1957).
83. Williams, D. F. and Riesfeld, R. A. Ann. N.Y. Acad. Sci. 121, 373(1964).
84. Davis, B. J. Ann. N.Y. Acad. Sci. 121, 404(1964).
85. Weber, K. and Osborn, M. J. Biol. Chem. 244, 4406(1969).

86. Wrigley, C. W. Science Tools 15, 17(1968).
87. Wrigley, C. W. Methods in Enzymology XXII, 559(1971).
88. Vesterberg, O. Biochim. Biophys. Acta. 243, 345(1971).
89. Yphantis, D. A. Biochemistry 3, 297(1964).
90. Dunker, A. K. and Reuckert, R. R. J. Biol. Chem. 244, 5074(1969).
91. Reshef, L. and Shapiro, B. Biochim. Biophys. Acta. 98, 73(1965).
92. Gopinathan, K. P. and DeMoss, R. D. Biochemistry 1, 1685(1968).
93. Heyl, D., Harris, S. A. and Feolker, K. J. Am. Chem. Soc. 70, 3429(1948).
94. Dixon, M. and Webb, E. C. Enzymes Academic Press, New York, chap. 8 (1964).
95. Enzymes and Isoenzymes: Structure, Properties and Function Vol. 18, ed. D. Shugar, Acad. Press, New York, pgs. 133-176 (1970).
96. Sodetz, J. M., Brockway, W. J. and Castellino, F. J. Biochemistry 11, 4451(1972).
97. Stein, S., Cherian, M. G. and Mazur, A. J. Biol. Chem. 246, 5287(1971).
98. Susor, W. A., Kochman, M., and Rutter, W. J. Science 165, 1260(1969).
99. Felig, P. and Wahren, J. Fed. Proceed. 33, 1092(1974).
100. Arinze, I. J., Garber, A. J. and Hanson, R. W. J. Biol. Chem. 248, 2266(1973).
101. Johnson, D. C., Brunsvold, R. A., Ebert, K. A. and Ray, P. D. J. Biol. Chem. 248, 763(1973).
102. Wicks, W. D., Barnett, C. A. and McKibbin, J. B. Fed. Proceed. 33, 1105(1974).

103. Manganiello, V. and Vaughan, M. J. Biol. Chem. 248, 7164(1973).
104. Thompson, W. J., Little, S. A. and Williams, R. H. Biochemistry 12, 1889(1973).
105. Goldberg, N., Haddox, M. K., Hartle, D. K., Haddon, J. W. in Proceedings of the Fifth International Congress of Pharmacology, San Francisco, 1972, vol. 5, Karger, Basel, pgs. 146-169 (1973).